การศึกษาจลนศาสตร์และสารตัวกลางที่เกิดขึ้นระหว่างการย่อยสลายด้วยแสงของสารกำจัดวัชพืช
ชนิดฟีนิลยูเรียโดยใช้ซิงค์ออกไซด์ขนาดนาโน

นางสาวกมลรัตน์ อภิชาติเสนีย์

INVESTIGATION OF KINETICS AND INTERMEDIATES OF

PHOTODEGRADATION OF PHENYLUREA HERBICIDES

ON NANOSIZED ZnO

Miss Kamonrat Apichatsanee

A Thesis Submitted in Partial Fulfillment of the Requirements

for the Degree of Master of Engineering Program in Chemical Engineering

Department of Chemical Engineering

Faculty of Engineering

Chulalongkorn University

Academic Year 2008

Thesis Title   INVESTIGATION OF KINETICS AND INTERMEDIATES OF PHOTODEGRADATION OF PHENYLUREA HERBICIDES ON NANOSIZED ZnO
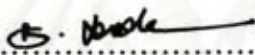
By   Miss Kamonrat Apichatsanee

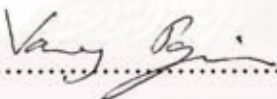Field of study   Chemical Engineering

Advisor   Assistant Professor Varong Pavarajarn, Ph.D.

Accepted by the Faculty of Engineering, Chulalongkorn University in Partial Fulfillment of the Requirements for the Master's Degree

…………………………………..… Dean of the Faculty of Engineering

(Associate Professor Boonsom Lerdhirunwong, Dr.Ing.)

THESIS COMMITTEE

………………………………………….. Chairman

(Associate Professor Muenduen Phisalaphong, Ph.D.)

…………………………………………. Advisor

(Assistant Professor Varong Pavarajarn, Ph.D.)

………………………………………….. Examiner

(Akawat Sirisuk, Ph.D.)

………………………………………….. External Examiner

(Chanchana Thanachayanont, Ph.D.)

กมลรัตน์ อภิชาติเสนีย์ : การศึกษาจลนศาสตร์และสารตัวกลางที่เกิดขึ้นระหว่างการย่อย
สลายด้วยแสงของสารกำจัดวัชพืชชนิดฟีนิลยูเรีย โดยใช้ซิงค์ออกไซด์ขนาดนาโน.
(INVESTIGATION OF KINETICS AND INTERMEDIATES OF
PHOTODEGRADATION OF PHENYLUREA HERBICIDES ON
NANOSIZED ZnO) อ. ที่ปรึกษาวิทยานิพนธ์หลัก: ผศ. ดร. วรงค์ ปวราจารย์, 103 หน้า.

การกำจัดสารกำจัดวัชพืชชนิดฟีนิลยูเรียออกจากน้ำด้วยปฏิกิริยาการย่อยสลายด้วยแสงได้
ถูกศึกษา โดยใช้ซิงค์ออกไซด์เป็นตัวเร่งปฏิกิริยา และสารกำจัดวัชพืชชนิดฟีนิลยูเรียที่ทำการศึกษา
ได้แก่ ไดยูรอน ลินูรอน และไอโซโปรทูรอน โดยทำการศึกษาผลการย่อยสลายจากอัตราการ
หายไปของสารประกอบฟีนิลยูเรีย และเปรียบเทียบประสิทธิภาพการย่อยสลายจากค่าจลนศาสตร์
เริ่มต้น ภายใต้เงื่อนไขที่กำหนดพบว่า ปริมาณตัวเร่งปฏิกิริยา ความเข้มข้นเริ่มต้นของ
สารประกอบฟีนิลยูเรีย ค่าพีเอชของสารละลาย และอุณหภูมิในการเกิดปฏิกิริยาส่งผลกระทบต่อ
อัตราการย่อยสลายของสารประกอบฟีนิลยูเรีย ปฏิกิริยาที่เร่งด้วยแสงโดยใช้ซิงค์ออกไซด์เป็น
ตัวเร่งปฏิกิริยานี้สามารถย่อยสลายสารประกอบฟีนิลยูเรียได้อย่างสมบูรณ์ โครงสร้างทางเคมีและ
ความเสถียรของสารประกอบฟีนิลยูเรียมีผลต่ออัตราการสลายตัว โดยไอโซโปรทูรอนซึ่งมี
โครงสร้างที่ว่องไวมากกว่าและมีความเสถียรน้อยกว่า จึงมีอัตราการสลายตัวที่เร็วกว่าไดยูรอนและ
ลินูรอน ทั้งนี้ได้เกิดสารตัวกลางขึ้นหลายชนิดในระหว่างกระบวนการการย่อยสลายด้วยแสงของ
สารกำจัดวัชพืชชนิดฟีนิลยูเรีย ซึ่งสารเหล่านี้เกิดขึ้นจากการเข้าทำปฏิกิริยาของอนุมูลไฮดรอกซีที่
ตำแหน่งต่างๆ ของสารประกอบฟีนิลยูเรีย

ภาควิชา	วิศวกรรมเคมี	ลายมือชื่อนิสิต กมลรัตน์ อภิชาติเสนีย์
สาขาวิชา	วิศวกรรมเคมี	ลายมือชื่อ อ.ที่ปรึกษาวิทยานิพนธ์หลัก
ปีการศึกษา	2551	

5070205221: MAJOR CHEMICAL ENGINEERING

KEYWORDS: ZINC OXIDE/ NANOSIZED/ PHENYLUREA HERBICIDE/ PHOTOCATALYTIC

KAMONRAT APICHATSANEE: INVESTIGATION OF KINETICS AND INTERMEDIATES OF PHOTODEGRADATION OF PHENYLUREA HERBICIDES ON NANOSIZED ZnO. ADVISOR: ASST. PROF. VARONG PAVARAJARN, Ph.D., 103 pp.

The practical elimination of phenylurea herbicides from water by photocatalytic reaction was studied using zinc oxide as photocatalyst and by choosing diuron, linuron, and isoproturon as representatives for the herbicides. The catalytic activities were investigated, based on the rate of phenylurea herbicides disappearance. In particular, comparison was made on their initial activities. Under identical conditions, it was found that the extent of the degradation of the phenylurea herbicide was obviously affected by amount of photocatalyst, initial phenylurea herbicide concentration, pH of the solution, and temperature. The photocatalytic reaction on the surface of zinc oxide can completely degrade the phenylurea herbicide existing in the solution. Chemical structure and stability of the phenylurea herbicide affect the rate of degradation. The higher activity or the less stability of isoproturon gives higher rate of degradation than that of diuron and linuron. Several degradation intermediates are generated by reactions of hydroxyl radical attacking to several sites of phenylurea structure, during the photocatalytic process.

Department : __Chemical Engineering__   Student's Signature : _Kamonrat Apichatsanee_

Field of Study : _Chemical Engineering_   Advisor's Signature : _____

Academic Year : _____2008_____

ACKNOWLEDGEMENTS

I would like to express my gratitude first to Assistant Professor Dr. Varong Pavarajarn, Ph.D., my thesis supervisor for his guidance, friendship, and support throughout the research and writing of this thesis. His patience and attention to details have helped me to remain on the path during the long and arduous course of my studies. Without him, there would be no thesis.

I am particularly grateful to Assistant Professor Alisa S. Vangnai, Ph.D. for her academic support and useful suggestion to my thesis.

My appreciation extends to the members of my thesis committee, Assistant Professor Muenduen Phisalaphong, Ph.D., Akawat Sirisuk, Ph.D. and Chanchana Thanachayanont, Ph.D.. Their comments and discussions have enriched and broadened the scope of the research.

I would like to thank Mektec Manufacturing Corporation (Thailand) Ltd. and all members for supporting the analytical equipments and their technical support.

I would also like to thank all my friends and all members of the Center of Excellent on Catalysis & Catalytic Reaction Engineering (Petrochemical Engineering Research Laboratory), Department of Chemical Engineering, Chulalongkorn University for their assistance and friendly encouragement.

Finally, I would like to dedicate this thesis to my parents and my families, who generous supported and encouraged me through the year spent on this study.

CONTENTS

Page

LIST OF TABLES

LIST OF FIGURES

Figure   **Page**

Figure Page

Figure **Page**

Figure   **Page**

CHAPTER I

INTRODUCTION

The use of agrochemicals such as herbicides and insecticides is one of the main environmental problems at presence because agrochemicals are commonly toxic and can contaminate both soil and aquatic systems for very long time. The causes of contamination are mainly due to the use in agricultural fields including washing of herbicide containers, and the discharge of industrial effluents that have not been treated before their disposal to the environment. Among such agrochemicals, diuron [3-(3,4-dichlorophenyl)-1, 1-dimethylurea], linuron [1-methoxy-1-methyl-3-(3,4-dichlorophenyl)urea], and isoproturon [3-(4-isopropylphenyl)-1,1-dimethylurea] were selected as target compounds in this study because they are herbicides belonging to the family of halogenophenylureas which are considered as highly toxic, bio-recalcitrant and chemically stable (Djebbar et al., 2008; Farré et al., 2007; Farré et al., 2008; Lapertot et al., 2007; Lopez et al., 2001; Madani et al., 2006; Mosleh et al., 2003)

The combined treatment processes including both physical and biological processes, such as flocculation, filtration and biological treatment are examples of wastewater treatment techniques. These processes are low in cost. However, such removal techniques are not able to remove low level of toxic inorganic and organic contaminants. Instead, the chemical methods have been used to remove the low level of toxic compounds from water to sufficiently safe concentration to reduce its environmental effect.

Advanced Oxidation Processes (abbreviated as AOPs) are special type of the chemical treatment process. All AOPs are characterized by the generation of highly oxidizing hydroxyl radicals (OH$^\bullet$), which are capable of achieving complete abatement of the pollutants through mineralization to carbon dioxide, water, and inorganic ions such as nitrate, chloride, sulfate and phosphate. Some of these processes involve the use of oxidizing chemicals, such as ozone and hydrogen

peroxide, while others combine such chemicals with UV/visible light irradiation. The combination of oxidants and irradiation has been found to significantly accelerate the degradation of the pollutants. Common photo-assisted AOPs are UV/Fenton, Ozone/UV, H_2O_2/UV and TiO_2/UV processes (Andreozzi et al., 1999).

Among all AOPs, semiconductor-assisted photocatalytic process is one of the waste treatment technologies for the elimination of toxic chemicals. Many kinds of semiconductor have been studied as photocatalysts. The most widely used semiconductor is TiO_2 due to its high efficiency, photochemical stability, non-toxic nature and low cost. On the other hand, ZnO is also a semiconductor having similar band gap as TiO_2. The advantage of ZnO, comparing to TiO_2, is that it absorbs over a larger fraction of UV spectrum and the corresponding threshold of ZnO is 425 nm (Behnajady et al., 2006).

In this research, the photocatalytic degradation of phenylurea herbicides on nanosized ZnO powder is investigated toward complete removal of harmful substances. This work not only investigates the degradation of phenylurea herbicides, but also interests in identifying the formation of intermediates during the photocatalytic degradation because the intermediate compounds formed could be even more toxic than the parent herbicides.

The objectives of this research are listed as following:

1. To investigate photocatalytic degradation of various phenylurea herbicides, using nanosized ZnO powder as catalyst. Effects of various parameters, i.e. initial concentration of herbicides, catalyst loading, pH of solution, and temperature on degradation of phenylurea herbicides and the external mass transfer of pollutant from bulk to surface of ZnO are investigated.

2. To investigate the degradation kinetics and the formation of intermediates during the photocatalytic degradation of various phenylurea herbicides.

The present study is arranged as follows:

Chapter I is the introduction of this work. Chapter II describes basic theory about phenylurea herbicides such as chemical, physical, and toxicological properties of phenylurea herbicides. Photocatalytic reaction, physical and chemical properties of zinc oxide, photocatalytic degradation of phenylurea herbicides are also described. Furthermore, literature reviews of the previous works related to this research are presented in this chapter as well. Chapter III shows experimental systems and procedures for the photocatalytic degradation. Chapter IV presents the experimental results and discussion. In the last chapter, the overall conclusions of this research and recommendations for the future work are given.

CHAPTER II

THEORY AND LITERATURE REVIEWS

Theory and literatures relating to properties of phenylurea herbicides, photocatalytic reaction, physical and chemical properties of zinc oxide, and photocatalytic degradation of phenylurea herbicides will be explained in this section.

2.1 Introduction of Phenylurea Herbicides

Since their discovery in 1950, phenylurea compounds have been widely used to prevent the growth of undesirable plants. They are mainly used for the control of germinating grass and broad-leaved weeds in many crops (Tixier et al., 2000). They prevent weeds growth by inhibiting the process of photosynthesis. However, the phenylureas are persistent herbicides. At high rates of application, they are useful as total weed killers, but at low rates, many can be used for selective weed control in a wide range of crops (Katsumata et al., 2005). They are toxic and non-biodegradable. They can contaminate both soil and aquatic systems for very long time. Therefore, the use of phenylurea herbicides is one of the main causes for the environmental pollution and public health. Examples of herbicides in this group are diuron, isoproturon, linuron, monuron and fenuron. In this work, diuron, isoproturon and linuron are selected as representatives for an investigation of phenylurea degradation by photocatalytic reaction.

The phenylurea herbicides discussed in this work are generally rather stable in the environment and undergo only limited decomposition or degradation under normal ambient conditions. Phenylurea herbicides are not particularly volatile, but because they tend to persist in the environment, they can circulate among water, soil, vegetation, and animals. Phenylurea herbicides can travel long distances via deposit in soil and water, so they can be often found away from their point of use. They can also be transported in foods and other products treated with them.

Because these phenylurea herbicides are fairly nonpolar molecules, they tend to dissolve readily in hydrocarbon-like environment, such as the fatty material in living matter. They are only slightly soluble in water. They adhere strongly to soils or sediments, where their local concentrations can increase, often exceeding those of surrounding water by orders of magnitude. Phenylurea herbicides in water and sediment tend to bioaccumulate in living tissues, particularly in fish and other aquatic organisms. They also bioaccumulate in plants, birds, terrestrial animals, agricultural livestock, and domestic animals, where their concentrations increase by orders of magnitude as they rise through the food web, particularly as they reach higher organisms.
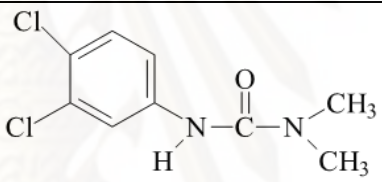
At low concentrations, phenylurea herbicides exhibit relatively low toxicty towards humans. However, they may mimic human hormones like estrogen, or possess other properties that may cause long-term health effects. At higher concentrations, phenylurea herbicides can be very harmful, causing a range of problems including mood change, headache, nausea, vomiting, dizziness, convulsions, muscle tremors, liver damage, and ultimately death. Because of observed effects on animals and plants in the environmental, and potential harmful effects to humans, uses of many phenylurea herbicides had long been banned in most of countries in the world.

The phenylurea herbicides are used for pre- and post-emergence weed control in a wide variety of crops and are widely applied throughout the world. In general, these herbicides have long lifetimes in the environment. For example, the half life in soil of diuron and linuron is 300 days and 3-4 months, respectively. Therefore, the occurrence of these herbicides as pollutants is of public concern.

2.1.1 Diuron

Diuron [3-(3,4-dichlorophenyl)-1, 1-dimethylurea], is a long acting herbicide, belonging to the family of halogenophenylureas. It has been one of the most commonly used herbicides for more than 40 years (Tomlin 2000). The plants absorb diuron via the root system. It kills weeds by inhibiting the process of photosynthesis, which means that plants cannot convert sunlight energy to grow. Diuron was selected for investigation of the photocatalytic degradation in this work because of high potential environmental contamination of soil and waterways by diuron run-off from agricultural areas, particularly into soil and aquatic systems. There are some human health concerns about the toxicity of some impurities in the active constituent of diuron as well. Its properties are shown in Table 2.1.
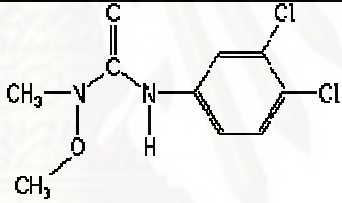
Table 2.1 Physicochemical properties of diuron.

Structure formula	
Molecular weight	233.10 g/mol
Molecular formula	$C_6H_{10}Cl_2N_2O$
Melting point	158 – 159°C
Vapor pressure	0.0041 Pa at 30°C
Appearance	White crystalline solid
Synonyms	Cekiuron; Crisuron; Dailon; Di-on; Krovar; Unidron; Vonduron; Xarmex; etc.
Solubility	42 ppm in water at 25°C
Toxicity	The concentrated material may cause irritation to eyes and mucous membrane, but a 50% -water paste is not irritating to the intact skin of mammal.
Half-life	Over 300 days in soil

2.1.2 Linuron

Linuron [1-Methoxy-1-methyl-3-(3,4-dichlorophenyl)urea], is one of the most important commercial ureas. It has good contact activity and it may kill emergent weed seedlings. Linuron is used to control annual and perennial broadleaf and grassy weeds on crop and non-crop sites. It is used as a pre- and a post-emergent herbicide. It works by inhibiting photosynthesis in plants. It is labeled for use in soybean, cotton, potato, corn, bean, pea, winter wheat, asparagus, carrot, and fruit crops. It is also used on crops stored in warehouses and storerooms. Half-life of linuron in soil ranges from 3 – 4 months. Therefore, this compound has been found as contaminant in surface and ground waters. The rapid and simple wastewater treatment of linuron is urgently required urgently. Its properties are shown in Table 2.2.
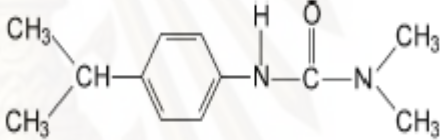
Table 2.2 Physicochemical properties of Linuron.

Structure formula	
Molecular weight	249.17 g/mol
Molecular formula	$C_9H_{10}Cl_2N_2O_2$
Melting point	85 – 94°C
Vapor pressure	0.0020 Pa at 24°C
Appearance	White crystalline solid
Synonyms	Afalon; Alafon; Cephalon; Garnitan; Linex; Linurex; Premalin; Rotalin; Sarclex; etc.
Solubility	75 ppm in water at 25°C
Toxicity	Excessive exposure to linuron may affect blood, and may cause cancer. Its effect to aquatic organism vary and likely to be harmful to other wildlife. It is considered as low toxicity herbicide.
Half -life	3-4 months in most soils

2.1.3 Isoproturon

Isoproturon [3-(4-isopropylphenyl)-1,1-dimethylurea or 3-*p*-cumenyl-1,1-dimethylurea], is a herbicide that inhibits photosynthetic electron transfer. It is mainly used for the control of annual grasses and many broad leaved weeds in the cereals and wheat. Isoproturon can be mobile in soil and it can be soluble in water. Moreover, isoproturon has low chemical and biochemical degradation rate, resulting in the fact that it is often found in contaminated surface water and ground water. Therefore, it becomes a potential risk for environment (Dupas et al., 1995; Nitschke and Schussler 1998; Parra et al., 2000; Sharma et al., 2008; Spliid and Koppen 1998; Tomlim 1994; Von wiren Lehr et al., 2001). Its properties are shown in Table 2.3.

Table 2.3 Physicochemical properties of isoproturon.

Structure formula	
Molecular weight	206.29 g/mol
Molecular formula	$C_{12}H_{18}N_2O$
Melting point	155 – 156°C
Vapor pressure	0.003 mPa at 20°C
Appearance	White crystalline solid
Solubility	72 ppm in water at 20°C
Toxicity	Low toxic, acute oral to mouse is over 10000 mg/kg
Half-life	30 days in water , 6.5 to 30 days in soil

2.2 Photocatalytic Reaction

Photocatalytic process is a technology for oxidation/degradation of organic contaminants in environmental control. It can use sunlight, which is available in abundance, as the energy source to initiate the photodecomposition of pollutants. The

end products of this treatment process are usually harmless compounds such as carbon dioxide, water and inorganic ions such as chloride and nitrate. It has been widely used as an alternative physical-chemical process for the elimination of toxic and hazardous organic substances in wastewater, drinking water, and air. In this process, a semi-conductor activated by ultra-violet (UV) radiation is used as a catalyst to destroy organic contaminants (Figure 2.1).
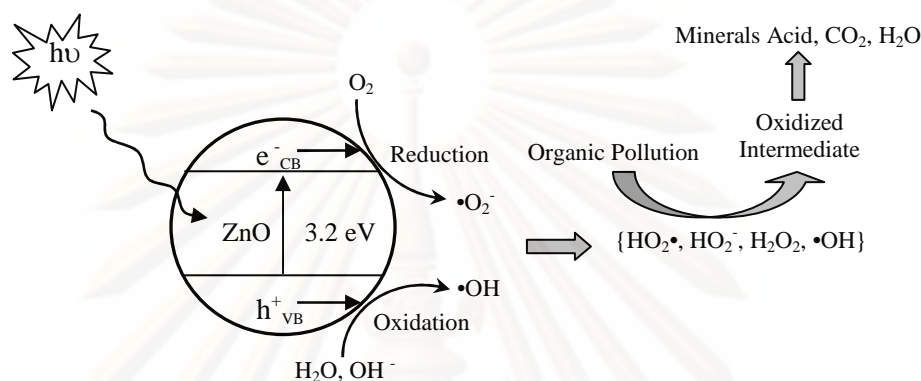
Figure 2.1. The photocatalytic reaction diagram.

The electron configuration in a semiconductor is formed into "bands" as a result of the combination of discrete energy levels of the constituent atoms. For a semiconductor such as zinc oxide, the highest filled band is termed the valence band (VB), and the lowest unoccupied level is the conduction band (CB). The separation between the top of the valence band and the bottom of the conduction band is called band gap. The band gap of a semiconductor is the minimum energy of light required to make electrons excited enough to get moving. When a photon of energy higher than or equal to the band gap energy is absorbed by a semiconductor particle. An electron from the valence band is promoted to the conduction band with simultaneous generation of an electronic vacancy or "hole" (h^+) in the valence band. The movement of electron within the system may occur in two different ways, i.e. the electron may move from the CB into an electron acceptor in the solution (reduction reaction) or the electron may move from the electron receiver in the solution into the hole in the VB (oxidation reaction). The hole can also react with water to produce the highly reactivity hydroxyl radical (OH^-). Both the holes and the hydroxyl radicals are very powerful oxidants and can be used to oxidize most organic materials (Fujishima et al., 1999).

The photocatalytic reaction starts with an exposure of photocatalyst to light. After light is absorbed by the photocatalyst, two types of carriers, i.e. electron (e^-) and holes (h^+) are generated. Semiconductor oxides such as TiO_2, ZnO, $SrTiO_3$, K_4NbO_2, Fe_2O_3 and SnO_2 are good photocatalyst because of the long time that both of these carriers are separated and can be used in photocatalytic process. The most widely used semiconductor is TiO_2 due to its high efficiency, photochemical stability, non-toxic nature and low cost. On the other hand, ZnO is also a semiconductor having similar band gap as TiO_2 (3.2 eV).
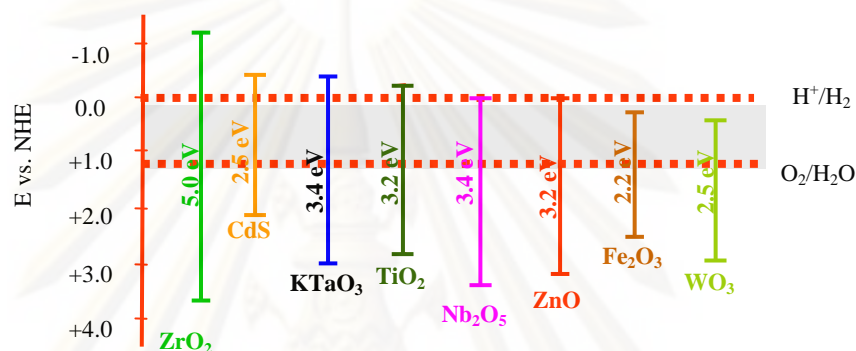
Figure 2.2. The semiconductor band gap.

The photocatalysis can be defined as the acceleration of a photoreaction by the presence of a semiconductor catalyst that can be activated by the adsorption of light of energy greater than its band gap. Since the contaminants are present in the aqueous phase, while the semiconductor is solid, this process can be called heterogeneous photocatalysis process. The generations of electron-hole pairs are represented in Eq. 2.1. The photo-generated holes and electrons give rise to oxidation and reduction processes, respectively. In an aqueous solution, water molecules adsorb onto surface of the catalyst. They are oxidized giving rise to $OH^\bullet$ radicals. As the process is usually carried out in aerobic conditions, the species to be reduced is oxygen, generating the superoxide radical (Eq. 2.2 to 2.4). Organic pollutants adsorb onto the surface of the catalyst are subsequently oxidized by $OH^\bullet$ radicals.

$$\text{Semiconductor} \;+\; hv \;\longrightarrow\; h^+ \;+\; e^- \tag{2.1}$$

$$h^+ \;+\; H_2O_{ads} \;\longrightarrow\; OH^\bullet \;+\; H^+ \tag{2.2}$$

$$h^+ \;+\; OH^-_{ads} \;\longrightarrow\; OH^\bullet \tag{2.3}$$

$$e^- \;+\; O_2 \;\longrightarrow\; O_2^- \tag{2.4}$$
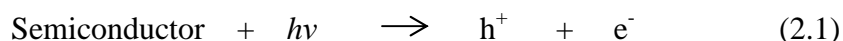
Support of the $OH^\bullet$ radical as the main reactive oxidant derives from the observation that intermediates detected during the photocatalytic degradation of halogenated aromatic compounds are typically hydroxyl structures, as those found when similar aromatics react with a known source of $OH^\bullet$ radicals.

The photocatalytic process has several advantages when compared to biological and traditional chemical oxidation processes. First, the photocatalytic reaction is not specific. Therefore, it is capable of destroying a spectrum of organic chemicals. These compounds include hydrocarbon fuels, halogenated solvents, surfactants, pesticides and many hazardous organic chemicals. Second, the process is very efficient. It often achieves a complete mineralization of organics. Third, the process is immune to organic toxicity. This advantage makes the photocatalytic process particularly attractive for the degradation of recalcitrant and toxic xenophobic compounds. Fourth, the process can be applied equally well to liquid and gaseous streams. Finally, there is a potential to utilize sunlight instead of an artificial light as an UV source. Thus, the energy cost for the process can be reduced.

2.3 Physical and Chemical Properties of Zinc Oxide

Zinc oxide is an amorphous white or yellowish powder. It occurs in nature as the mineral zincite. It is nearly insoluble in water or alcohol, but it is soluble in acids and alkalies. Zinc oxide particles may be spherical, acicular or nodular depending on the manufacturing process. The particle shape is important for maximizing physical properties. Zinc oxide absorbs all UV light radiation at wavelengths below 360 nm. Zinc oxide has received considerable attention because of its unique optical, semiconducting, piezoelectric, and magnetic properties. ZnO nanostructures exhibit interesting properties including high catalytic efficiency and strong adsorption ability.

ZnO is able to degrade a wide range of recalcitrant organics and inorganic pollutants due to its ability to generate highly oxidizing and reducing species. It could be photo-excited by absorbing light of suitable wavelength to generate two types of electronic carriers, i.e. electrons (e^-; the reducing species) and holes (h^+; the oxidizing species).

Zinc oxide is a II-VI compound semiconductor of which the ionicity resides at the borderline between covalent and ionic semiconductor. The crystal structures shared by zinc oxide are wurtzite, zinc blende, and rocksalt, as schematically shown in Figure 2.3. At ambient conditions, the thermodynamically stable phase is wurtzite. The zinc-blende structure can be formed only by the growth of ZnO on cubic substrate. The rocksalt structure may be obtained at relatively high pressure.

(a)   (b)   (c)
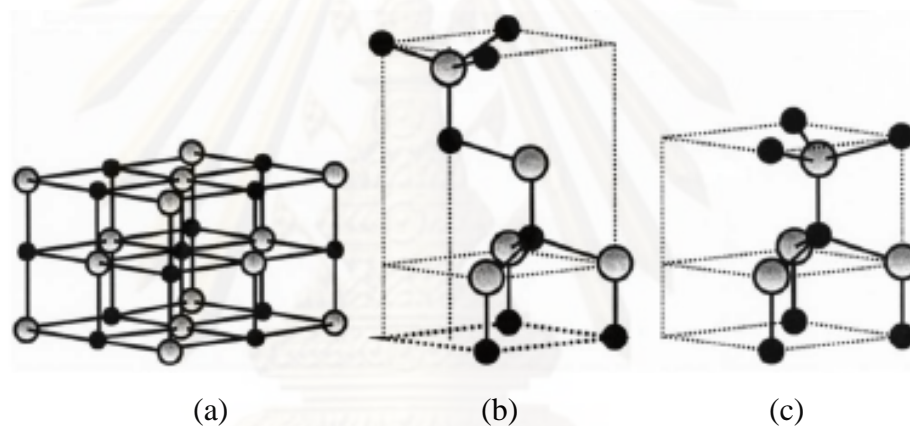
Figure 2.3. Stick and ball representation of zinc oxide crystal structures:
(a) cubic rocksalt, (b) cubic zinc blende, and (c) hexagonal wurtzite.
The shaded gray and black spheres denote Zn and O atoms, respectively.

Zinc oxide is an n-type semiconductor with a band gap of 3.20 eV and the free excitation energy of 60 meV, which makes it very high potential for room temperature light emission. This also gives zinc oxide strong resistance to high temperature electronic degradation during operation. Therefore, it is attractive for many opto-electronic applications in the range of blue and violet light as well as UV devices for wide range of technological applications. Zinc oxide also exhibits dual semiconducting and piezoelectric properties. A summary of the physical and chemical properties of zinc oxide are given in Table 2.4.

Table 2.4 Physical and chemical properties of zinc oxide.

Molecular formula	ZnO
Molecular weight	81.38 g/mole
Lattice parameters at 300 K	
a	0.32495 nm
c	0.52069 nm
a/c	1.602 (ideal hexagonal structure is 1.633)
Density	5.606 g/cm^3
Melting point	1970 – 1975 °C (decomposes)
Thermal conductivity	130 W/m.K
Linear expansion coefficient	a: 6.5 x 10^{-6}
(/^{o}C)	c: 3.0 x 10^{-6}
Static dielectric constant	8.656
Energy gap	3.2 eV, direct
Excitation binding energy	60 meV
Appearance	White solid
Synonyms	Zinc white; Zinc flowers; Calamine; C.I. pigment white 4
Solubility	Insoluble in water and alcohols. Soluble in acids and bases.
Physicochemical stability	Stable under normal conditions of handling and storage.

Zinc oxide occurs in nature as mineral. Zinc oxide is prepared in industrial scale by vaporizing zinc metal and oxidizing the generated zinc vapor with preheated air. Zinc oxide has numerous industrial applications. It is a common white pigment in paints. It is used to make enamel, white printing ink, white glue, opaque glasses, and floor tiles. It is also used in cosmetics, pharmaceutical applications such as antiseptic and astringent, dental cements, batteries, electrical equipments, and piezoelectric devices. Other applications are the use as flame retardant, and UV absorber in plastics. Nevertheless, the current major application of zinc oxide is in the preparation of most zinc salts.

2.4 Electronic Structure of Semiconductor

In solid-state physics, semiconductors (and insulators) are defined as solids in which the upper most band of occupied electron energy states, known as the valence band, is completely full at absolute zero temperature (0 K). In the other words, the Fermi energy of the electrons lies within the forbidden band gap. The Fermi energy or Fermi level can be thought of as the energy up to which available electron states are occupied at absolute zero temperature.

At room temperature, there is the smearing of the energy distribution of electrons, such that a small, but not insignificant number of electrons have enough energy to cross the energy band gap into the conduction band. These electrons break loose from the covalent bonding among neighboring atoms in the solid, and they are free to move around, hence conducting charges. The covalent bonds from which these excited electrons had previously occupied now have missing electrons, or holes, which are free to move around as well. It should be noted that the hole itself does not actually move, but a neighboring electron can move to fill the hole, leaving a hole where it originally come from. By this way, the holes appear to move.

It is an important distinction between conductors and semiconductors such that, in semiconductors, movement of charge (current) is facilitated by both electrons and holes. For the conductors where the Fermi level lies within the conduction band, the band is only half filled with electrons. Therefore, only small amount of energy is needed for the electrons to find other unoccupied states in the conductor. On the contrary, the Fermi level in semiconductors lies in the valence band. The excitation of electrons from the valence band to the conduction band in semiconductors depends on the band gap.

The current-carrying electrons in the conduction band are known as "free electrons" although they are often simply called "electrons" if context allows this usage to be clear. The holes in the valence band behave very much like positively-charged counterparts of electrons, and they are usually treated as if they are real charged particles.
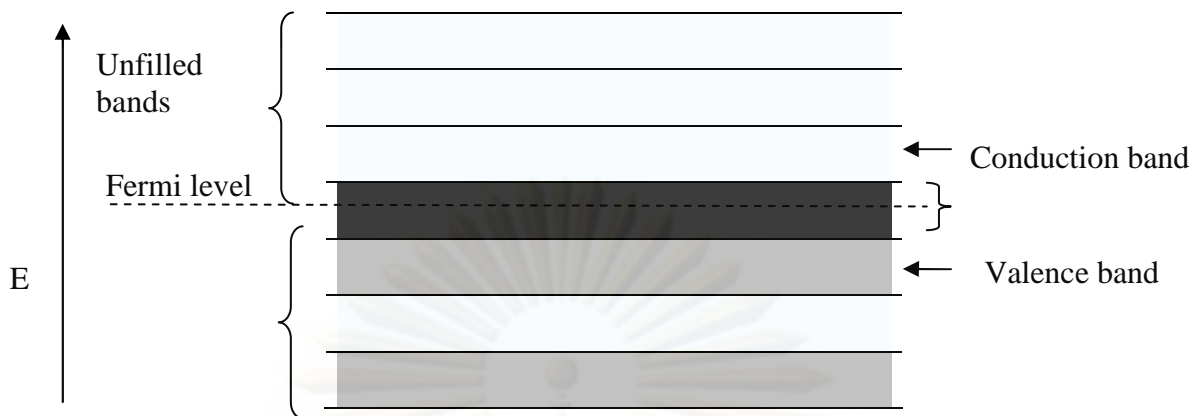
Figure 2.4. Band structure of a semiconductor showing a full valence band and an empty conduction band. The Fermi level lies within the forbidden band gap.

2.4.1 Direct and indirect band gap semiconductors

The band gap energy of semiconductor can be classified into direct and indirect band gap energy.

Direct band gap means that the conduction band lies directly above the valence band. A semiconductor with direct band gap can be used to emit light. The prime example of a direct band gap semiconductor is gallium arsenide, a material commonly used in laser diodes.

Indirect band gap semiconductors are inefficient in emitting light. This is because any electrons present in the conduction band quickly settle into the minimum energy of that band. Electrons in this minimum require source of momentum to overcome the offset and fall into the valence band. Momentum of photons is very small comparing to this energy offset. Since the electron cannot rejoin the valence band by irradiative recombination, conduction band electrons typically last quite some time before recombining through less efficient means. Silicon is an indirect bandgap semiconductor, and hence is not generally useful for light-emitting diodes or laser diodes. Indirect bandgap semiconductors can absorb light, however this only occurs

for photons with significantly more energy than the band gap. This is why pure silicon appears dark grey and opaque, rather than clear.

2.4.2 The fundamental absorption process

The most important light absorption process in semiconductors involves the transition of electrons from the valence band to the conduction band. Because of its importance, the process is referred to as *fundamental absorption*.

In fundamental absorption, an electron absorbs an incident photon and jump from the valence band to the conduction band. Therefore, the energy of photon must be equal to or greater than the band gap energy (E_g), or the frequency of the incident photon (ν) must be;

$$\nu \geq E_g/h \qquad\qquad (2.5)$$

where, h is Planck constant (4.135×10^{-15} eV.s).

The frequency of photon which corresponding exactly to the band gap energy is referred to as the absorption edge (ν_0), where $\nu_0 = E_g/h$.

The absorption edge is useful for determining band gap energy in semiconductors. It has replaced the earlier method that based on conductivity and has been a standard procedure for band gap determination, because of its accuracy and convenience. The optical method also reveals many more details about the band structure than the conductivity method.

To fine the absorption edge, the optical absorbance spectra of the sample, as shown in Figure 2.5, must be obtained (e.g. form UV-Visible spectrophotometer). The wavelength where the absorbance becomes 50% of the maximum absorbance (i.e. excitonic peak) is called $\lambda_{1/2}$. Meulenkamp and coworkers (1998) have reported that the frequency calculated from $\lambda_{1/2}$ is analogous to the absorption edge (Meulenkamp,

1998). This method gives the result comparable to other studies and can reduce errors from the spectra with broad absorption edge (Madler et al., 2002).
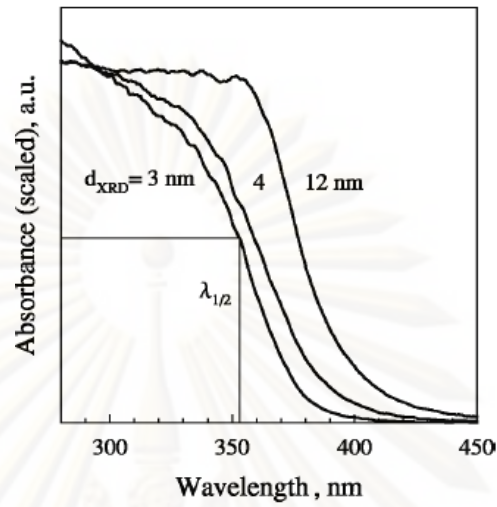
Figure 2.5. Determination of $\lambda_{1/2}$ from the optical absorbance spectra (Madler et al., 2002).

For semiconductor film, band gap can be calculated by other equations, depending on characteristic of the semiconductors.

For a *direct band gap semiconductor*:

$$\alpha_d = A(hv - E_g)^{1/2} \qquad (2.6)$$

where α_d = Absorption coefficient, which can be calculated by using the formula of Pankove (Pankove, 1971; Mott et al., 1979).

$$\alpha_d = \frac{1}{d}\ln\left[\frac{(1-R)^2}{2T} + \left\{\frac{(1-R)^4}{4T^2} - R^2\right\}^{0.5}\right] \qquad (2.7)$$

A = Constant involving the properties of the bands

R = Reflectance data

T = Transmittance data

d = film thickness (nm)

In 2005, Weng and coworkers synthesized zinc oxide thin film by electrochemical deposition. The band gap energy of samples were determinate from relationship in equation (2.6) by extrapolation of the linear part in the plot of (absorbance)^2 versus the excitation energy, *hv* (Weng et al., 2005). It should be noted that the use of (absorbance) ^{2} is in accordance with $(\alpha_d)^2$ in equation (2.6). The methods are given in Figure 2.6.
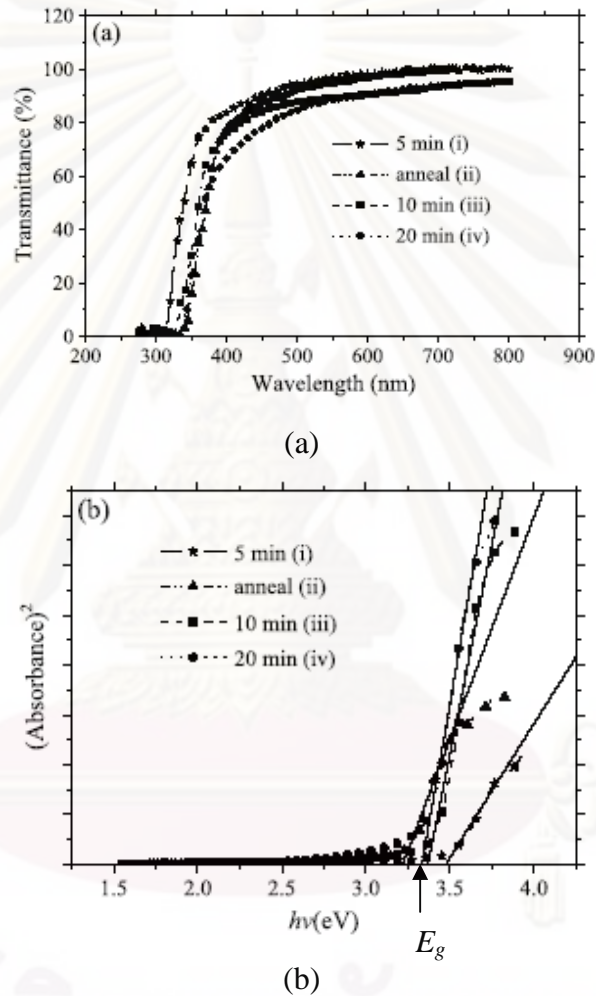
Figure 2.6. (a) Optical absorbance spectra of samples

(b) The band gap energy are determinated by extrapolation of the linear part of the plot of α ^{2} versus *hv* on x-axis (Weng et al., 2005).

For an *indirect band gap semiconductor*:

$$\alpha_i = A'(T) \, (hv - E_g)^2 \tag{2.8}$$

where $A'(T)$ = Constant containing parameters pertaining to the bands and the
temperature (Blatt, 1968).

2.5 Photocatalytic Degradation of Phenylurea Herbicides

Advanced Oxidation Processes (AOPs) are alternative and very useful for the degradation of non-biodegradable organic pollutants. They are much more efficient than conventional techniques such as flocculation, precipitation and adsorption on activated coal. The chemical processing by AOPs could lead to the complete mineralization of pollutants. AOPs are based on the generation of the hydroxyl radicals and use them as primary oxidant for the degradation of organic pollutants.

Nanosized ZnO powder has been widely studied as catalyst for AOPs. In recent years, ZnO has been used as effective, inexpensive, nontoxic semiconductor for the degradation of wide range of organic chemicals. Gouvea et al. have reported that the activity of nanosized ZnO is higher than nanosized TiO_2. They also compared three methods used to prepare the nanosized ZnO, and the results indicated that the smaller the particle, the higher the photocatalytic activity (Akyol et al., 2004; Gouvea et al., 2000; Lizama et al., 2002; Pal and Sharon, 2002; Sakthivel et al., 2003; Su et al., 2008; Yatmaz et al., 2004).

The mechanisms of photocatalytic degradation of organic matter on nanosized ZnO powder can be expressed by applying the research of N. Daneshvar (2007). The photocatalytic degradation of organic matter in the solution is initiated by photoexcitation of the semiconductor, followed by the formation of electron–hole pairs on the surface of the catalyst (Eq.2.9). The high oxidative potential of the hole (h_{VB}^{+}) in the catalyst permits the direct oxidation of organic matter (herbicide) into reactive intermediates (Eq. 2.10). Very reactive hydroxyl radicals can also be formed either by the decomposition of water (Eq. 2.11) or by the reaction of the hole with OH^{-} (Eq. 2.12). The hydroxyl radical is an extremely strong, non-selective oxidant that brings about the degradation of organic chemicals as well (Behnajady 2006; Daneshvar et al., 2004; Khodja et al., 2001).

$$\text{ZnO} \quad + \quad hv \quad\quad\quad \rightarrow \quad \text{ZnO} \; (e_{CB}^{-} \; + \; h_{VB}^{+}) \quad\quad\quad (2.9)$$

$$h_{VB}^{+} \quad + \quad \text{herbicide} \; \rightarrow \; \text{oxidative products of the herbicide} \quad (2.10)$$

$$h_{VB}^{+} \quad + \quad H_2O \quad\quad \rightarrow \quad H^{+} \; + \; OH^{\bullet} \quad\quad\quad (2.11)$$

$$h_{VB}^{+} \quad + \quad OH^{-} \quad\quad \rightarrow \quad OH^{\bullet} \quad\quad\quad\quad (2.12)$$
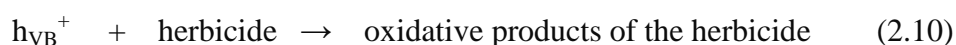
Electrons in the conduction band (e_{CB}^{-}) on the catalyst surface can reduce molecular oxygen to superoxide anion (Eq. 2.13). This radical, in the presence of organic scavengers, may form organic peroxides (Eq. 2.14) or hydrogen peroxide (Eq. 2.15).

$$e_{CB}^{-} \quad + \quad O_2 \quad\quad\quad \rightarrow \quad O_2^{\bullet -} \quad\quad\quad\quad (2.13)$$

$$O_2^{\bullet -} \quad + \quad \text{herbicide} \; \rightarrow \; \text{herbicide} - OO^{\bullet} \quad\quad\quad (2.14)$$

$$O_2^{\bullet -} \; + \; HO_2^{\bullet} \; + \; H^{+} \quad \rightarrow \quad H_2O_2 \; + \; O_2 \quad\quad\quad (2.15)$$
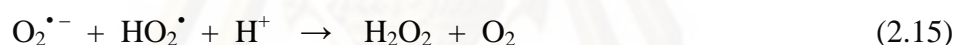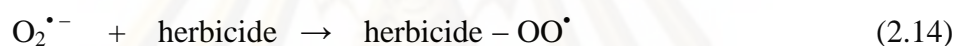
Electrons in the conduction band are also responsible for the production of hydroxyl radicals, which have been indicated as the primary cause of organic matter mineralization (Eq. 2.16) (Daneshvar, 2004; Konstantinou and Albanis, 2004).

$$OH^{\bullet} \quad + \quad \text{herbicide} \quad \rightarrow \quad \text{degradation of the herbicide} \quad (2.16)$$

Many papers on photocatalytic processes have been presented in recent years (Daneshvar et al., 2007; Daneshvar et al., 2007; Djebbar, 2008; Farré, 2007; Klongdee et al., 2005; Lapertot, 2007; Madani, 2006; Pérez et al., 2006; Sobana and Swaminathan, 2007; Thatt Yang Timothy TAN, 2003). These papers offer extensive details on the photocatalytic degradation of various non-biodegradable organic pollutants such as insecticides, herbicides, and wastewater from textile and some other industries contain residual dyes. The common photocatalytic degradation processes employs either semiconductor/UV or UV/Fenton processes. According to these papers, the photocatalytic processes are able to degrade non-biodegradable organic pollutants. They have also found that the kinetic model for, the photocatalytic

reaction is the Langmuir – Hinshelwood model, in which the substrates have to be adsorbed on the catalyst surface sites for bond breaking or bond formation. The adsorption of substrates and the availability of sites are hence important parameters in photocatalytic reactions. The rate of substrate conversion is proportional to the available active sites. As the reaction proceeds, the amount of substrate adsorbed on the catalysts surface will decrease until the substrate is completely converted. In general, kinetic models are often formulated to describe photocatalytic reactions with respect to the initial substrate concentrations. The kinetic models for photocatalytic reactions are derived based on the classical Langmuir – Hinshelwood kinetic model. This model assumes that the reaction occurs on the surface and the reaction rate (r) is proportional to the fraction of surface coverage by the substrate (θ):

$$r = -\frac{dC}{dt} = k_r\theta = k_r\frac{KC}{1+KC} \qquad (2.17)$$

where k_r is the reaction rate constant, K is the adsorption constant and C is the substrate concentration at any time t. Integrating the above expression yields:

$$\ln\frac{C_0}{C} + K(C_0 - C) = k_rKt \qquad (2.18)$$

Moreover, the results of some papers indicated that the photocatalytic process is very efficient because it often achieves a complete mineralization of organics. For example, María José Farré et al. (2006) have studied photo-Fenton and biological treatment coupling for diuron and linuron removal from water. They have found that complete disappearance of the herbicides from water was achieved after the photo-Fenton process. N. Daneshvar et al. (2006) have investigated the removal of C.I. acid orange 7 from aqueous solution by UV irradiation in the presence of ZnO nanopowders. The results showed that the complete removal of color, after selection of desired operational parameters, could be achieved within a relatively short time of about 60 min.

However, the disappearance of the initial compound is not sufficient to demonstrate the effectiveness of the photocatalytic process because the intermediate compounds formed during the reaction could be even more toxic and resilient towards degradation than the parent compound. It is hence of interest not only to monitor the degradation of the parent compound but also to identify the intermediate compounds formed. In general, the oxidation of straight-chained hydrocarbon is relatively easy, while dearomatisation of aromatic compounds has been found to be harder, longer and involves the formation of many intermediate compounds before mineralization is achieved.

In this work, nuclear magnetic resonance spectroscopy (NMR) and liquid chromatography coupled with mass spectrometer (LC-MS) are used to identify intermediate compounds while the phenylurea herbicides degradation are periodically monitored by using a reverse-phase liquid chromatography system, with UV detector (HPLC-UV). The kinetics study has been based on the initial disappearance of phenylurea herbicides to measure the intrinsic activities, avoiding the interference of the intermediate products.

CHAPTER III

EXPERIMENTAL

3.1 Characterizations of zinc oxide

3.1.1 Scanning Electron Microscopy (SEM)

Surface morphology and size of the zinc oxide particles were observed by using a scanning electron microscope (Hitachi S3400) at a research laboratory collaborated between Mektec Manufacturing Corporation (Thailand) Ltd. and Chulalongkorn University, operating in SE mode with aperture number 3, acceleration voltage of 15 kV, pressure below 1 Pa, working distance 500-10000 μm.

3.1.2 Surface area measurement

The multipoint BET surface area of zinc oxide particles was measured by micromeritics model ASAP 2020 using nitrogen as the adsorbate at the Center of Excellence on Catalysis and Catalytic Reaction Engineering, Chulalongkorn University. The operating conditions are as follows:

Sample weight	~ 0.2 g
Degas temperature	$200^{\circ}C$
Vacuum pressure	< 10 mmHg

3.1.3 UV/Vis spectrophotometer

The band gap of zinc oxide was measurement by UV/VIS spectrophotometer (PerkinElmer Lambda 650, wavelength between 220 and 800 nm and step size 1 nm.) at a research laboratory collaborated between Mektec Manufacturing Corporation (Thailand) Ltd. and Chulalongkorn University. The spectra recorded at wavenumber 400-800 cm^{-1}.

The band gap energy of zinc oxide was estimated by using the relation $\nu = E_g/h$ where h is Planck constant (4.135×10^{-15} eV.s), ν is the frequency of photon at the absorption edge and E_g is the band gap energy (Omar, 1975). The frequency, ν, is related with wavelength by the relationship $\nu = c/\lambda$ where c is the speed of light (3×10^{17} nm.sec^{-1}). To fined the absorption edge, the wavelength where the absorbance becomes 50% of the maximum absorbance was selected and called $\lambda_{1/2}$. Then, $\lambda_{1/2}$ is replaced into the aforementioned equations to calculate the band gap energy. This method gives the result comparable to other studies and can reduce errors from the spectra with broad absorption edge (Madler et al., 2002).

3.1.4 Point of zero charge determination

The point of zero charge (abbreviated as pH_{pzc}) of the zinc oxide was determined by the solid addition method (Mishra et al., 2003). Batch experiments were performed in a series of 125-ml Erlenmeyer flasks. The 45 ml of KNO_3 solution of known concentration was poured into a series of 125 ml Erlenmeyer flasks. The initial pH values of the solution were roughly adjusted from 3 to 12 by adding either 0.1 N HNO_3 or NaOH. The total volume of the solution in each flask was made up exactly to 50 ml by adding the KNO_3 solution of the same concentration. The initial pH values of the solution were then accurately noted. One gram of ZnO sample was added to each flask and the flask was securely capped immediately. The suspensions were allowed to equilibrate for 48 hours while shaking. The pH values of the supernatant liquid were noted. The difference between initial and final values (ΔpH) was plotted against the initial pH. The point of intersection of the resulting curve at which ΔpH = 0 gave the pH_{pzc}. The procedure was repeated for different concentrations of KNO_3 (0.1M, 0.01M, and 0.001M).

3.2 Photocatalytic Degradation of Phenylurea Herbicides

3.2.1 Herbicides

1. Diuron [3-(3,4-dichlorophenyl)-1,1-dimethylurea or N´-(3,4-dichlorophenyl)-N, N-dimethyl urea], 98% was purchased from Sigma-Aldrich Chemical Company.

2. Linuron [3-(3,4-dichlorophenyl)-1-methoxy-1-methyl urea or N´-(3,4-dichlorophenyl) N´-methoxy- N´-methyl urea], 99% was purchased from Chem Service.

3. Isoproturon [3-(4-isopropylphenyl)-1,1-dimethylurea or 3-*p*-cumenyl-1,1-dimethylurea], 99% was purchased from Chem Service.

3.2.2 Experimental procedures

The photodegradation was conducted in aqueous system. Diuron, linuron, and isoproturon were selected as target compounds for photocatalytic degradation of phenylurea herbicides. The nanosized ZnO powder was used as photocatalyst for UV-induced photocatalytic degradation (UV/ZnO process) of phenylurea herbicides.

For the photodegradation of each herbicide, a 550 ml solution containing known concentration of the herbicide was transferred to 600 ml Pyrex reactor. Then, ZnO nanoparticles (obtained from Univenture PLC, Thailand) were added into the solution in the ratio of 1 mg of ZnO to 10 ml of solution. The mixture was kept in the dark for 30 min to allow the complete adsorption of herbicides on the surface of ZnO. The photocatalytic reaction was initiated by irradiating the mixture with light from 6 UV-A lamps (Phillips TLD 15W/05). The light intensity was 7.43 Wm^{-2} measured by IL 1700 Research Radiometer. The temperature during the experiment was maintained at 30 ± 2 $^{\circ}C$ using cooling coil. During the experiment, the mixture was constantly agitated by a magnetic stirrer to keep mixture homogeneous. The diagram of the equipment setup for photocatalytic reaction is shown in Figure 3.1. The mixture was sampled after an appropriate illumination time. Before determination of concentration of the herbicide, samples were filtered through 0.45 µm cellulose acetate filter to remove ZnO particles. The concentration of the herbicide in each degraded sample was determined using a reverse-phase liquid chromatography

system, with UV detector (HPLC-UV, Agilent Technologies, series 1200) and C-18 column (ZORBAX SB-C18, 5 µm particle size, 4.6x150mm). Isocratic elution conditions were applied. The mobile phase composition was acetronitrile/deionization water at a ratio 70/30. The flow rate was 1.5 ml/min and the sample injection volume was 20 µl.

Under these conditions, the retention time for diuron, linuron, and isoproturon was about 1.5, 1.9, and 1.4 min, respectively. The calibration curves were calculated on the basis of the peak height obtained with standardized samples analyzed under the same HPLC conditions, as shown in Appendix B.

Intermediate products from the photocatalytic reaction of herbicides were fractionated using the HPLC-UV, Agilent Technologies, series 1100 and C-18 column (ZORBAX Eclipse XDS-C18 PrepHT, 7 µm particle size, 21.5x250mm). The solution of 70% acetronitrile-30% water was used as mobile phase (flow rate of 5 ml/min). The sample injection volume was 2,700 µl. The nuclear magnetic resonance spectroscopy (NMR) and liquid chromatography coupled with mass spectrometer (LC-MS) were used to identify intermediate compounds.

Effect of various parameters, i.e. catalyst loading (0.5, 1.0, 1.5, 2.0, 2.5, 3.0, 3.5 mg of ZnO to 10 ml of solution), initial concentration of herbicides (1, 5, 10 ppm), pH of solution (The pH values of the herbicide solution were adjusted to the desired value in the range of 3 to 11 by using either dilute H_2SO_4 and NaOH.), temperature during the degradation of phenylurea herbicides in range of $10 - 50$ ^{o}C, and the external mass transfer of pollutant from bulk to surface of ZnO were investigated.
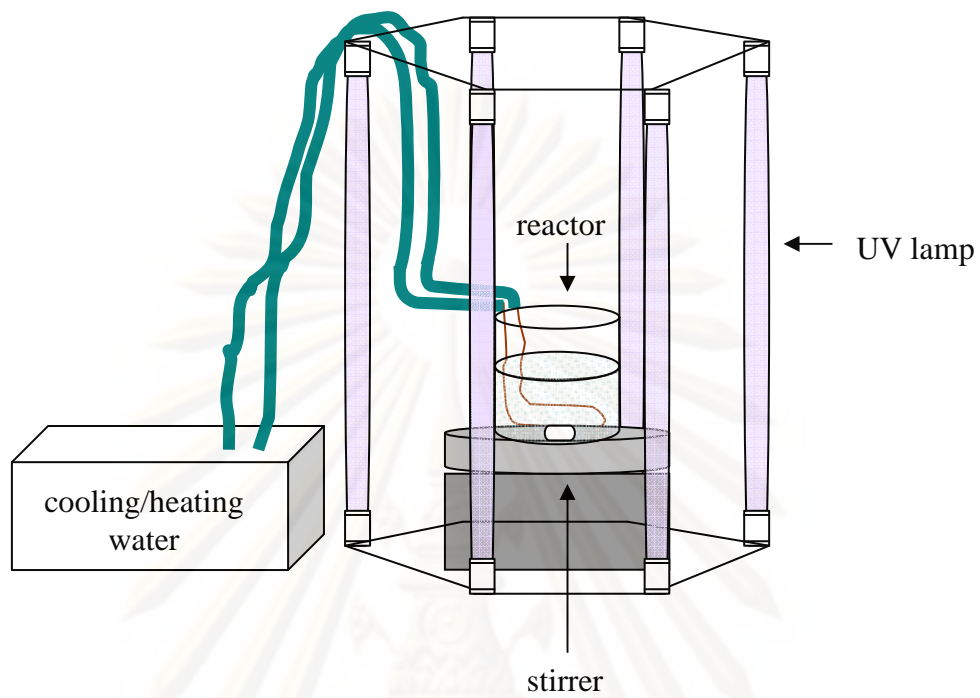
Figure 3.1. Diagram of the equipment setup for the photocatalytic degradation.

CHAPTER IV

RESULTS AND DISCUSSION

Photocatalytic degradation can be applied to remove many organic compounds from wastewater. In this study, zinc oxide was used as photocatalyst to eliminate phenylurea herbicides from water. Diuron, linuron, and isoproturon were chosen as model molecules representing the herbicides. Although the total photomineralization of phenylurea herbicides can be obtained as indicated by the total organic carbon (TOC) disappearance, one has to get rid of the interference from intermediate products for better comparison of the intrinsic activities. This is why we based our kinetics comparison on initial kinetics (Madani et al., 2006).

4.1 General Description for Photocatalytic Degradation Results
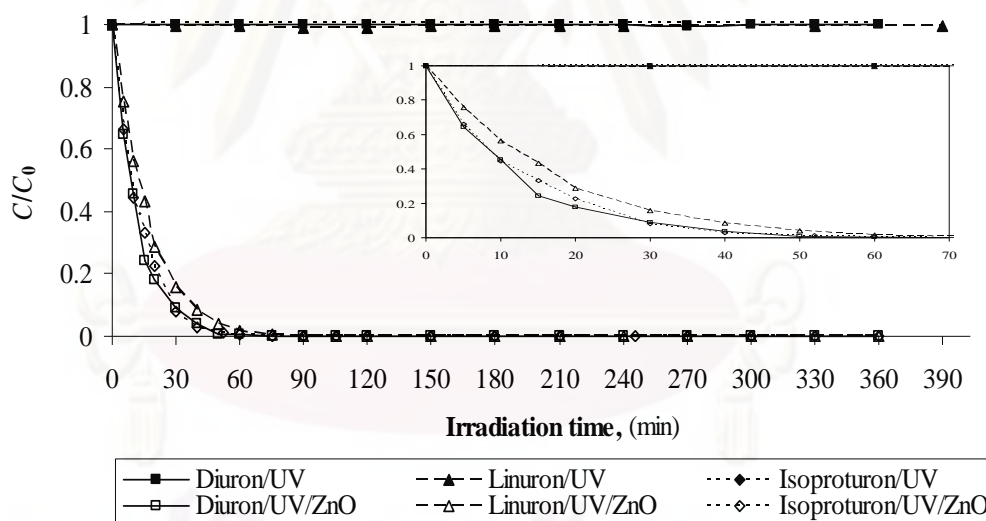
Figure 4.1. Effect of UV light and ZnO on photocatalytic degradation of phenylurea herbicides at the initial concentration of 10 ppm.

The focus here is on fundamental photocatalytic parameters and therefore the photolytic effect will be discussed from this point of view. Figure 4.1 shows the results of several degradation experiments including self-degradation of the herbicides under UV-light without catalyst. The experiments were performed in order to find out

the decomposition rate without the catalyst (ZnO). No detectable degradation of diuron was observed, which is similar to the result reported for self-degradation in the dark at room temperature indicating that hydrolysis of diuron can be neglected (Madani et al., 2006). Although organic pollutants absorb light over a wide range of wavelengths, such natural photodegradation is usually very slow. On the other hand, it can be seen from the figure that, in the presence of both ZnO and UV light, 100% removal of the herbicides could be achieved within short period of time. These experiments have demonstrated that both UV light and a photocatalyst, such as ZnO, are needed for the effective degradation of the herbicides.

4.2 Effect of External Mass Transfer of Herbicide from Bulk Liquid to Catalyst Surface

The effect of the external mass transfer of the herbicide from bulk liquid to the surface of ZnO on the photocatalytic degradation was studied by varying the stirring speed from 100, 150, 200 and 250 rpm, respectively. For this parameter, the photodegradation was conducted using the initial phenylurea herbicide concentration of about 10 ppm. The amount of ZnO powder added into the solution was in the ratio of 2 mg of ZnO to 10 ml of solution. The results are illustrated in Figure 4.2.
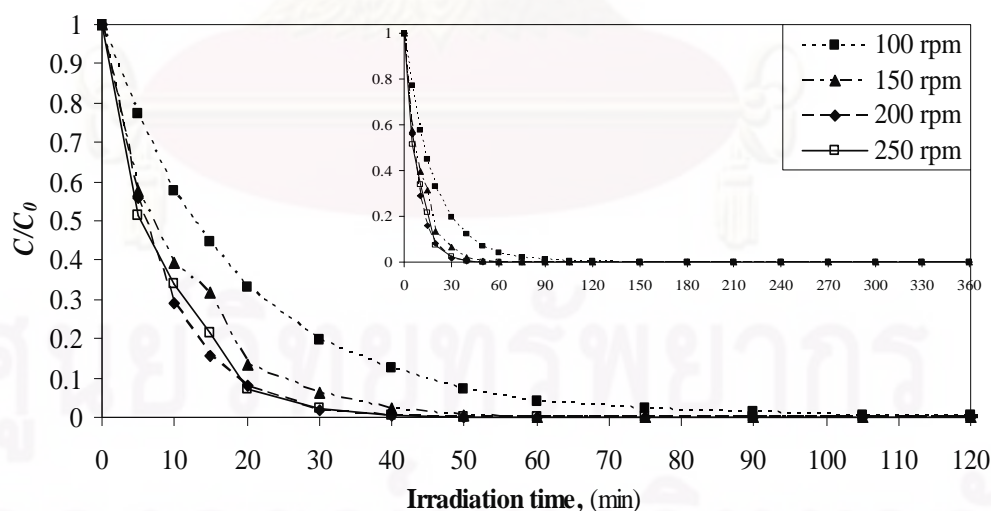

Figure 4.2. Effect of the external mass transfer of the herbicide from bulk liquid to the surface of ZnO on photodegradation of diuron.

It can be observed that each condition can result in 100% degradation of the herbicide existing in the solution. The results indicate that the extent of the photodegradation is increased with the increasing stirring speed up to 200 rpm, after which the increase in rpm does not significantly affect the degradation. It is indicated that the stirring speed slower than 200 rpm results in mass transfer resistance for the diffusion of the herbicide molecule to the catalyst surface. Therefore, in all experiments in this research, the photodegradation was conducted under the stirring speed of 200 rpm to avoid the effect of external mass transfer.

4.3 Effect of Catalyst Loading

The effect of catalyst loading on the degradation of phenylurea herbicides was investigated using ZnO in the range of 0.5 to 3.5 mg in 10 ml solution. The results are shown in Figure 4.3. Experiments performed with different concentration of ZnO have shown that the photodegradation efficiency is increased with an increase in ZnO loading. The data shown in Figure 4.3 were fitted against the Langmuir- Hinshelwood kinetic model, using multi-variables linear regression technique. The results are shown in Table 4.1 and Figure 4.4. It can be seen from Figure 4.4 that the trend of reaction rate constant of the photodegradation of each phenylurea herbicide is increased with increasing catalyst loading. It can be explained that increasing catalyst loading bring about the increase in total active surface area, hence the degradation efficiency. The adsorption constant of the photocatalytic degradation of phenylurea herbicides with various catalyst loading are listed in Table 4.1. It is shown that the adsorption constants are quite similar for all experiments.
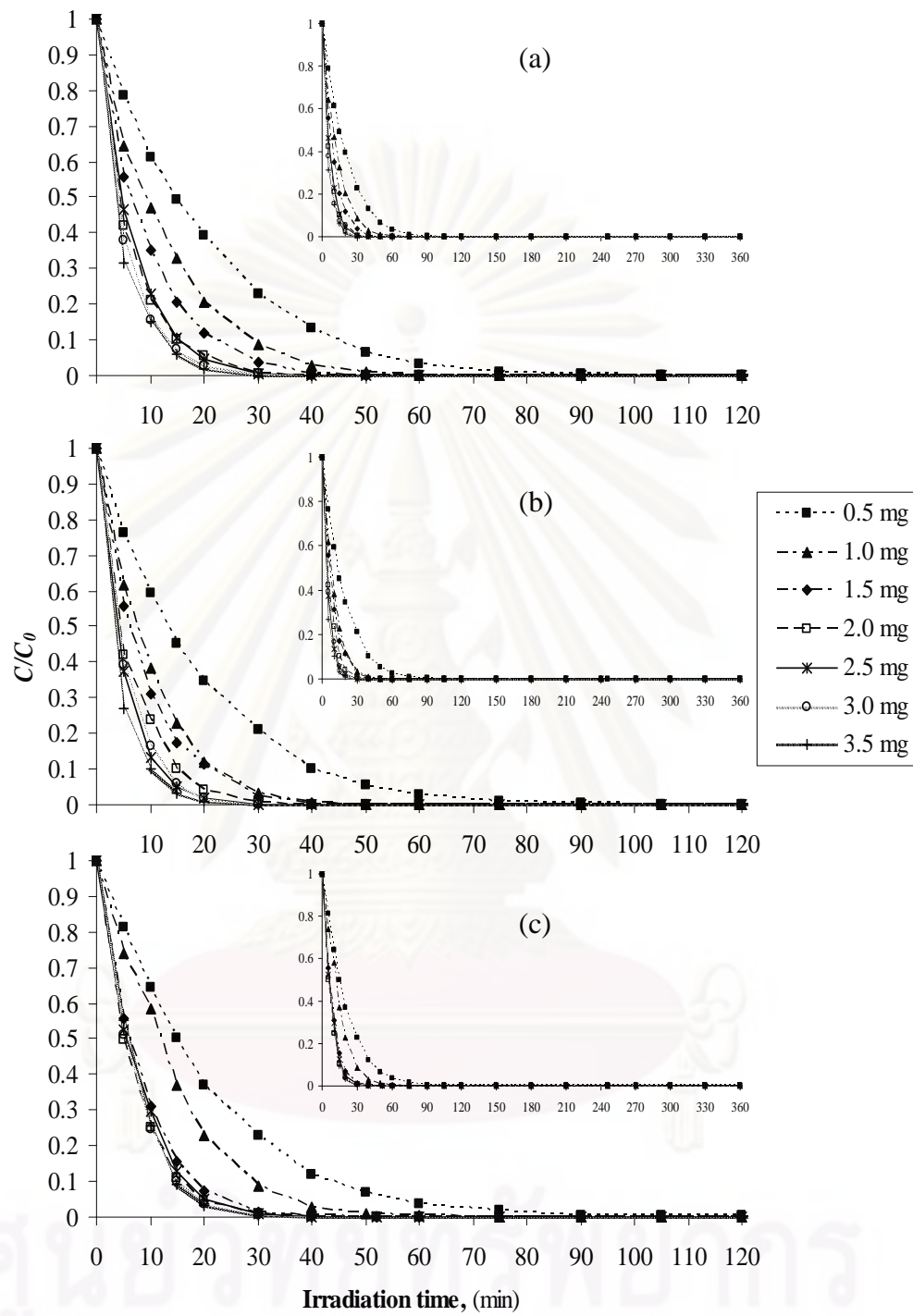
Figure 4.3. Effect of amount of ZnO on photodegradation of diuron (a), linuron (b) and isoproturon (c), without pH adjustment, using initial herbicide concentration of 10 ppm.

Table 4.1. The reaction rate constants (k_r) and the adsorption constant (K_{ads}) for the photocatalytic degradation of phenylurea herbicides using various catalyst loading.

mg ZnO:10ml solution		k_r, (ppm/min)	K_{ads}, (ppm^{-1})	R^2
0.5	Diuron	1.1092	0.0609	0.9946
	Linuron	1.5217	0.0447	0.9954
	Isoproturon	1.1415	0.0564	0.9996
1.0	Diuron	1.1898	0.0933	0.9979
	Linuron	2.1586	0.0607	0.9994
	Isoproturon	0.8635	0.1416	0.9947
1.5	Diuron	1.1656	0.1357	0.9967
	Linuron	3.0323	0.0450	0.9928
	Isoproturon	2.4252	0.0645	0.9992
2.0	Diuron	2.5746	0.0752	0.9944
	Linuron	4.9599	0.0355	0.9989
	Isoproturon	3.5309	0.0495	0.9998
2.5	Diuron	2.3861	0.0830	0.9983
	Linuron	5.3744	0.0422	0.9980
	Isoproturon	2.0200	0.0934	0.9988
3.0	Diuron	4.5400	0.0459	0.9978
	Linuron	6.0980	0.0346	0.9990
	Isoproturon	2.2401	0.0890	0.9995
3.5	Diuron	4.1918	0.0549	0.9932
	Linuron	19.9942	0.0124	0.9959
	Isoproturon	2.2401	0.0890	0.9995

Figure 4.4. Reaction rate constant (k_r) for the degradation of diuron, linuron and isoproturon using various catalyst loading.
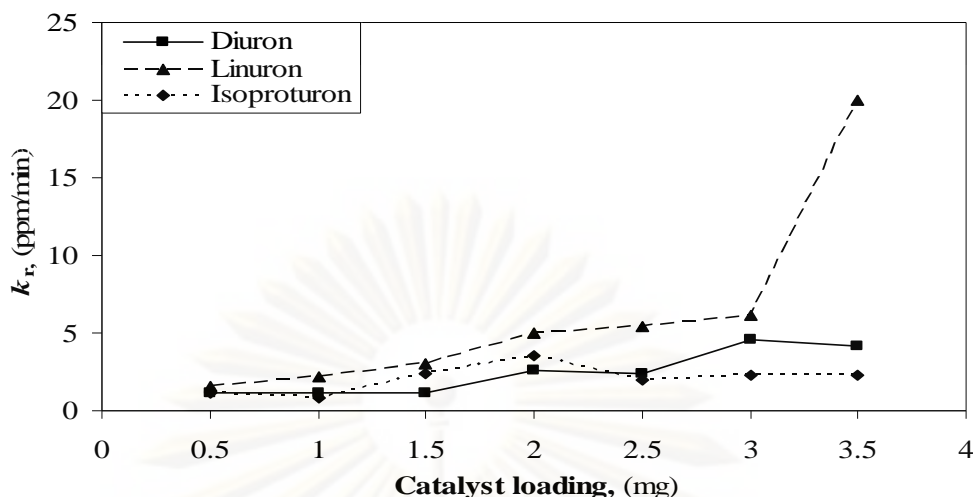
For the amount of ZnO up to 2 mg per 10 ml of the solution, the degradation reaches almost 100% of the initial concentration within about 40 min. At higher catalyst loading, degradation reaches the level of about 100% within roughly the same period of time, as shown in Figure 4.5. This observation can be explained in term of availability of active sites on the catalyst surface and the penetration of UV light into the suspension. The total active surface area increases with increasing catalyst dosage. At the same time, when the catalyst loading is high, UV light penetration is decreased due to an increase in the turbidity of the suspension, which decreases the photoactivated volume of the suspension. Moreover, it is difficult to maintain the suspension homogenous at high catalyst loading due to particles agglomeration, which also decreases the number of active sites. In any given application, this optimum catalyst mass has to be found in order to avoid excess catalyst and ensure total absorption of efficient photons. However, it does not seem to be necessary to test a very wide range of ZnO loading. Usually, the initial kinetic increases quickly with the amount of ZnO. At higher catalyst content, the rate of the photocatalytic reaction decreases. When the optimum point is found, it is not really necessary to continue checking the effect of catalyst loading any higher level because no more useful information is going to be obtained.
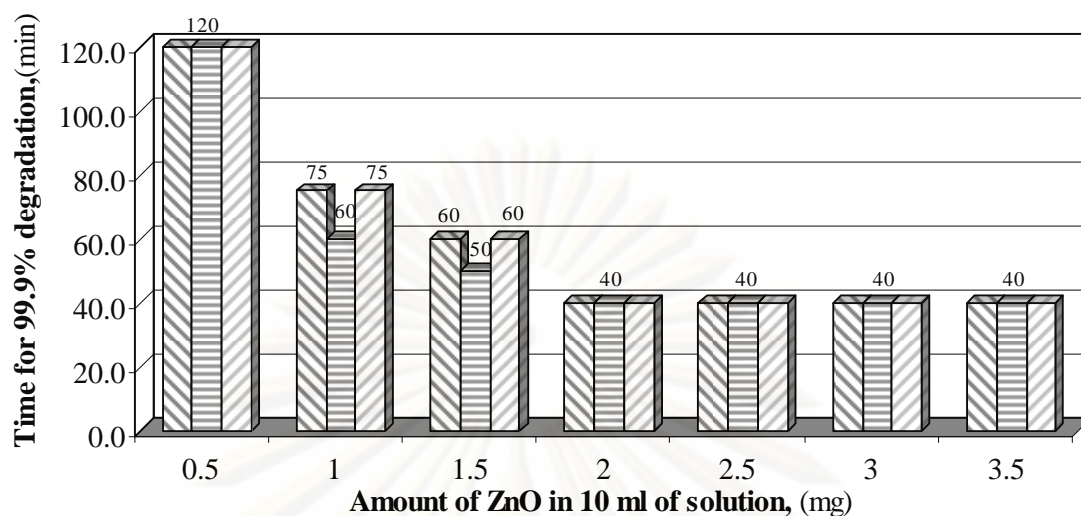
Figure 4.5. Effect of catalyst loading on the time of photodegradation that reached
99.9% of initial concentration, when the initial concentration of herbicides
is 10 ppm: ▨ Diuron, ▨ Linuron, ▨ Isoproturon.

4.4 Effect of Initial Herbicide Concentration

The effect of initial concentration of aqueous phenylurea herbicide solution on
the photocatalytic degradation was studied by varying the initial concentration from 1,
5, and 10 ppm, respectively. For this parameter, the amount of ZnO powder added
into the solution was fixed at the ratio of 1 mg of ZnO to 10 ml of solution. The
results are illustrated in Figure 4.6.
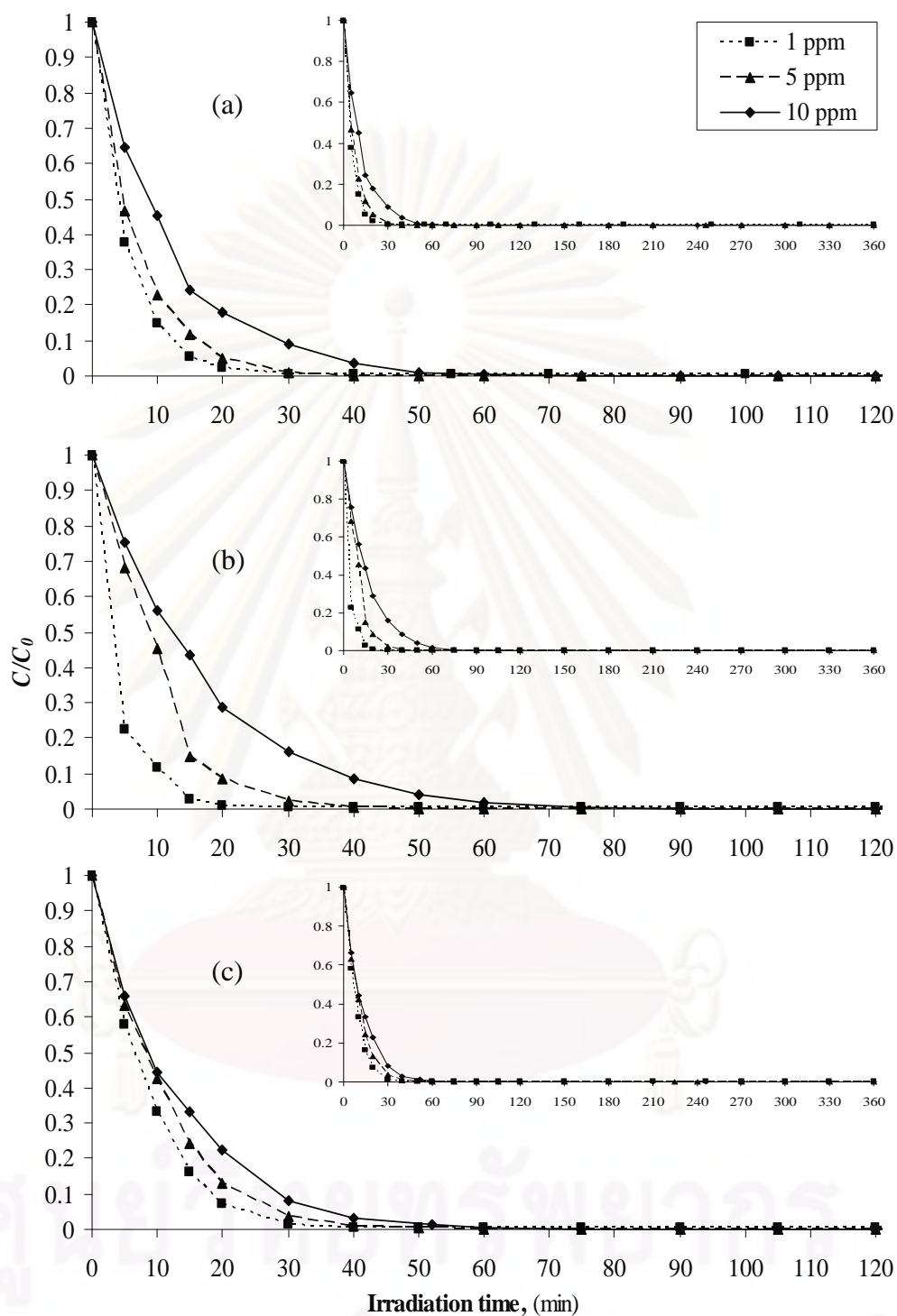
Figure 4.6. Effect of initial herbicide concentration on photodegradation efficiency of
diuron (a), linuron (b) and isoproturon (c). The reaction was conducted
using 1 mg of ZnO per 10 ml of solution, without pH adjustment.

It can be observed that each herbicide is fully degraded within less than 40 min when the initial herbicide concentration is 1 or 5 ppm. In the case of the initial concentration of 10 ppm, the irradiation time of 60 min is sufficient to degrade almost 100% of the herbicide existing in the solution. It can be seen from Figure 4.6 that the degradation rate of each herbicide in high concentration is only slightly less than that observed in low concentration. The increasing initial herbicide concentration can be related to the faster consumption of photogenerated hydroxyl radicals by higher concentrated organic molecules. Then, the photostationary concentration of hydroxyl radical is decreased. Consequently, lower concentration of hydroxyl radicals reduces a probability of the recombination of hydroxyl radicals with electrons trapped on surface of zinc oxide particles (Macounova, 2003).

Moreover, it is shown that the degradation of isoproturon is relatively fast. Almost complete disappearance of isoproturon is observed in the shortest period of irradiation time. The difference in the degradation rate between isoproturon and diuron can be discussed from the fact that an initial degradation rate is directly related to the electron-donating or electron-withdrawing character of different functional group attaching to the aromatic ring of herbicides, which can alter the reactivity of the aromatic ring with the OH radical. The OH radical generated from the interaction between photoexcited electron/hole and water as previously mentioned is very reactive in oxidation of organic substances. Isoproturon is more active than diuron as witnessed from shorter half-life in nature. This is probably due to the presence of the $CH(CH_3)_2$ group in isoproturon, which is benzene ring activating group (Parra, 2002). On the contrary, the presence of halogen group in diuron causes the aromatic to be more stable and results in lower reactivity of diuron toward the decomposition, comparing to isoproturon.

For the investigation on the photodegradation results of linuron, it can be seen that linuron disappearance rate is generally lower than diuron and isoproturon. Linuron exhibits slow degradation rate because the stability of linuron is higher than diuron. Chlorine group consisting in the structure of both diuron and linuron is an aromatic ring deactivating group, while the alkyl group attaching to an aromatic ring in isoproturon has more reactive structure and tends to release electron easier (Graham, 1996). In the other words, the electrophilic attack of the OH radical to

isoproturon is easier than diuron and linuron. For this reason it can be explained why the degradation rate of diuron and linuron is less than that of isoproturon. Between diuron and linuron, the $-NHCON(CH_3)_2$ group attaching to the aromatic ring of diuron and $-NHCON(OCH_3)(CH_3)$ group in linuron are not so different that it can cause significantly difference in the electron-releasing habit of these groups. Instead, the steric effect of organic substance is employed to explain the difference in the degradation of these two compounds. The $-NHCON(OCH_3)(CH_3)$ group in linuron is more difficult to be attacked by OH radical. Nevertheless, further investigation is needed.

Table 4.2 shows the calculated reaction rate constants (k_r) and the calculated adsorption constant (K_{ads}) of the photocatalytic degradation of phenylurea herbicides for the investigation of initial herbicide concentration effect, based on the Langmuir-Hinshelwood kinetic model. However, the model fitting for the case of the 1 ppm of linuron failed, which indicates that the reaction does not follow the mechanism described by the Langmuir- Hinshelwood kinetic model. For other cases, the calculated adsorption constants are quite similar to that observed for the effect of catalyst loading.

Table 4.2. The reaction rate constants (k_r) and the adsorption constant (K_{ads}) for the photocatalytic degradation of phenylurea herbicides for the investigation of initial herbicide concentration effect.

Initial Concentration, (ppm)		k_r, (ppm/min)	K_{ads}, (ppm^{-1})	R^2
1	Diuron	5.6628	0.0347	0.9998
	Linuron	-	-	-
	Isoproturon	0.1791	0.9430	0.9991
5	Diuron	1.7579	0.0983	0.9976
	Linuron	1.1539	0.1351	0.9928
	Isoproturon	1.2169	0.1032	0.9978
10	Diuron	3.4295	0.0274	0.9949
	Linuron	5.4544	0.0122	0.9988
	Isoproturon	3.0527	0.0307	0.9955

Then, the concentrations of the herbicides are recalculated, using the Langmuir- Hinshelwood kinetic model. The fitted results for the photodegradation reaction are compared with the experimental data, as shown in Figure 4.7-4.9.

Figure 4.7. Comparison between experimental data (■) and calculated results from the Langmuir-Hishelwood model (———) for the photodegradation of diuron, using the initial diuron concentration of : (a) 1 ppm, (b) 5 ppm and (c) 10 ppm. The reaction was conducted using 1 mg of ZnO per 10 ml of solution, without pH adjustment.
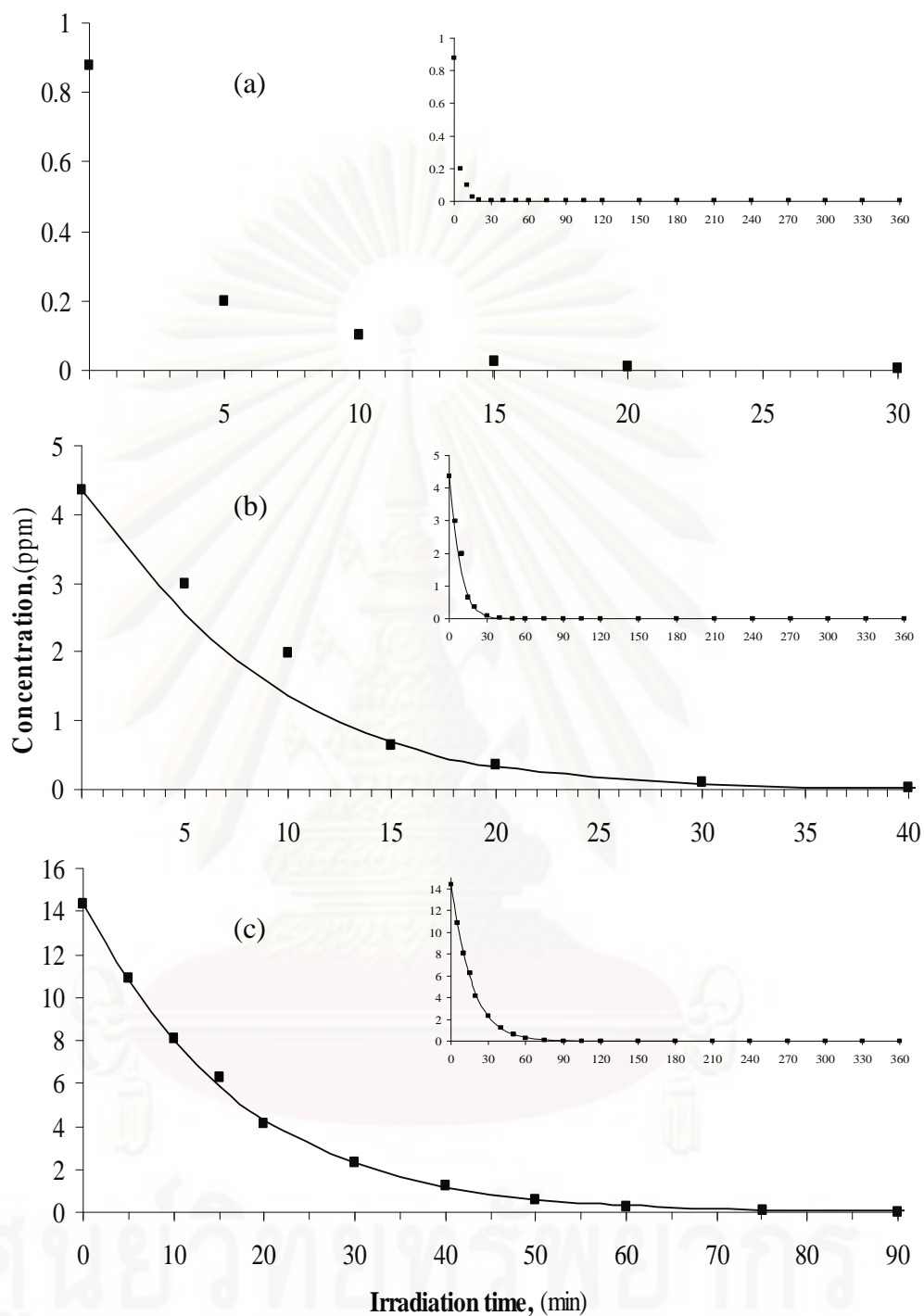
Figure 4.8. Comparison between experimental data (■) and calculated results from the Langmuir-Hishelwood model (———) for the photodegradation of linuron, using the initial linuron concentration of : (a) 1 ppm, (b) 5 ppm and (c) 10 ppm. The reaction was conducted using 1 mg of ZnO per 10 ml of solution, without pH adjustment.
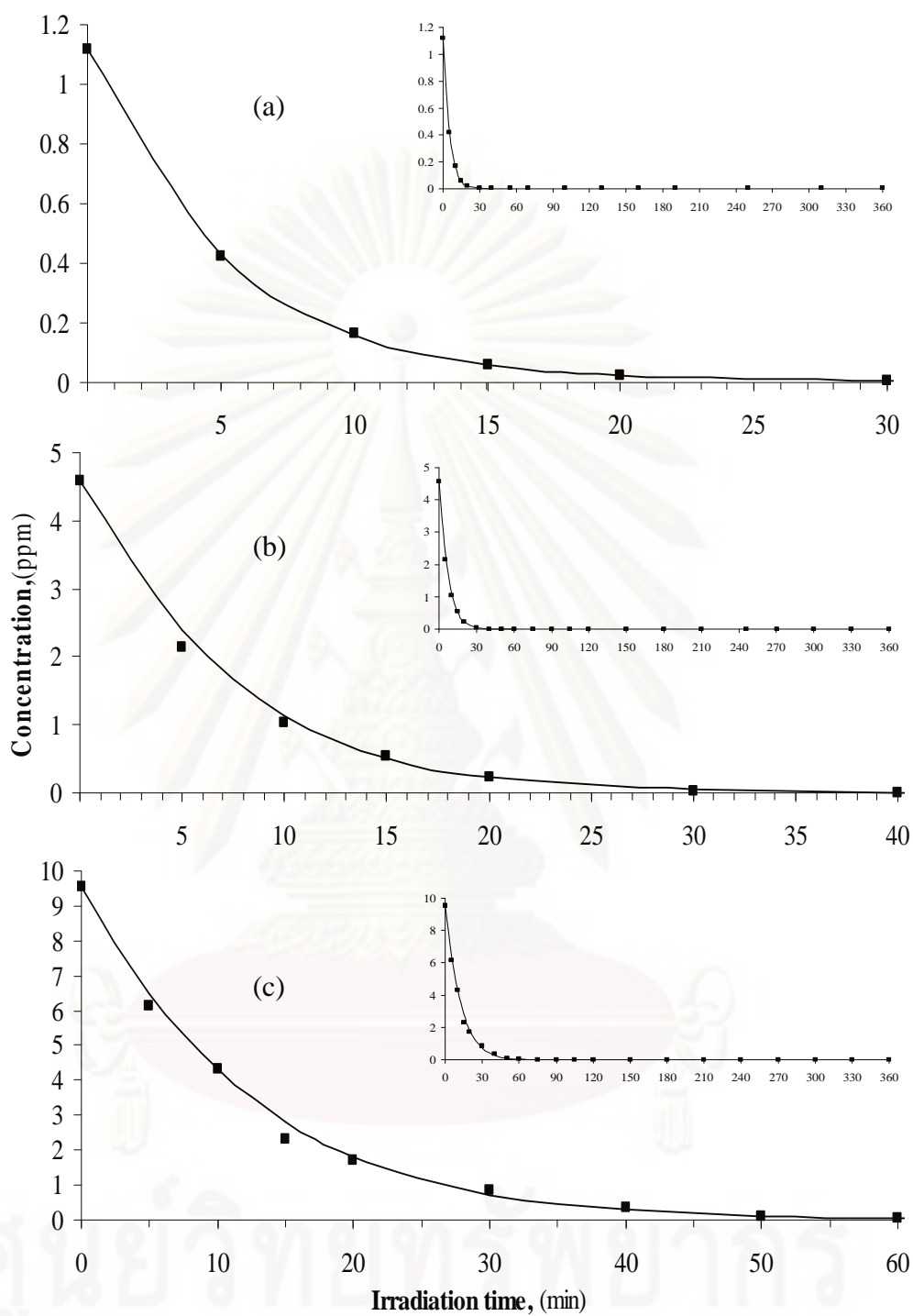
Figure 4.9. Comparison between experimental data (■) and calculated results from the Langmuir-Hishelwood model (——) for the photodegradation of isoproturon, using the initial isoproturon concentration of : (a) 1 ppm, (b) 5 ppm and (c) 10 ppm. The reaction was conducted using 1 mg of ZnO per 10 ml of solution, without pH adjustment.
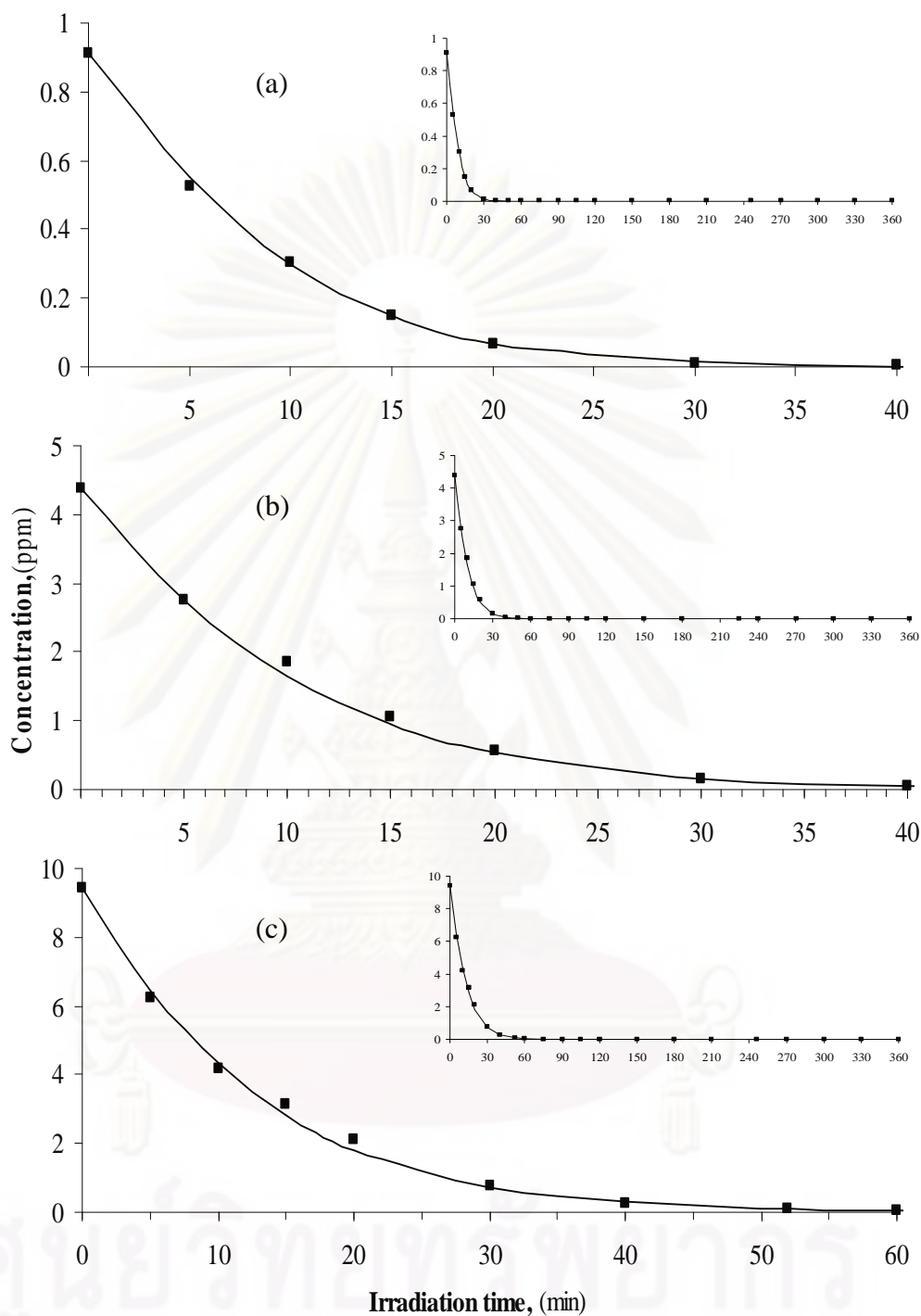
It can be observed from Figure 4.7-4.9 that the degradation can be well represented by the Langmuir- Hinshelwood model. The degradation result of each phenylurea herbicide predicted by the model is quite similar to the actual experiment data.

As indicated by the results, the rate of degradation depends upon the initial concentration. At high concentration of phenylurea herbicides, greater amount of phenylurea herbicides adsorb on the surface of ZnO, which can bring about the decrease in the number of available active sites on the catalyst surface. Moreover, as the concentration of the phenylurea herbicide solution is increased, the photons from the irradiated UV light are intercepted by the herbicide molecules in the solution before they can reach the catalyst surface, hence decreases the photoexcitation of the catalyst by photons. Consequently, the degradation efficiency is reduced.

4.5 Effect of pH of the Solution

The effect of pH of the aqueous phenylurea herbicide solution on the photocatalytic degradation was studied. The pH value of the herbicide solution was adjusted to the desired value in the range of 3 to 11 by using either dilute H_2SO_4 or NaOH. For the study of this parameter, the amount of ZnO powder added into the solution was fixed at the ratio of 1 mg of ZnO to 10 ml of solution.

The pH can be one of the most important parameters for the photocatalytic process. So, it was of interest to study its influence on the photocatalytic degradation of phenylurea herbicide. In Figure 4.11-4.16 and Table 4.4, the extent of photodegradation of each phenylurea herbicide is reported in the pH range of 3–11. The pH of the solution is adjusted before irradiation and it is not controlled during the course of the reaction. Table 4.3 shows the pH value of the herbicide solution during the experiment. It can be observed that the pH of the solution during the experiment do not change much. The results for the degradation are illustrated in Figure 4.11.

Table 4.3. The pH value of the herbicide solution during the photocatalytic degradation reaction of phenylurea herbicides.

| pH of solution before adding ZnO		pH of the solution at different irradiation time				Mean value and deviation
		0 min	60 min	120 min	360 min	
3.0	Diuron	5.11	5.67	6.04	5.68	5.58±0.465 (8.34%)
	Linuron	5.65	6.07	5.14	6.02	5.61±0.465 (8.29%)
	Isoproturon	5.71	5.77	5.43	5.98	5.71±0.275 (4.82%)
4.0	Diuron	6.38	6.88	6.13	6.51	6.51±0.375 (5.76%)
	Linuron	6.15	6.87	6.21	6.45	6.51±0.360 (5.53%)
	Isoproturon	6.23	6.17	6.42	6.75	6.46±0.290 (4.49%)
6.0	Diuron	6.37	5.38	5.73	5.79	5.88±0.495 (8.43%)
	Linuron	5.68	5.87	6.33	5.92	6.01±0.325 (5.41%)
	Isoproturon	6.22	5.94	5.23	5.97	5.73±0.495 (8.64%)
9.0	Diuron	7.04	6.61	6.27	6.19	6.62±0.425 (6.42%)
	Linuron	6.64	6.17	7.06	6.36	6.62±0.445 (6.73%)
	Isoproturon	6.98	6.74	6.02	6.99	6.51±0.485 (7.46%)
11.0	Diuron	11.26	11.11	11.23	10.89	11.08±0.185 (1.67%)
	Linuron	11.39	11.48	11.05	11.07	11.27±0.215 (1.91%)
	Isoproturon	10.80	11.36	11.12	11.19	11.08±0.280 (2.53%)
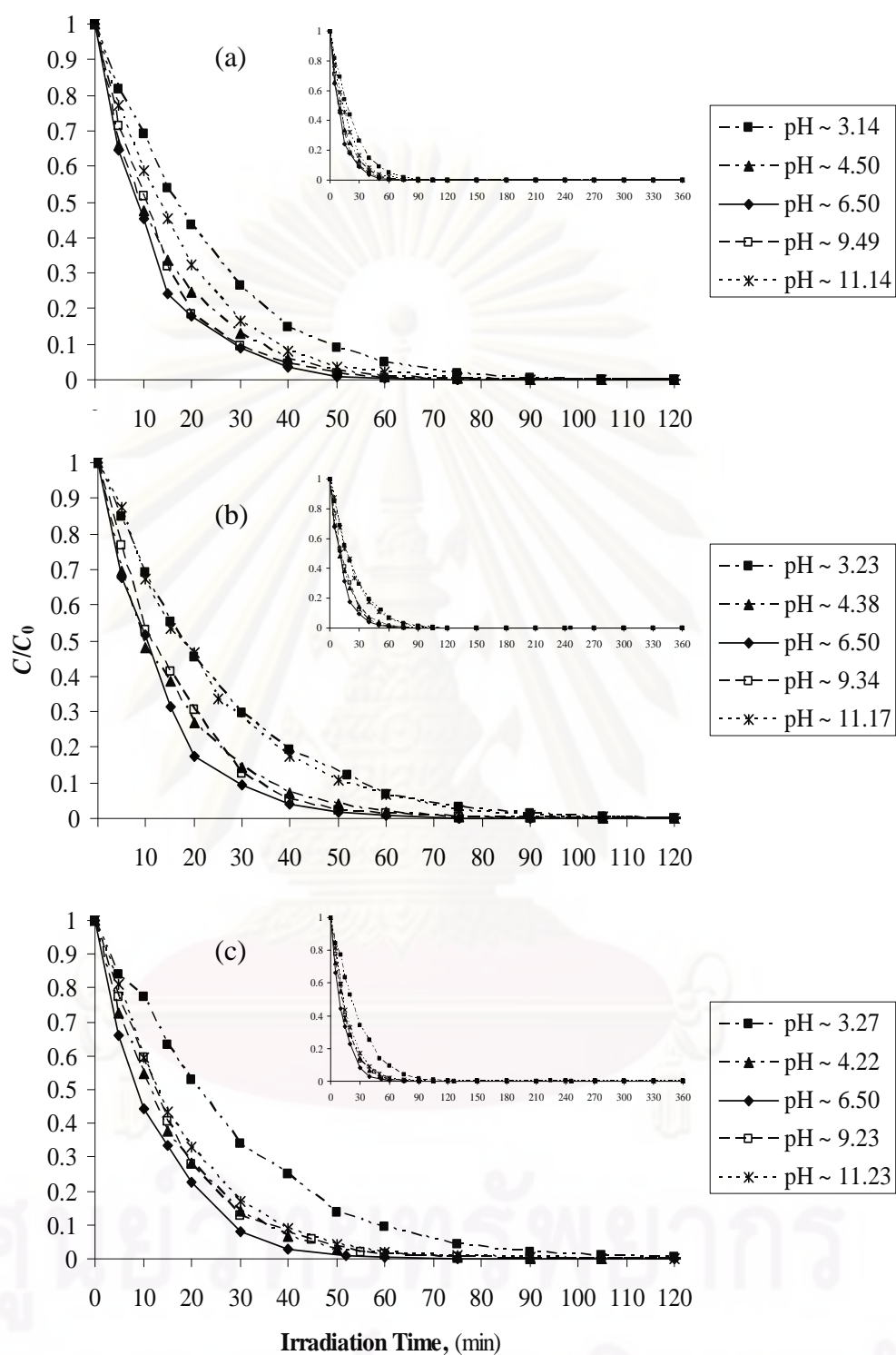
Figure 4.11. Effect of pH of the solution on photodegradation efficiency of
diuron (a), linuron (b) and isoproturon (c). The reaction was conducted
using 1 mg of ZnO per 10 ml of solution.

The results indicate that the extent of photodegradation is increased with increasing pH up to pH 6, beyond which the degradation decreases. Generally, the effect of pH on organic degradation assisted by the semiconductor oxides has been related to the establishment of acid–base equilibria governing the surface chemistry of metal oxides in water (M.A. Fox et al., 1993; T.C.-K. Yang, et al., 2001; K. Tanaka et al., 2000; B. Zielinska et al., 2001), as shown in the following reactions.

$$ZnOH_2^+ \quad \Leftrightarrow \quad ZnOH \; + \; H^+ \qquad [pKa_1] \tag{4.1}$$

$$ZnOH \; + \; OH^- \quad \Leftrightarrow \quad ZnO^- \; + \; H_2O \qquad [pKa_2] \tag{4.2}$$

The pH at which the surface of an oxide is uncharged is defined as the point of zero charge (pH_{pzc}). From the preliminary experiments, it was found that the point of zero charge for ZnO is about 7.5. The effect of pH on the photocatalytic performance can thus be explained in terms of electrostatic interaction between the catalyst surface and the target substrate. Such interaction can be expected to affect the encounter probability of the hydroxyl radical with the herbicide. It follows that the overall reaction would be enhanced or hindered depending on whether attractive or repulsive forces prevail, respectively. Each herbicide is negatively charged above its pKa, whereas catalysts are positively charged below pH~7.5. As expected, optimal conditions were found at $pK_a^{herbicide} < pH < pH_{pzc}^{ZnO}$ at which the positively charged ZnO and negatively charged herbicide molecules should readily attract each other. Unfortunately, the mere electrostatic argument is unable to exhaustively account for the relative photocatalytic behavior as a function of pH. Other concomitant effect can come into play. For example ZnO can undergo photocorrosion through self-oxidation (Eq. 4.3) (M.A. Fox et al., 1993 and B. Neppolian et al., 2002):

$$ZnO \; + \; 2h^+ \quad \rightarrow \quad Zn^{2+} \; + \; 0.5O_2 \tag{4.3}$$
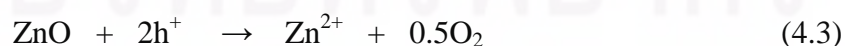
In particular, ZnO powder exhibit tendency to dissolve with decreasing the pH (Eq. 4.4) (N. Daneshvar et al., 2004):

$$ZnO \; + \; 2H^+ \quad \rightarrow \quad Zn^{2+} \; + \; H_2O \tag{4.4}$$
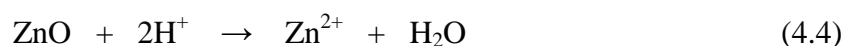
In a strongly alkaline environment, ZnO can undergo dissolution according to

$$ZnO \ + \ H_2O \ + \ 2OH^- \ \rightarrow \ Zn(OH)_4{}^{2-} \qquad (4.5)$$
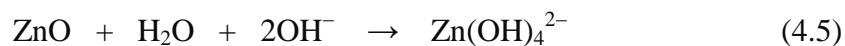
Moreover, the possible formation of photocatalytically inert $Zn(OH)_2$ surface layers upon UV irradiation (Eq. 4.6) has also to be considered in aqueous media (R. Comparelli et al., 2005):

$$2ZnO \ + \ 4H_2O \ + \ 4h^+ \ \rightarrow \ 2Zn(OH)_2 \ + \ O_2 \ + \ 4H^+ \qquad (4.6)$$
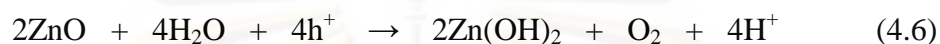
Therefore, the reduction of photocatalytic activity of ZnO at exceedingly low and high pH values can originate from either acidic/photochemical corrosion of the catalyst (Eq. 4.3 and 4.4), from alkaline dissolution (Eq. 4.5) and/or surface passivation with $Zn(OH)_2$ (Eq. 4.6).

Table 4.4 shows the calculated reaction rate constants (k_r) and the calculated adsorption constant (K_{ads}) of the photocatalytic degradation of phenylurea herbicides for the investigation of pH of the solution effect, based on the Langmuir-Hinshelwood kinetic model. The calculated adsorption constants are quite similar to that observed for the effect of catalyst loading and the effect of initial herbicide concentration.

Table 4.4. The reaction rate constants (k_r) and the adsorption constant (K_{ads}) of the photocatalytic degradation of phenylurea herbicides for the investigation of the effect of pH of the solution.

pH of solution		k_r, (ppm/min)	K_{ads}, (ppm^{-1})	R^2
3.0	Diuron	2.9682	0.0191	0.9846
	Linuron	0.7032	0.0807	0.9976
	Isoproturon	0.5606	0.0947	0.9975
4.0	Diuron	2.1958	0.0356	0.9975
	Linuron	2.2227	0.0324	0.9967
	Isoproturon	1.5019	0.0529	0.9995
6.0	Diuron	3.4295	0.0274	0.9949
	Linuron	1.4495	0.0552	0.9986
	Isoproturon	3.0527	0.0307	0.9955
9.0	Diuron	1.8604	0.0497	0.9974
	Linuron	1.0831	0.0870	0.9972
	Isoproturon	0.7280	0.1626	0.9966
11.0	Diuron	1.1678	0.0651	0.9992
	Linuron	0.7164	0.0845	0.9981
	Isoproturon	1.1678	0.0651	0.9992

Then, the concentrations of the herbicides are recalculated, using the Langmuir- Hinshelwood kinetic model. The fitted results for the photodegradation reaction are compared with the experimental data, as shown in Figure 4.12-4.16, from which it can be observed that the degradation can be well represented by the Langmuir-Hinshelwood model.
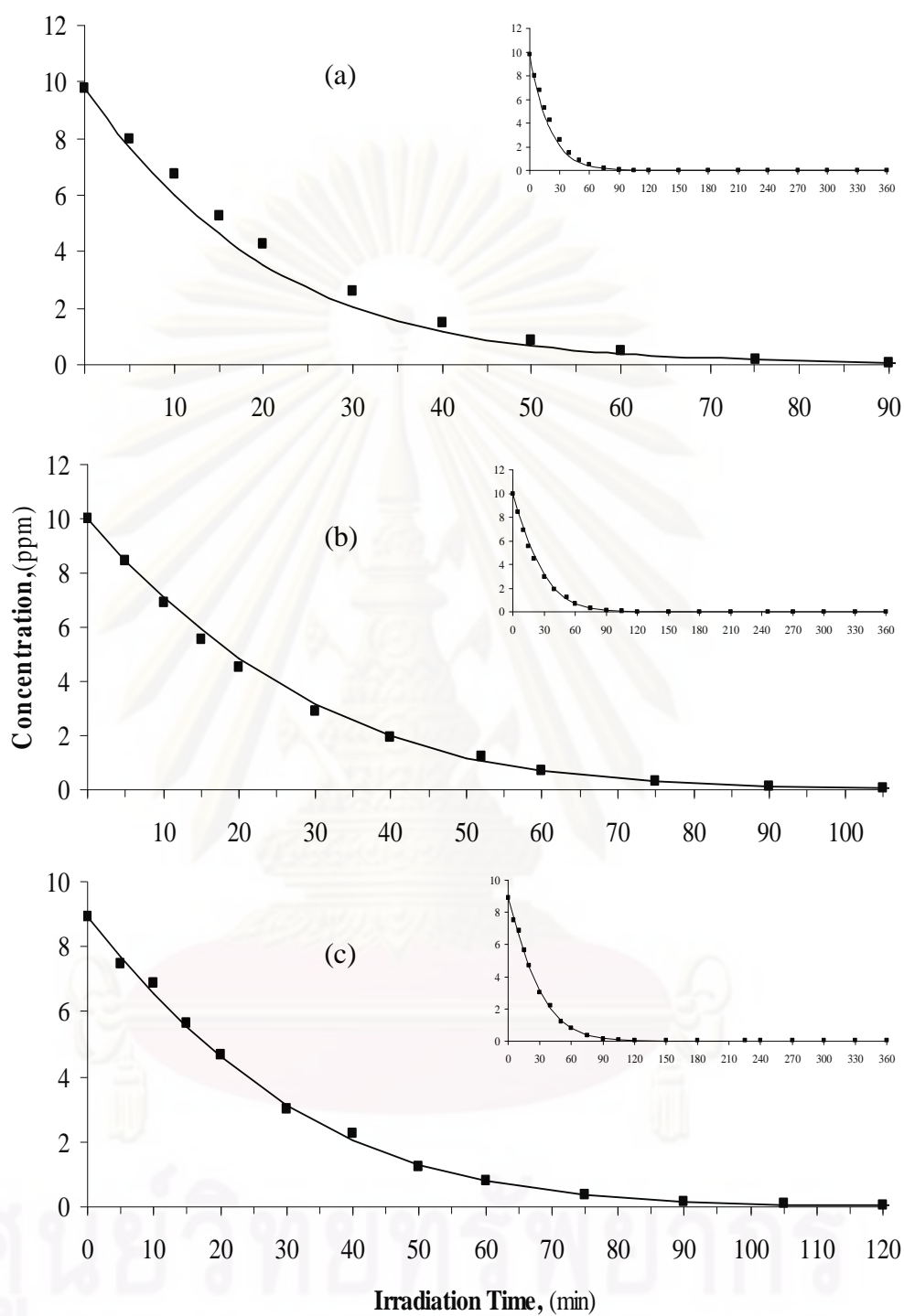
Figure 4.12. Comparison between experimental data (■) and calculated results from the Langmuir-Hishelwood model (——) for the photodegradation of diuron (a), linuron (b) and isoproturon (c), using the initial concentration of herbicides is 10 ppm. The reaction was conducted using 1 mg of ZnO per 10 ml of solution with initial pH of solution ~ 3.
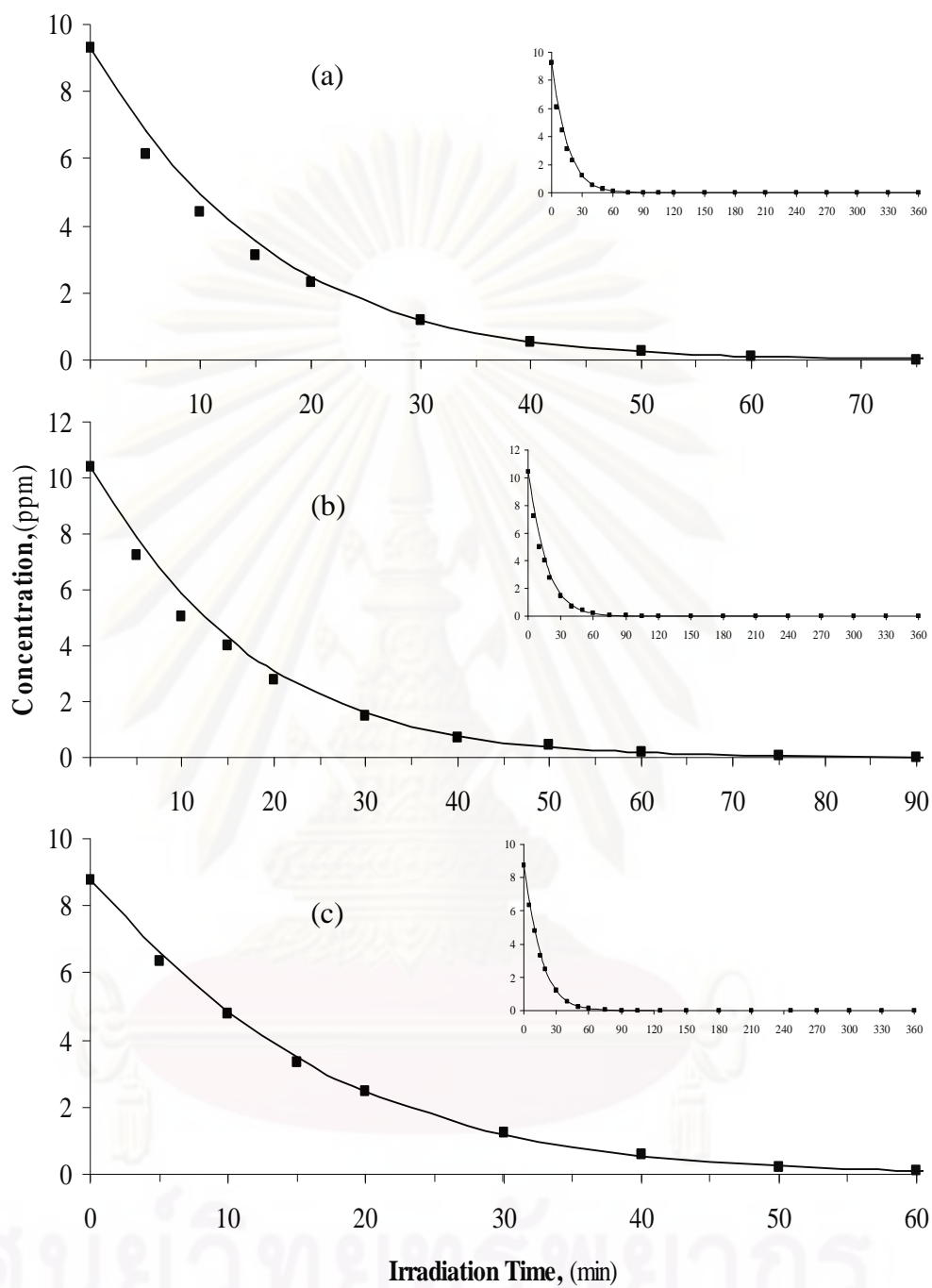
Figure 4.13. Comparison between experimental data (■) and calculated results from the Langmuir-Hishelwood model (——) for the photodegradation of diuron (a), linuron (b) and isoproturon (c), using the initial concentration of herbicides is 10 ppm. The reaction was conducted using 1 mg of ZnO per 10 ml of solution with initial pH of solution ~ 4.
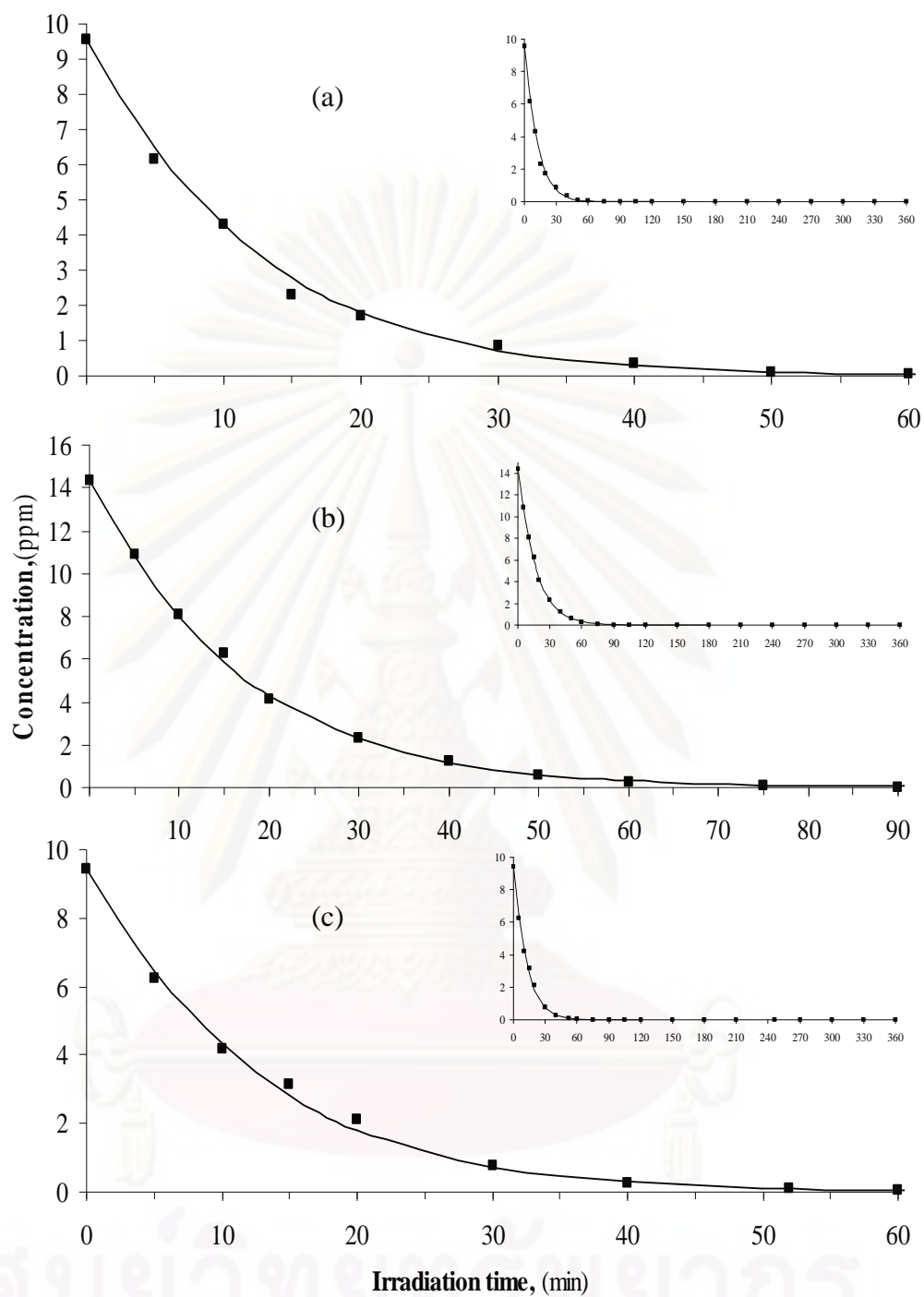
Figure 4.14. Comparison between experimental data (■) and calculated results from the Langmuir-Hishelwood model (——) for the photodegradation of diuron (a), linuron (b) and isoproturon (c), using the initial concentration of herbicides is 10 ppm. The reaction was conducted using 1 mg of ZnO per 10 ml of solution with initial pH of solution ~ 6.
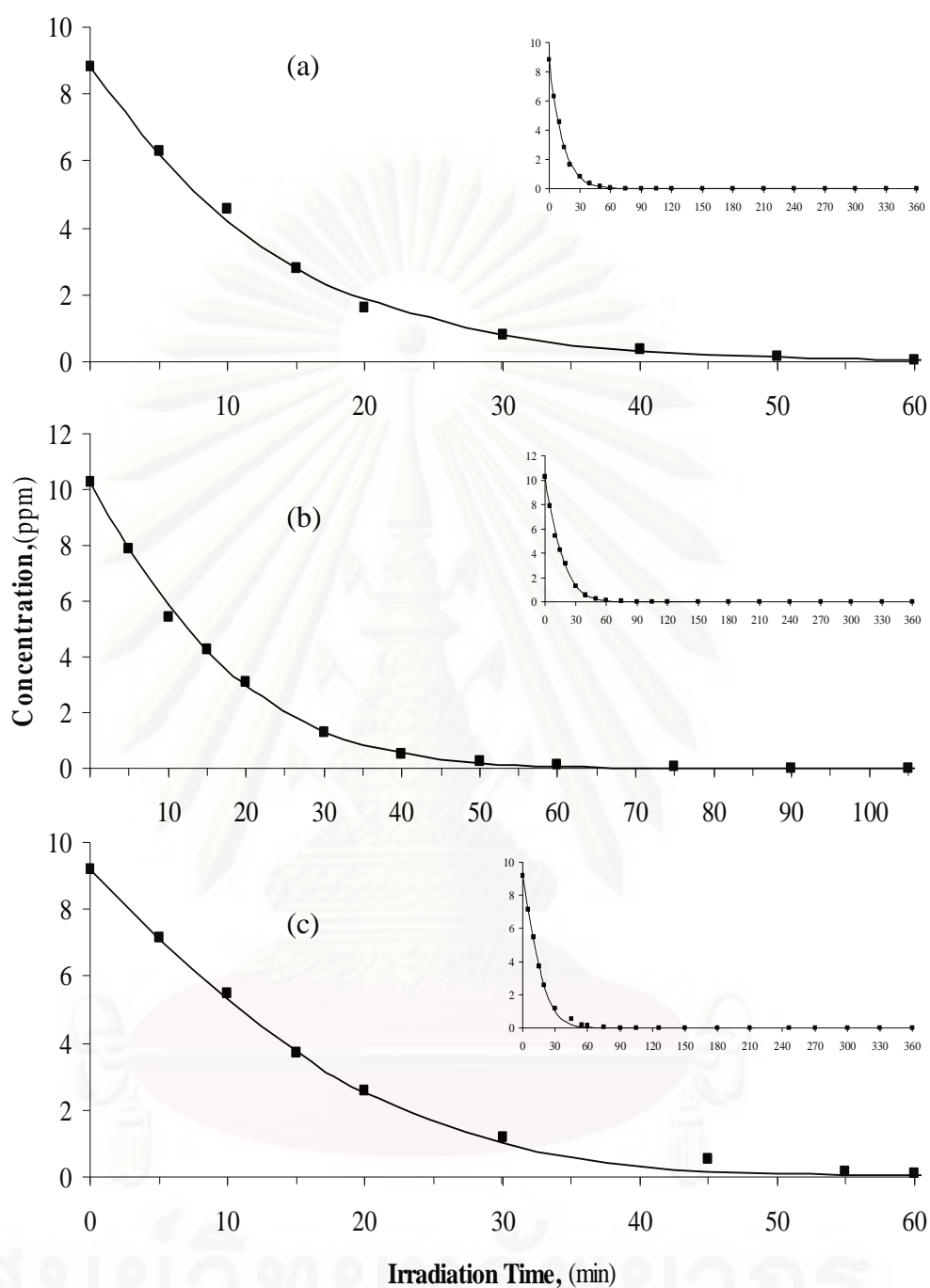
Figure 4.15. Comparison between experimental data (■) and calculated results from
the Langmuir-Hishelwood model (——) for the photodegradation of
diuron (a), linuron (b) and isoproturon (c), using the initial concentration
of herbicides is 10 ppm. The reaction was conducted using 1 mg of ZnO
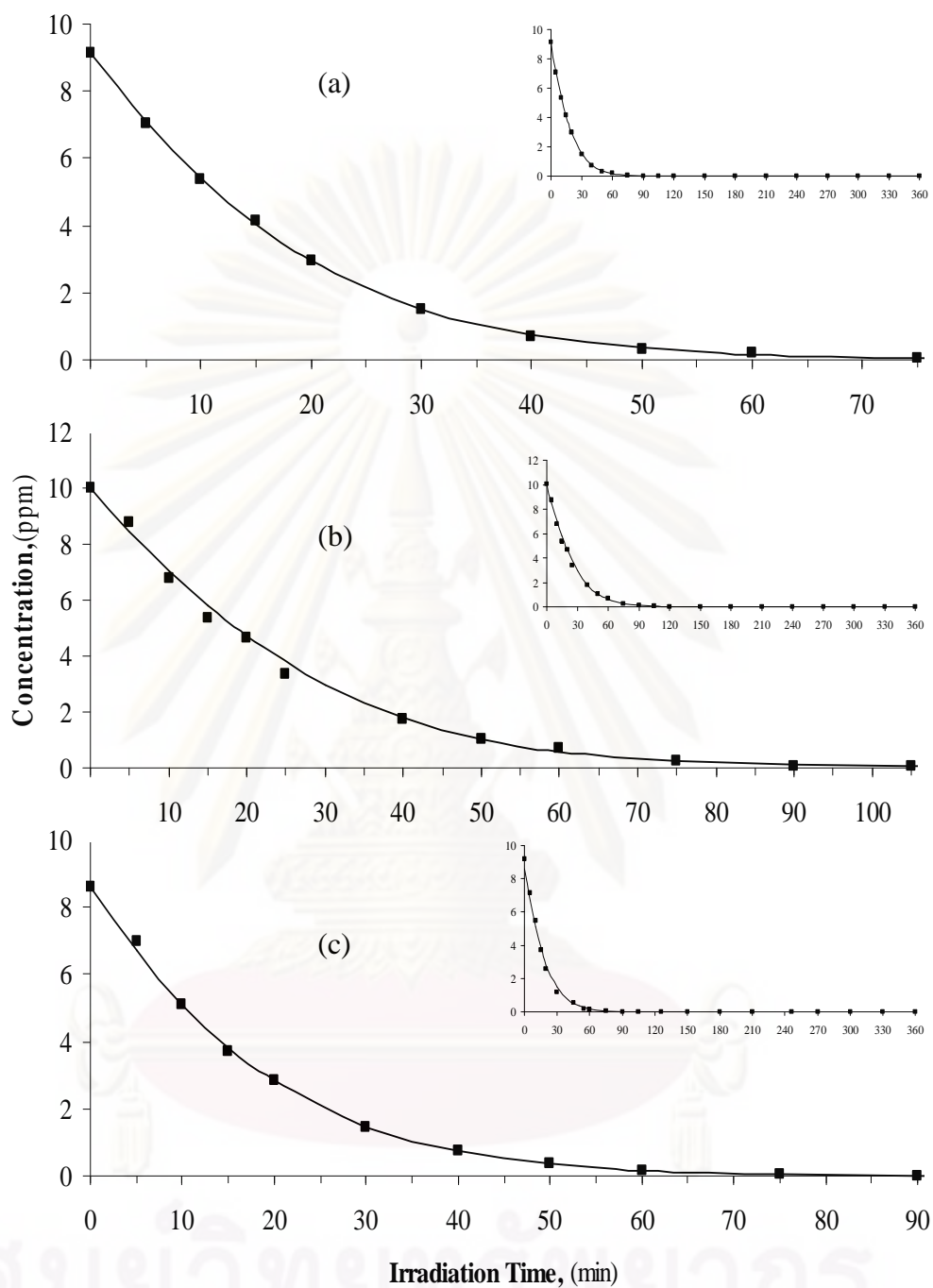per 10 ml of solution with initial pH of solution ~ 9.

Figure 4.16. Comparison between experimental data (■) and calculated results from the Langmuir-Hishelwood model (——) for the photodegradation of diuron (a), linuron (b) and isoproturon (c), using the initial concentration of herbicides is 10 ppm. The reaction was conducted using 1 mg of ZnO per 10 ml of solution with initial pH of solution ~ 11.

4.6 Effect of Temperature

The effect of temperature of the aqueous phenylurea herbicide solution on the photocatalytic degradation was studied at temperature in range 10 – 50 $^{\circ}$C. For this parameter, the initial phenylurea herbicide concentration was about 10 ppm and the amount of ZnO powder added into the solution was fixed at the ratio of 1 mg of ZnO to 10 ml of solution. The results are illustrated in Figure 4.17.

It can be observed that each herbicide could be fully degraded at all temperatures. Table 4.5 shows the calculated reaction rate constants (k_r) and the calculated adsorption constant (K_{ads}) of the photocatalytic degradation of phenylurea herbicides at different temperature, based on the Langmuir- Hinshelwood kinetic model. However, the model fitting for the case of the 50 $^{\circ}$C of linuron failed, which indicates that the reaction does not follow the mechanism described by the Langmuir-Hinshelwood kinetic model. For other cases, the calculated adsorption constants are quite similar to that observed for the effect of catalyst loading, the effect of initial herbicide concentration and the effect of pH of the solution.
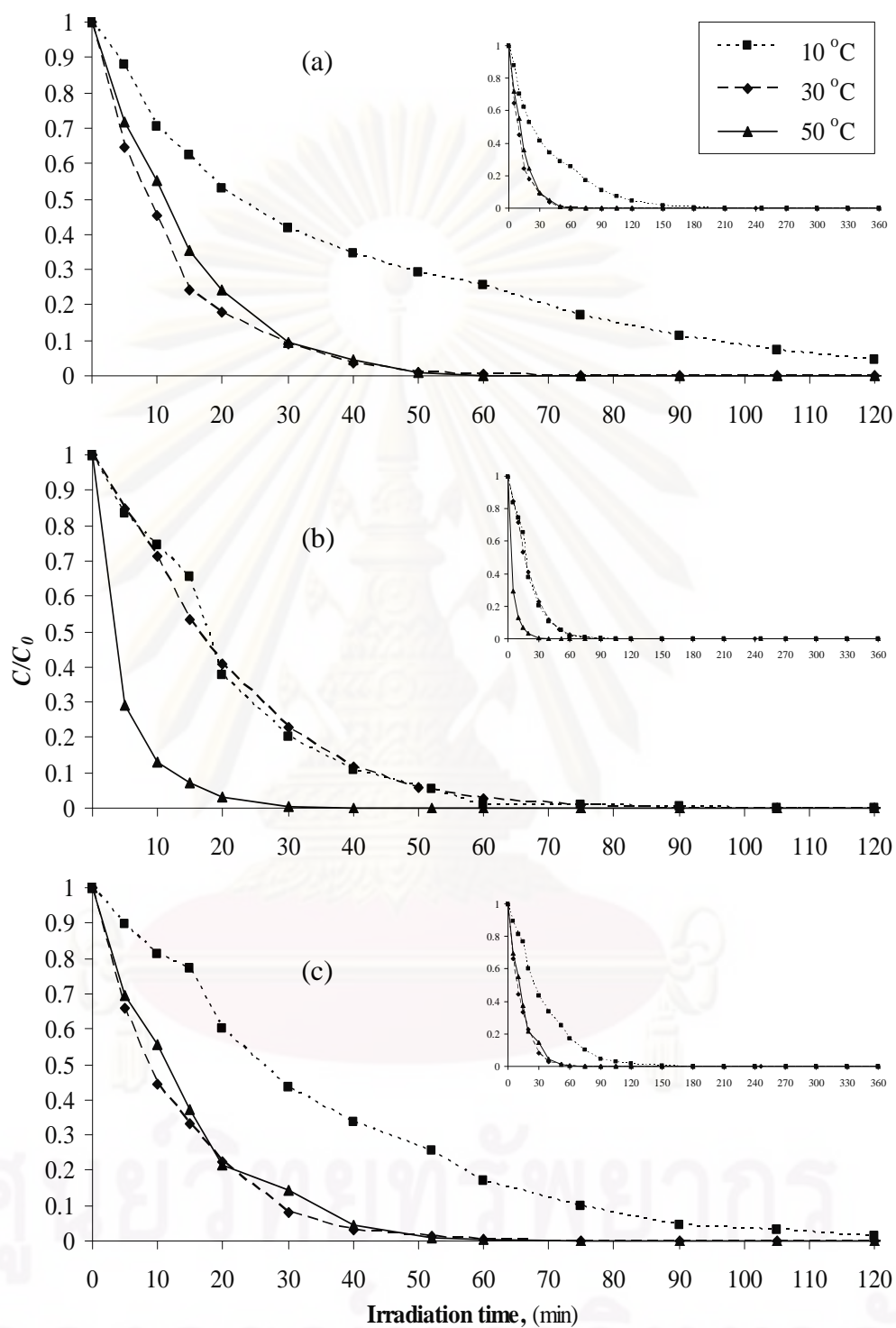
Figure 4.17. Effect of temperature on photodegradation of diuron (a), linuron (b) and isoproturon (c). The reaction was conducted using 1 mg of ZnO per 10 ml of solution, without pH adjustment.

Table 4.5. The reaction rate constants (k_r) and the adsorption constant (K_{ads}) for the photocatalytic degradation of phenylurea herbicides for the investigation of temperature effect.

Temperature, (°C)		k_r, (ppm/min)	K_{ads}, (ppm^{-1})	R^2
10	Diuron	0.7496	0.0375	0.9897
	Linuron	0.5668	0.1746	0.9691
	Isoproturon	0.3969	0.1136	0.9921
30	Diuron	3.4295	0.0274	0.9949
	Linuron	1.4495	0.0552	0.9986
	Isoproturon	3.0527	0.0307	0.9955
50	Diuron	0.7922	0.1553	0.9891
	Linuron	N/A	N/A	N/A
	Isoproturon	0.6700	0.1734	0.9876

Then, the concentrations of the herbicides are recalculated, using the Langmuir- Hinshelwood kinetic model. The fitted results for the photodegradation reaction are compared with the experimental data, as shown in Figure 4.18-4.20.
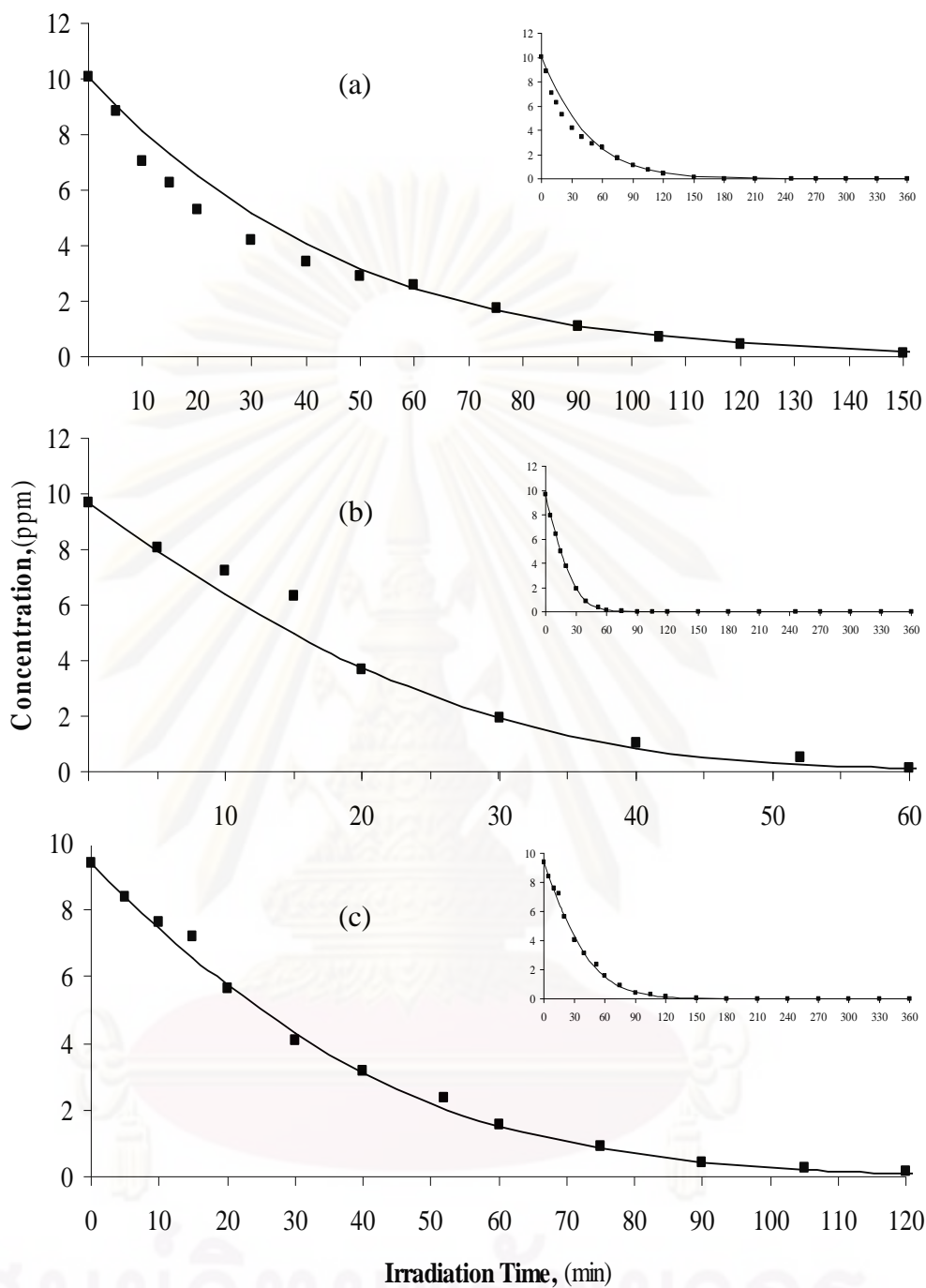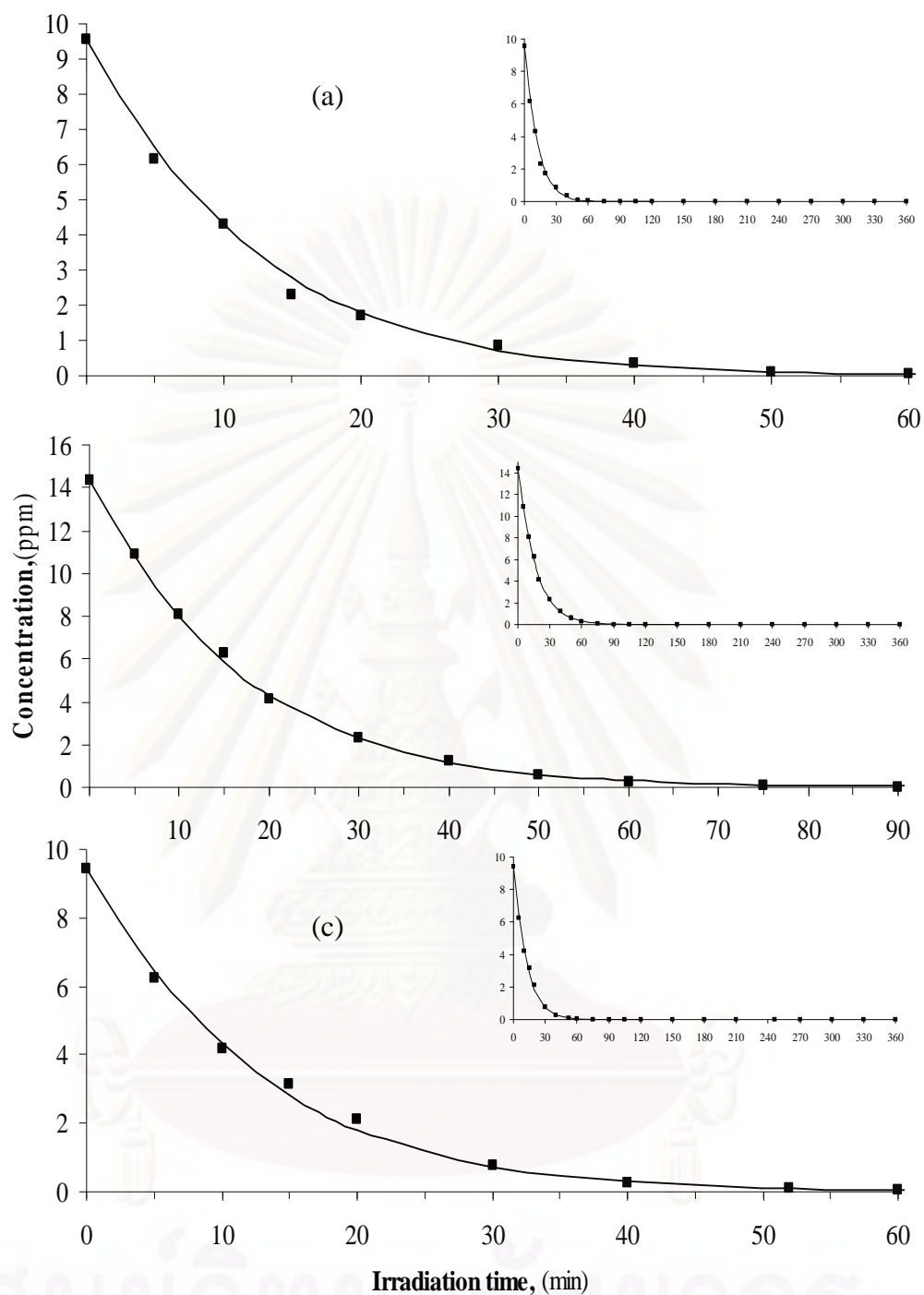
Figure 4.18. Comparison between experimental data (■) and calculated results from the Langmuir-Hishelwood model (——) for the photodegradation of diuron (a), linuron (b) and isoproturon (c), using the initial concentration of herbicides is 10 ppm. The operating temperature was 10 ^{o}C and the reaction was conducted using 1 mg of ZnO per 10 ml of solution, without pH adjustment.

Figure 4.19. Comparison between experimental data (■) and calculated results from the Langmuir-Hishelwood model (——) for the photodegradation of diuron (a), linuron (b) and isoproturon (c), using the initial concentration of herbicides is 10 ppm. The operating temperature was 30 ^{o}C and the reaction was conducted using 1 mg of ZnO per 10 ml of solution, without pH adjustment.
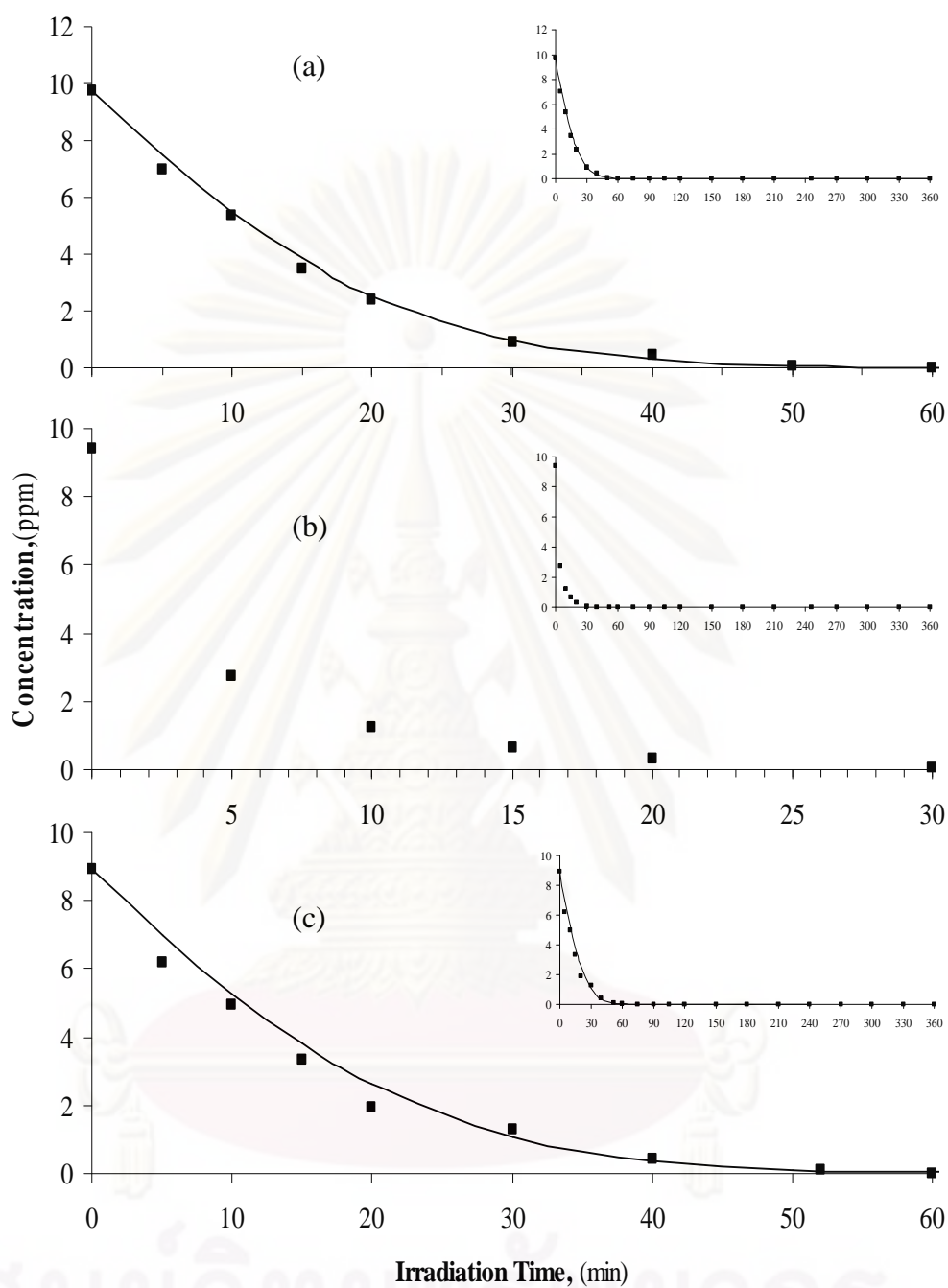
Figure 4.20. Comparison between experimental data (■) and calculated results from
the Langmuir-Hishelwood model (——) for the photodegradation of
diuron (a), linuron (b) and isoproturon (b), using the initial concentration
of herbicides is 10 ppm. The operating temperature was 50 ^{o}C and the
reaction was conducted using 1 mg of ZnO per 10 ml of solution,
without pH adjustment.

It can be observed from Figure 4.18-4.20 that the degradation can be represented by the Langmuir- Hinshelwood model. The concentration predicted by the model is relatively close to the experimental data. As indicated in the results, the rate of degradation depends upon the temperature.

4.7 Activation Energy

The reaction rate constant k is not truly a constant, but is merely independent of the concentrations of the species involving in the reaction. The quantity k is also referred to as the specific reaction rate (constant). It is almost always strongly dependent of temperature. In gas phase reactions, it depends on the catalyst and may be a function of total pressure. In liquid systems it can also be function of total pressure, and in addition can depend on other parameters, such as ionic strength and choice of solvent. These other variables normally exhibit much less effect on the specific reaction rate than temperature does. So, for the purposes of the material presented here, it will be assumed that k depends only on temperature. This assumption is valid in most laboratory and industrial reactions and seems to work quite well.

The activation energy is determined experimentally by carrying out the reaction at several different temperatures.

$$\ln k = \ln k_0 - (E/R)(1/T) \tag{4.7}$$

where k_0 = preexponential factor

E = activation energy, J/mol or cal/mol

R = gas constant = 8.314 J/mol·K = 1.987 cal/mol·K

T = absolute temperature, K

Equation 4.7 is called Arrhenius equation. It can be seen that a plot of $\ln k$ versus $1/T$ should be a straight line, of which slope is proportional to the activation energy.

For this section, the initial phenylurea herbicide concentration was about 10 ppm and the amount of ZnO powder added into the solution was fixed at the ratio of 1 mg of ZnO to 10 ml of solution.
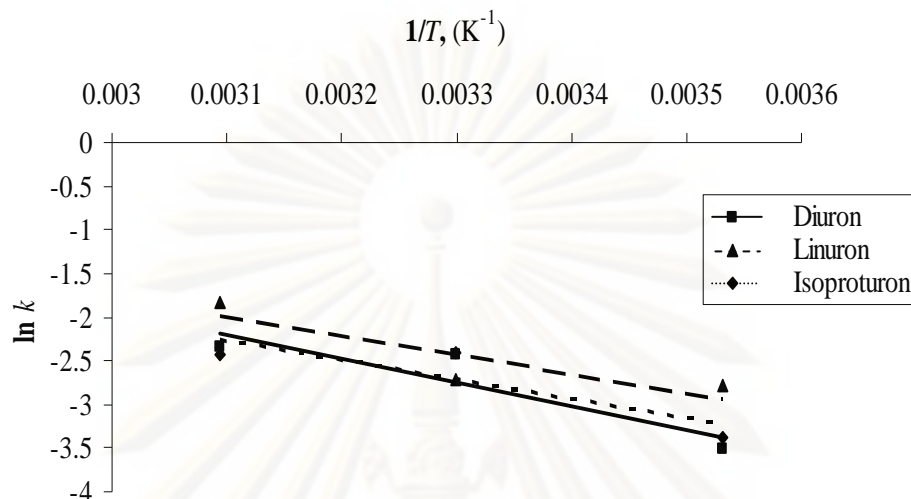

Figure 4.21. Linear transform, according to the Arrhenius equation, of the photocatalytic degradation of phenylurea herbicides.

Table 4.6. The activation energy (E) and preexponential factor (k_0) were calculated from the slopes and ordinates at the origin of the linear transforms of Figure 4.3.1.
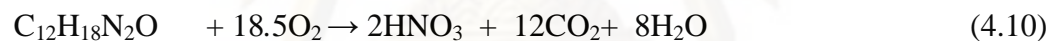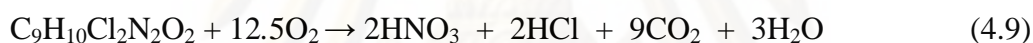
Herbicide	linear equation	R^2	k_0, (min^{-1})	E, (J/mol)
Diuron	$y = -2730.8x + 6.2735$	0.8299	530.33	22,703.9
Linuron	$y = -2144.9x + 4.6430$	0.7731	103.86	17,832.7
Isoproturon	$y = -2235.7x + 4.6609$	0.7713	105.73	18,587.6

As indicated in the results, the calculated activation energy is very low in kJ/mol. It can be seen from the calculation that in the presence of both ZnO and UV light, the activation energy could be reduced and bring about achieve the complete degradation of herbicides in the short time.

4.8 Evaluation of Degradation Intermediates

The focus here is the identification of intermediate compounds formed during photocatalytic degradation. In general, the oxidation of straight-chained hydrocarbon is relatively easy, while dearomatisation of aromatic compounds has been found to be harder, longer and involves the formation of many intermediate compounds before mineralization is achieved. However, this monitoring is not always easy since by-products generated in such oxidation processes can be small polar compounds represented in low concentration.

The stoichiometry of the complete mineralization of diuron, linuron and isoproturon can be expressed with the following global equations:

$$C_9H_{10}Cl_2N_2O \ + \ 13O_2 \ \rightarrow 2HNO_3 \ + \ 2HCl \ + \ 9CO_2 \ + \ 3H_2O \qquad (4.8)$$

$$C_9H_{10}Cl_2N_2O_2 + 12.5O_2 \rightarrow 2HNO_3 \ + \ 2HCl \ + \ 9CO_2 \ + \ 3H_2O \qquad (4.9)$$

$$C_{12}H_{18}N_2O \quad + 18.5O_2 \rightarrow 2HNO_3 \ + \ 12CO_2+ \ 8H_2O \qquad (4.10)$$

Although there has been no consensus on the detailed mechanism of the photocatalytic reaction on zinc oxide, it is generally agreed that the reaction involves generation of electron-hole pairs upon illumination of UV light on zinc oxide. The photogenerated holes can be subsequently scavenged by oxidizing species such as H_2O or OH^- and result in highly reactive hydroxyl radicals, which are the key for decomposition of most organic contaminants.

4.8.1 Degradation of diuron

Diuron has the chemical structure which is consisted of an aromatic ring attached by one urea group and two chorine atoms. During the photocatalytic degradation, active radicals generated from zinc oxide react with diuron, resulting in intermediate products. Structure of the functional groups attaching to aromatic ring of diuron is the mainly responsible for the structure of the intermediates formed. Diuron clearly offers two sites for the reaction, i.e. the aromatic ring and the aliphatic side

chain (Hincapie 2005). In this work, five kinds of intermediate were detected by HPLC during the photocatalytic treatment of diuron proceeds as shown in Figure 4.22. Concentrations of these intermediate are expected to be very low, suspected from the observation that the intensities of HPLC signals for the intermediates are much lower than that of diuron (see Figure 4.23). It can be suggested that nitrogen containing in diuron forms ammonia, urea and nitrate. Carbon dioxide is also the main product of oxidation reaction (Malato 2003). However these small molecules are not detectable by HPLC analysis.
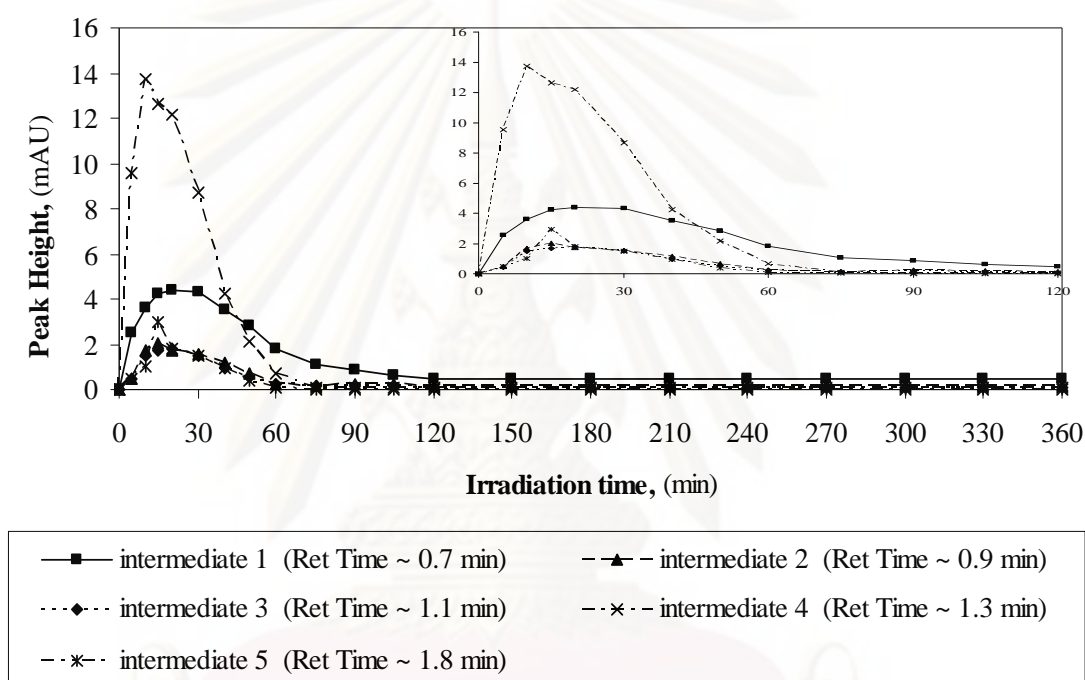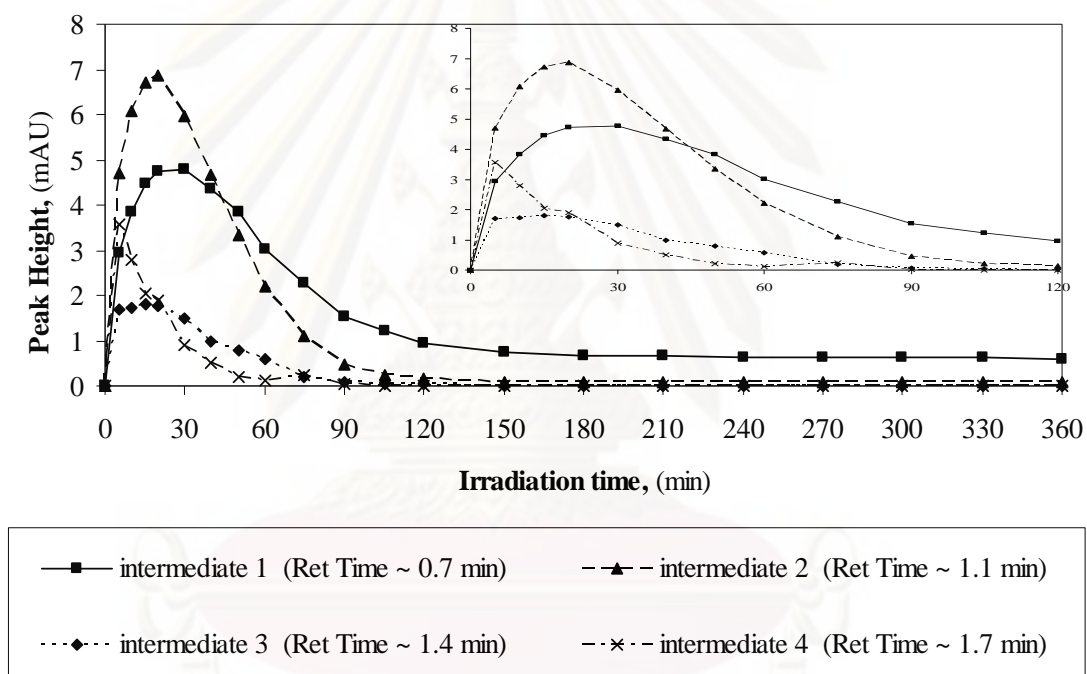

Figure 4.22. Intermediates generated during photocatalytic treatment of diuron.
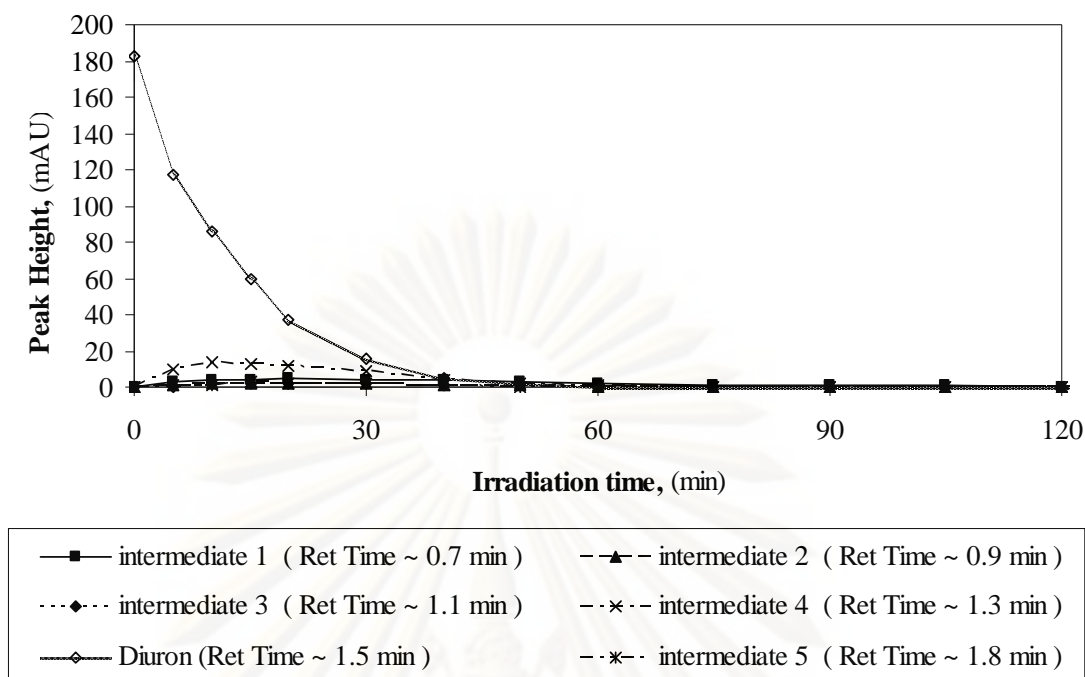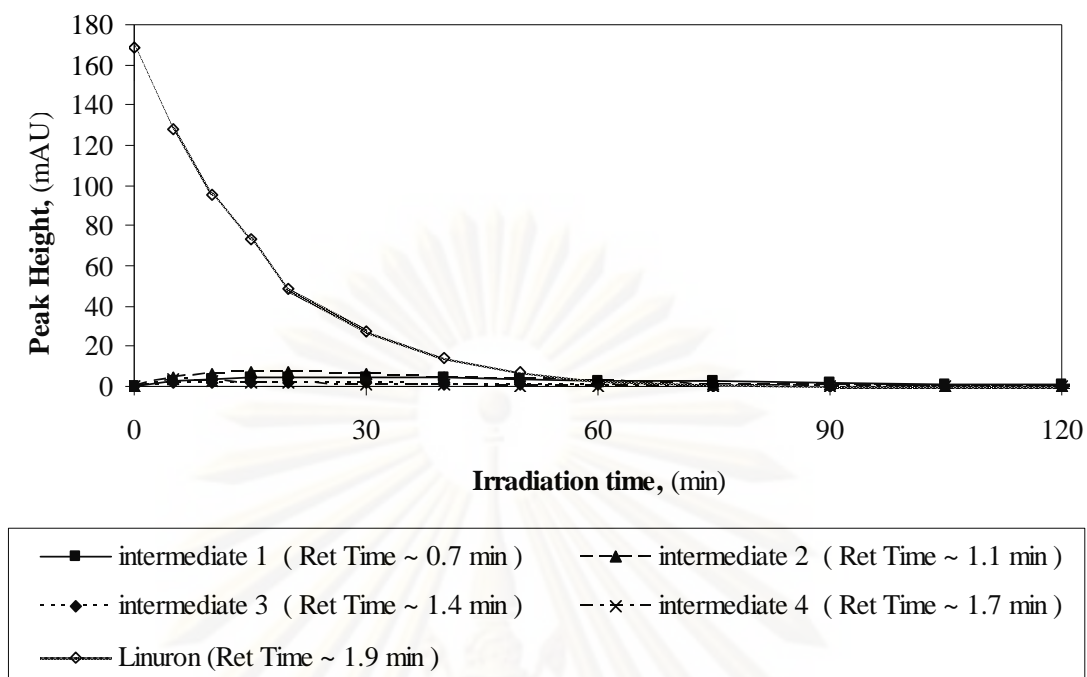
Figure 4.23. Comparison of the HPLC signals from intermediates and that from diuron during the course of photocatalytic degradation.

According to Figure 4.22-4.23, all intermediates are formed in the highest concentration within the first 20 min of the reaction. Then, subsequent degradation of the intermediates occurs. The intermediates 4 and 5 could not be detected after 90 min of irradiation time. However, some intermediates, e.g. intermediates 1-3, remain stable at low concentration even after 6 h of the reaction.

4.8.2 Degradation of linuron

Linuron consists of an aromatic ring attached with two chlorine groups and one uretic group with methoxyl group substituted in urea moiety. Photochemical behavior of linuron involves photohydrolysis as the main transformation pathway. The urea moiety is substituted by methoxyl group and demethoxylation is a competition between N-demethoxylation reaction or oxidation of methyl group (Amine-Khodja 2004). The possible degradation pathway for linuron is proposed in these steps (Katsumata 2005);

(a) The attack on the aromatic ring by OH$^\bullet$ radical without dechlorination or alkyl chain.

(b) A series of oxidation processes that eliminated alkyl groups and chlorine atom.

(c) The oxidative opening of aromatic ring, leading to small organic ion and inorganic species.

It should be noted that linuron has molecular structure that is less reactive than diuron and isoproturon. Therefore, the less number of intermediate substances appear in the solution during the degradation process. HPLC analysis shows four intermediate fractions as shown in Figure 4.24. Concentration of the intermediates generated in the process changes with irradiation time.

Figure 4.24. Intermediates generated during photocatalytic treatment of linuron.

Figure 4.25. Comparison of the HPLC signals from intermediates and that from linuron during the course of photocatalytic degradation.

According to Figures 4.24-4.25, all intermediates are formed in the highest concentration within the first 30 min of the reaction. Then, subsequent degradation of the intermediates occurs. The intermediates 3 and 4 could not be detected after 90 min of irradiation time. However, some intermediates, e.g. intermediates 1 and 2, remain stable even after 6 h of the reaction. These two intermediates appear at similar retention time as the stable intermediate observed in the degradation of diuron (at retention time of 0.7 and 1.1 min, respectively).

4.8.3 Degradation of isoproturon

Isoproturon is a phenylurea herbicide consisting of an aromatic ring with an alkyl chain and one uretic group. The molecular structure of isoproturon allows OH radical attack at different sites, following by several chain reactions. The first hydroxylation can occur at the aromatic ring, at the alkyl groups and at the secondary nitrogen of the uretic group, leading to monohydroxylated products. Subsequent hydroxylation at the remaining sites results in di-hydroxylated and tri-hydroxylated products (Gora 2006). Figure 4.26 shows intermediates generated during photocatalytic treatment of isoproturon. It should be noted that isoproturon has

molecular structure that is more reactive than diuron, due to the presence of the $CH(CH_3)_2$ group, instead of halogen substituents, as previously discussed. HPLC analysis gave five intermediated fractions as shown in Figure 4.26.

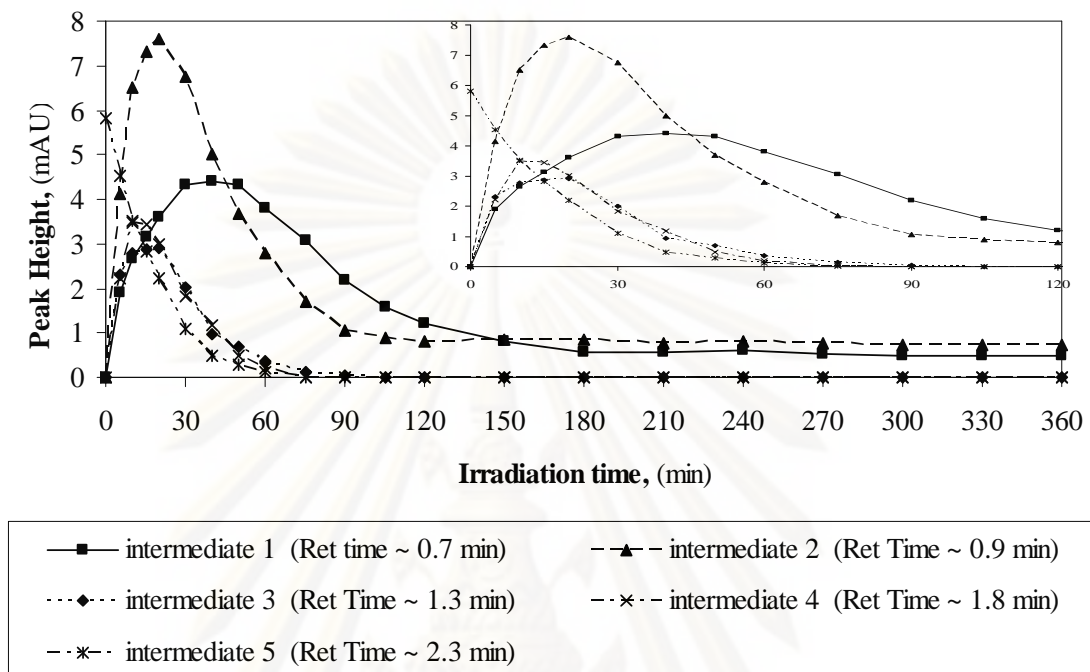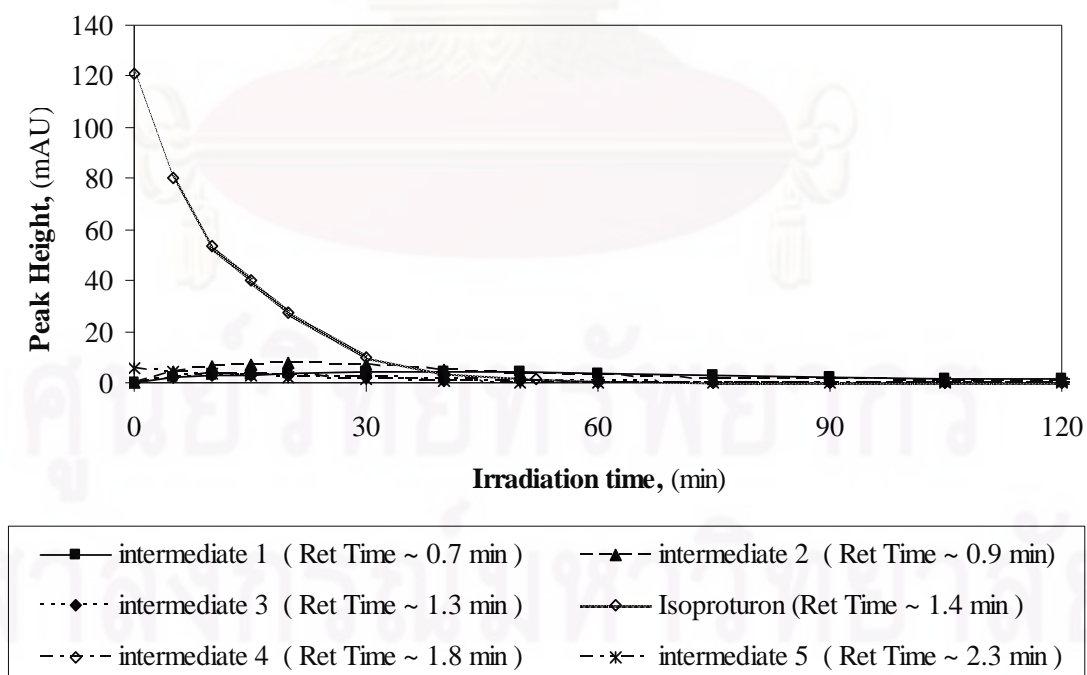**Figure 4.26.** Intermediates generated during photocatalytic treatment of isoproturon.

Figure 4.27. Comparison of the HPLC signals from intermediates and that from isoproturon during the course of photocatalytic degradation.

According to Figures 4.26-4.27, intermediates 1-4 are formed in the highest concentration within the first 20 min of the reaction, after which the degradation of the intermediates occurs. The intermediates 3 and 4 could not be detected after 90 min of irradiation time. On the other hand, intermediates 1 and 2, remain stable even after 6 h of the reaction. The intermediate 1 (appears at retention time of 0.7 min) is similar to the intermediate observed in diuron and linuron degradations. The intermediate 2, which appears at retention time of 0.9 min is also observed in the diuron degradation.

Unlike all intermediates previously discussion, an intermediate 5 at retention time of 2.3 min is already presented in the solution even before the photodegradation. This species should be the result from the reaction between isoproturon and water and it is not the product from photodegradation.

Although the chemical structures of the intermediates were not identified in this work, the result confirms that the degradation of each phenylurea herbicide generates lots of intermediates. According to the detailed mass spectra shown in Appendix C, the intermediate compounds generated during phenylurea herbicides degradation tend to conjugate into larger molecules than the parent compounds. An example of the mass spectra is shown in Figure 4.28. In this study, the investigation of the intermediates by using NMR was inconclusive (see Figure 4.29 and more detail in Appendix D). It can be the result from the fact that the concentrations of all unknown intermediates are very low. Therefore, signals from unknown intermediates are very low and does not explicit.
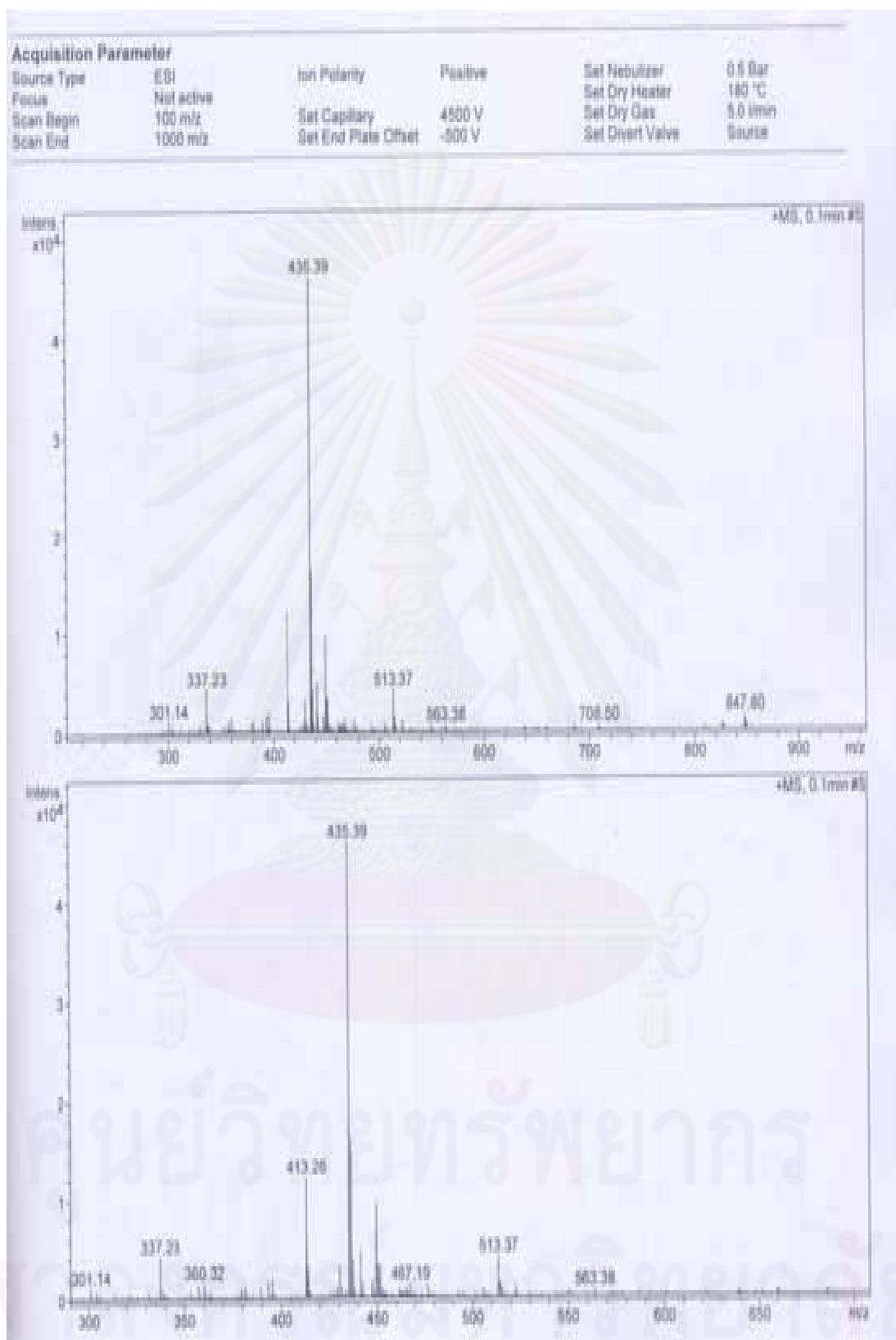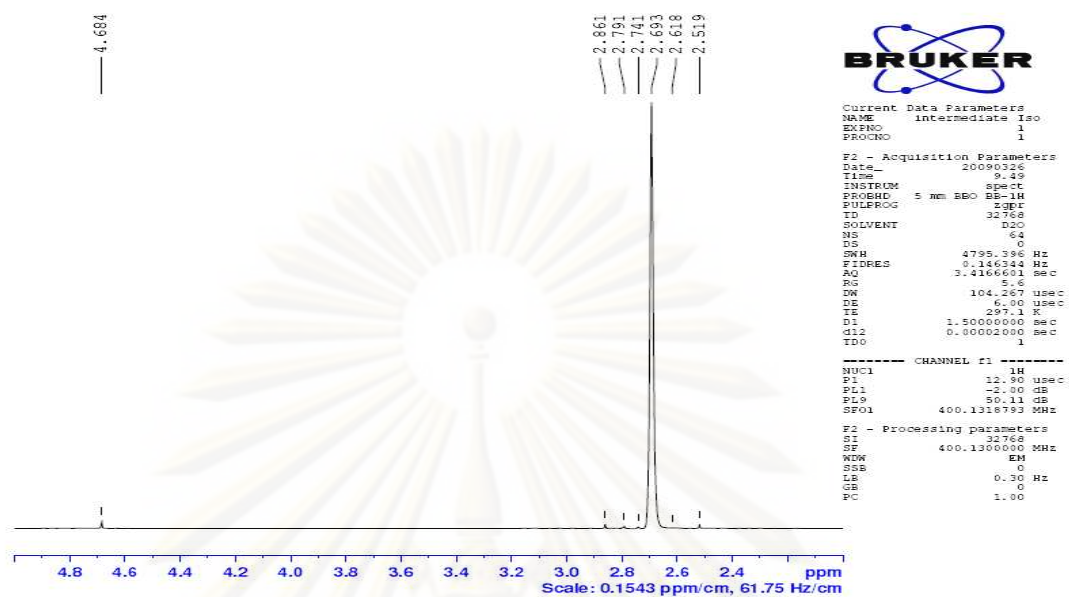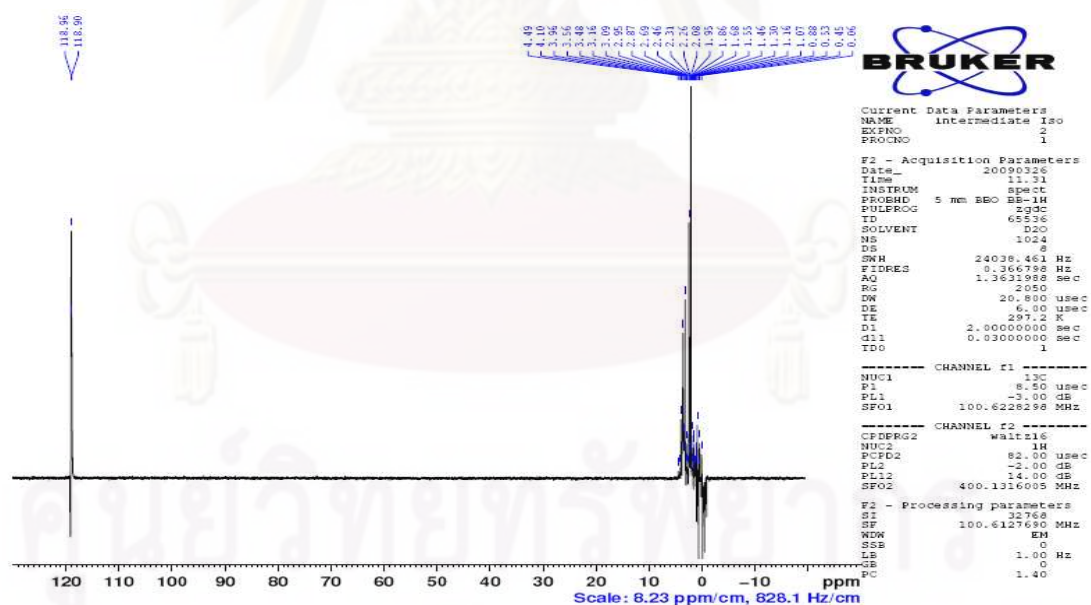
Figure 4.28. Example of mass spectra of intermediate 1 from the degradation of isoproturon.

(a)

(b)

Figure 4.29. Example of NMR signal appears for proton mode (a) and carbon mode (b) from intermediate 1 obtained from the degradation of isoproturon.

CHAPTER V

CONCLUSIONS AND RECOMMENDATIONS

5.1 Conclusions

The conclusions of the present research are the following:

1. The treatment is not feasible without a catalyst.

2. Zinc oxide has high activity toward the photocatalytic degradation of phenylurea herbicide in aqueous solution. Complete degradation can be achieved within relatively short period of time.

3. The degradation follows the Langmuir-Hinshelwood kinetics model.

4. The degree of degradation of phenylurea herbicide was obviously affected by photocatalyst amount, initial phenylurea herbicide concentration, pH of solution, and temperature.

5. Many intermediates are formed during the degradation of phenylurea herbicide.

5.2 Recommendations for the Future Studies

Regarding the previous conclusions, the following recommendations for the future studies are proposed.

1. Investigate photocatalytic degradation of phenylurea herbicides by coating zinc oxide on various supports.

2. Study the regeneration of used zinc oxide.

3. Evaluate total organic compound (TOC) generated during photodegradation process.
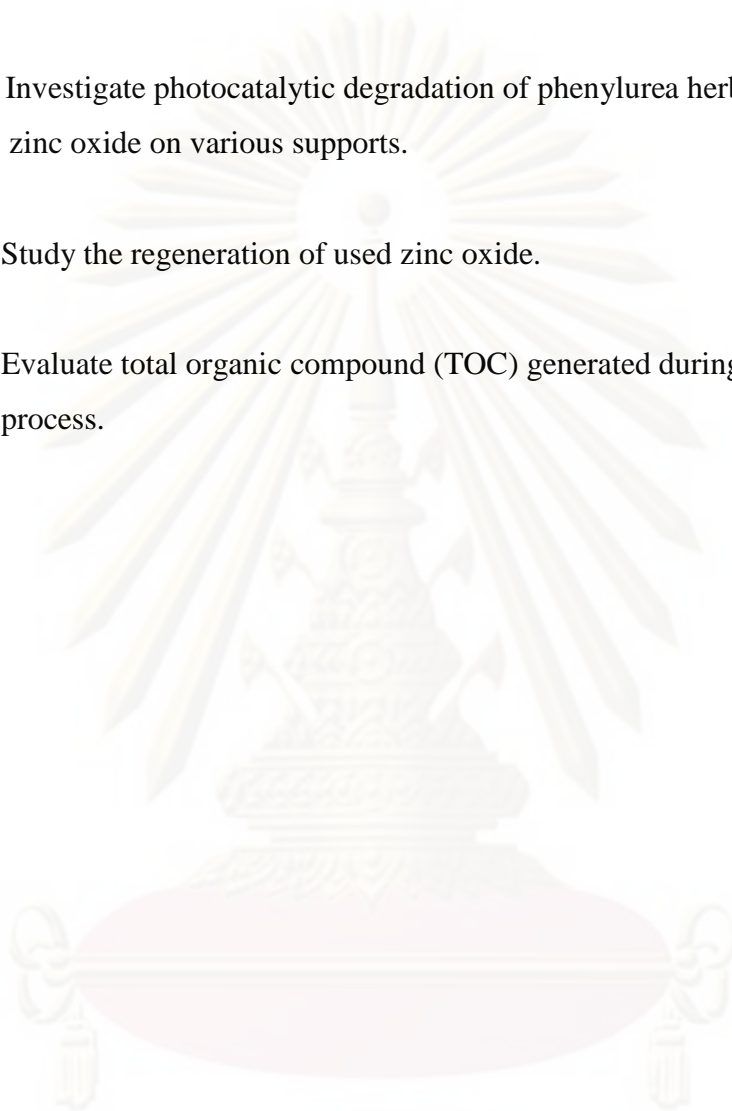
REFERENCES

Akyol, A., H.C. Yatmaz, and M. Bayramoglu. 2004. Applied Catalysis B: Environmental 54: 19.

Alpert, A.J. 1990. Journal of Chromatogram. 499 : 177–196.

Amine-Khodja, A., Boulkamh, A. and Boule, P. 2004. Photochemical Behavior of Phenylurea Herbicides. Photochemical & Photobiological Sciences 3: 145-156.

Amorisco, A., Losito, I., Palmesano, F., Zambonin, P.G. 2005. Photocatalytic degradation of the herbicide isoproturon: characterisation of by-products by liquid chromatography with electrospray ionisation tandem mass spectrometry, Rapid Commun. Mass Spectrom 19: 1507–1516.

Andreozzi, R., C. V., A. Insola, and R. Marotta. 1999. Advanced Oxidation Processes (AOP) for Water Purification and Recovery. Catalysis Today 53: 51-59.

Behnajady, M.A., N. Modirshahla, and R. Hamzavi. 2006. Kinetic study on photocatalytic degradation of C.I. Acid Yellow 23 by ZnO photocatalyst. Journal of Hazardous Materials B. 133: 226–232.

Blatt, F. J. 1968. Physics of Electronic Conduction in Solids New York, Mc Graw-Hill.

Daneshvar, N., D. Salari, and A.R. Khatayee. 2004. Photocatalytic degradation of azo dye acid red 14 in water on ZnO as an alternative catalyst to TiO_2. Journal of Photochemistry and Photobiology A: Chemistry 162: 317-322.

Daneshvar, N., M.H. Rasoulifard, A.R. Khatayee, and F. Hosseinzadeh. 2007. Removal of C.I. Acid Orange 7 from aqueous solution by UV irradiation in the presence of ZnO nanopowder. Journal of Hazardous Materials 143: 95-101.

Daneshvar, N., S. Aber, M.S.S. Dorraji, A.R. Khatayee, and M.H. Rasoulifard. 2007. Photocatalytic degradation of the insecticide diazinon in the presence of

prepared nanocrystalline ZnO powders under irradiation of UV-C light. Separation and Purification Technology Chemospher 58: 91-98.

Djebbar, K.E., A. Zertal, N. Debbache, and T. Sehili. 2008. Comparison of Diuron degradation by direct UV photolysis and advanced oxidation processes. Journal of Environmental Management 88 (4): 1505-1512.

Dupas, S., P. Scribe, H. Etcheber, and A. Saliot. 1995. Phenylurea and triazine herbicides in the Garonne river (France) during high flood and low water periods. International Journal of Environmental Analytical Chemistry 58: 397–409.

Farré, M.J., S. Brosillon, X. Domènech, and J. Peral. 2007. Evaluation of the intermediates generated during the degradation of Diuron and Linuron herbicides by the photo-Fenton reaction. Journal of Photochemistry and Photobiology A: Chemistry 189: 364–373.

Farré, M.J., M.I. Maldonado, W. Gernjak, I. Oller, S. Malato, X. Domènech, and J. Peral. 2008. Coupled solar photo-Fenton and biological treatment for the degradation of diuron and linuron herbicides at pilot scale. Chemosphere 72: 622–629.

Fujishima, A., K. Hashimoto, and T. Watanabe. 1999. TiO_2 Photocatalysis Fundamental and Applications. BKC, Inc.

Gora, A., Toepfer, B., Puddu, Valeria, A. and Puma, G.L 2006. Photocatalytic Oxidation of Herbicides in Single-Component and Multicomponent Systems: Reaction Kinetics Analysis. Applied Catalysis B: Environmental 65: 1-10.

Gouvea, C.A.K., F. Wypych, S.G. Moraes, N. Duran, N. Nagata, and P.P. Zamora. 2000. Chemosphere 40: 433.

Hincapie, M., Maldonado, M.I., Oller, I., Gernjak, W., Sanchez-Perez, J.A., Ballesteros, M.M. and Malato, S. 2005. Solar Photocatalytic Degradation and Detoxification of EU Priority Substances. Catalysis Today 101: 203-210.

Katsumata, H., S. Kaneco, T. Suzuki, K. Ohta, and Y. Yobiko. 2005. Degradation of linuron in aqueous solution by the photo-Fenton reaction. Chemical Engineering Journal 108: 269-276.

Khodja, A.A., T. Sehili, J. Pilichowski, and P. Boule. 2001. Photocatalytic degradation of 2 phenyl-phenol on TiO2 and ZnO in aqueous suspension. Journal of Photochemistry and Photobiology A: Chemistry 141: 231-239.

Keith, L.H., Telliard, W.A. 1979. Environmental Science Technology 13 : 416–424.

Klongdee, J., W. Petchkroh, K. Phuempoonsathaporn, P. Praserthdam, A.S. Vangnai, and V. Pavarajarn. 2005. Activity of nanosized titania synthesized from thermal decomposition of titanium (IV) n-butoxide for the photocatalytic degradation of diuron. Science and Technology of Advanced Materials 6 (3-4): 290-295.

Konstantinou, I.K. and T.A. Albanis. 2004. TiO_2-assisted photocatalytic degradation of azo dyes in aqueous solution: kinetic and mechanistic investigation. Applied Catalysis B: Environmental 49: 1–14.

Lapertot, M., S. Ebrahimi, S. Dazio, A. Rubinelli, and C.e. Pulgarin. 2007. Photo-Fenton and biological integrated process for degradation of a mixture of pesticides. Journal of Photochemistry and Photobiology A: Chemistry 186 34–40.

Lizama, C., J. Freer, J. Baeza, and H.D. Mansilla. 2002. Catalysis Today 76: 235.

Lopez, A., G. Mascolo, R. Ciannarella, and G. Tiravanti. 2001. Formation of volatile halogenated by-products during chlorination of isoproturon aqueous solutions. Chemosphere. 45: 269-274.

M., P. 2001. Degradation of organic compounds in paper and textile industrial wastewaters by advanced oxidation processes. Escola Tècnica Superior d'Enginyeria Química, Doctoral dissertation. Unisersitat Politècnica de catalunya.

Madani, M.E., C. Guillard, N. Pe´rol, J.M. Chovelon, M.E. Azzouzi, A. Zrineh, and J.M. Herrmann. 2006. Photocatalytic degradation of diuron in aqueous solution in presence of two industrial titania catalysts, either as suspended powders or deposited on flexible industrial photoresistant papers. Applied Catalysis B: Environmental 65: 70–76.

Madler, L., W. J. Stark and S. E. Pratsinis 2002. Rapid synthesis of stable ZnO quantum dots. Journal of Applied Physics 92: 6537.

Malato, S., Caceres, J., Fernandez-Alba, A.R., Piedra, L., Hernando, M.D., Aguera, A. and Vial, J. 2003. Photocatalytic Treatment of Diuron by Solar Photocatalysis: Evaluation of Main Intermediates and Toxicity. Environmental Science & Technology 37(11): 2516-2524.

Mishra, S. K., Kanungo, S. B., and Rajeev. 2003. Adsorption of sodium dodecyl benzene sulfonate onto coal. Journal of Colloid and Interface Science 267(1): 42-48.

Mott, M. F. and E. A. Davis 1979. Electronic Process in Non-Crystalline Materials. Clarendon Press, Oxford.

Mosleh, Y.Y., S. Paris-Palacios, M. Couderchet, and G. Vernet. 2003. Effects of the herbicide isoproturon on survival, growth rate, and protein content of mature earthworms (Lumbricus terrestris L.) and its fate in the soil. Applied Soil Ecology 23: 69–77.

Nitschke, L. and W. Schussler. 1998. Surface water pollution by herbicides from effluents of waste water treatment plants. Chemosphere 36: 35–41.

Pal, B. and M. Sharon. 2002. Chemical Physics: 76: 82.

Pankove, J. I. 1971. Optical Processes in Semiconductors. Dover Publications: New York.

Parra, S., V. Sarria, S. Malato, P. Peringer, and C. Pulgarin. 2000. Photochemical versus coupled photochemical–biological flow system for the treatment of two

biorecalcitrant herbicides: metobromuron and isoproturon. Applied Catalysis B: Environmental 27: 153–168.

Parra, S., Olivero, J., Pulgarın, C. 2002. Relationships between physicochemical properties and photoreactivity of four biorecalcitrant phenylurea herbicides in aqueous TiO2 suspension. Applied Catalysis B: Environmental 36: 75–85.

Pérez, M.H., G. Peñuela, M.I. Maldonado, O. Malato, P. Fernández-Ibáñez, I. Oller, W. Gernjak, and S. Malato. 2006. Degradation of pesticides in water using solar advanced oxidation processes. Applied Catalysis B: Environmental 64: 272–281.

Sakthivel, S., B. Neppolian, M.V. Shankar, B. Arabindoo, M. Palanichamy, and V. Murugesan. 2003. Solar Energy Materials and Solar Cell 77: 65.

Sharma, M.V.P., V.D. Kumari, and M. Subrahmanyam. 2008. Photocatalytic degradation of isoproturon herbicide over TiO_2//Al-MCM-41 composite systems using solar light. Chemosphere 72: 644-651.

Sobana, N. and M. Swaminathan. 2007. The effect of operational parameters on the photocatalytic degradation of acid red 18 by ZnO. Separation and Purification Technology 56: 101–107.

Spliid, N.H. and B. Koppen. 1998. Occurrence of pesticides in Danish shallow ground water. Chemosphere 37: 1307–1316.

Su, S., S.X. Lu, and W.G. Xu. 2008. Photocatalytic degradation of reactive brilliant blue X-BR in aqueous solution using quantum-sized ZnO. Materials Research Bulletin 43: 2172–2178.

Thatt Yang Timothy TAN, B.E. 2003. Photocatalytic Reduction of Selenate and Selenite: Water/Wastewater Treatment and The Formation of Nano-Selenium Compounds. Chemical Engineering and Industrial Chemistry. Doctor of Philosophy, New South Wales, Sydney.

Tixier, C., P. Bogaerts, M. Sancelme, F. Bonnemoy, L. Twagilimana, A. Cuer, J. Bohatier, and H. Veschambre. 2000. Fungal biodegradation of phenylurea

herbicide, Diuron: structure and toxicity of metabolites. Pest Management Science 56: 455–462.

Tomlim, C. 1994. The Pesticide Manual, ed. 10th: The Bath Press, UK.

Tomlin, C. 2000. *The Pesticide Manual*, ed. 12th: British Crop Protection Council.

Von wiren Lehr, S., M.D. Castillo, L. Torstensson, and I. Scheunert. 2001. Degradation of isoproturon in biobeds. Biology and Fertility of Soils 33: 535–540.

Weng, J., Y. Zhang, G. Han, Y. Zhang, L. Xu, J. Xu, X. Huang and K. Chen 2005. Electrochemical deposition and characterization of wide band semiconductor ZnO thin film. Thin Solid Films 478: 25-29.

Yatmaz, H.C., A. Akyol, and M. Bayramoglu. 2004. Industrial & Engineering Chemistry Research 43: 6035.

APPENDICES

APPENDIX A

PROPERTIES OF ZINC OXIDE

A.1 Morphology of Zinc Oxide

The SEM micrographs of zinc oxide is shown in Figure A.1.

S3400 15.0kV 9.7mm x20.0k SE 9/3/2008 14:38   2.00um
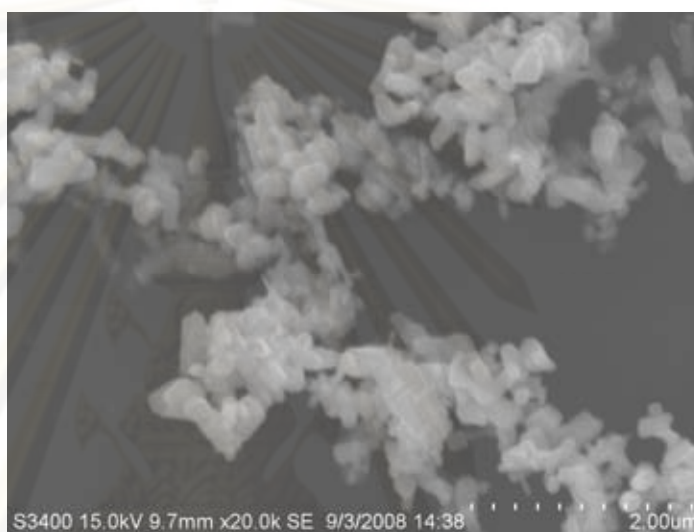
Figure A.1. SEM micrographs of zinc oxide.

A.2 Surface Area Measurement

The BET surface area of zinc oxide particles is 4.1871 m²/g.

A.3 Band Gap Energy Calculation

The band gap energy of zinc oxide was studied from absorption wavelength data from UV-Visible spectroscopy. The zinc oxide shows substantial absorption at wavelength below 380 nm, which is in the range of UV-A (315 – 400 nm). For wavelength higher than 400 nm, no significant absorption is observed.

The absorption edge from absorption spectra use to calculate the band gap energy by equation

$$\nu_0 \; = \; E_g/h \tag{A.1}$$

Where ν_0 is frequency at absorption edge. Substitution $\nu = \dfrac{c}{\lambda_{1/2}}$ into equation (A.1).

$$E_g = \frac{c.\,h}{\lambda_{1/2}} \tag{A.2}$$

Where

c = light velocity (3×10^8 m/s)

h = Planck constant (4.135×10^{-15} eV.s)

$\lambda_{1/2}$ = wavelength at absorption edge (nm)

E_g = band gap energy (eV)

The wavelength at half-absorption intensity $(\lambda_{1/2})$ form the UV- Vis absorption spectra of zinc oxide are shown in Figure A.2.1. It can be seen $\lambda_{1/2}$ is about 380 nm. Substitution $\lambda_{1/2}$ =380 nm into Eq. (A.2).

$$E_g = \frac{(3 \times 10^8 \; m/s)(4.135 x 10^{-15} eV.s)}{(380 x 10^{-9} \; m)}$$

We get the band gap energy of zinc oxide is 3.26 eV, which is close to the value reported in literature (Srikant et al., 1998).
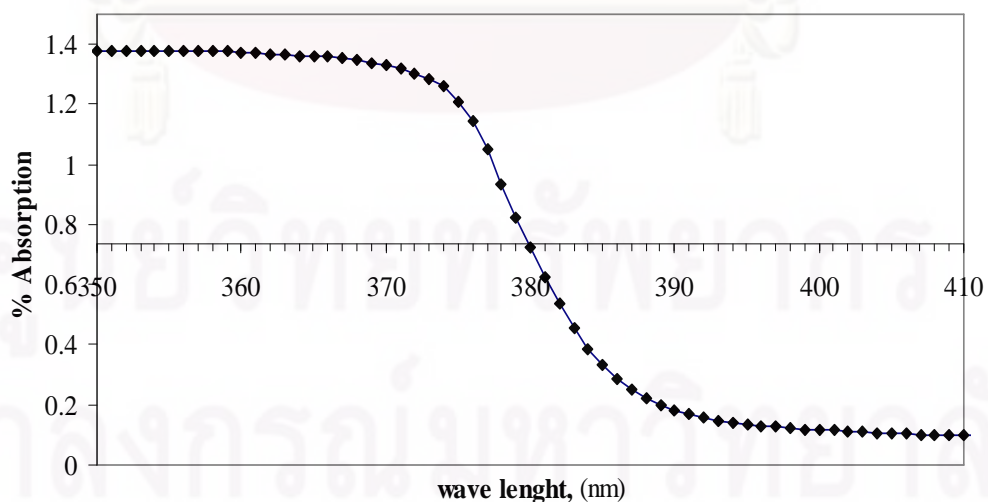
Figure A.2.   The UV-Vis absorption spectra of zinc oxide. The wavelength at half-absorption intensity $(\lambda_{1/2})$ is the band-gap energy of the material.

A.3 Point of Zero Charge Determination
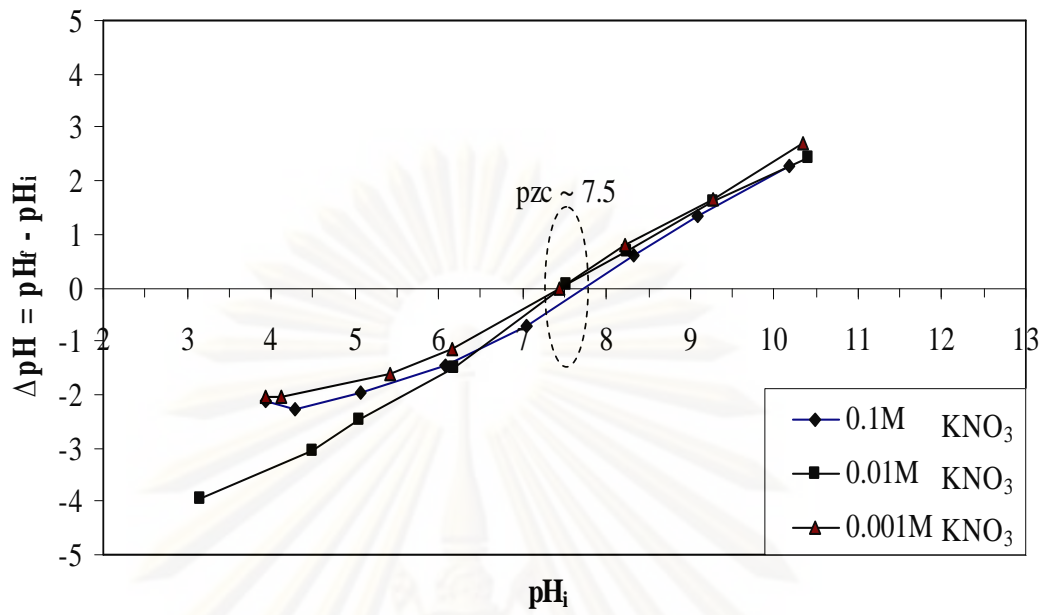
Figure A.3. Determination of the point of zero charge of zinc oxide.

Figure A.3 shows that the $\Delta pH = 0$ lies at the initial pH value of about 7.5, which is considered as the pH_{pzc} of ZnO.

APPENDIX B

CALIBRATION CURVE FOR DETERMINANTION OF
PHENYLUREA HERBICIDE CONCENTRATION
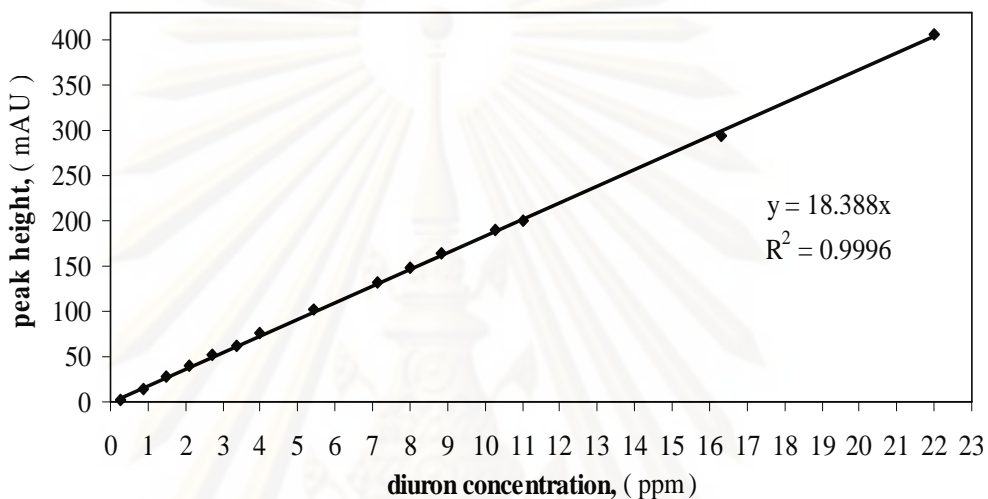
Figure B.1.   The calibration curve of diuron.

$y = 18.388x$
$R^2 = 0.9996$
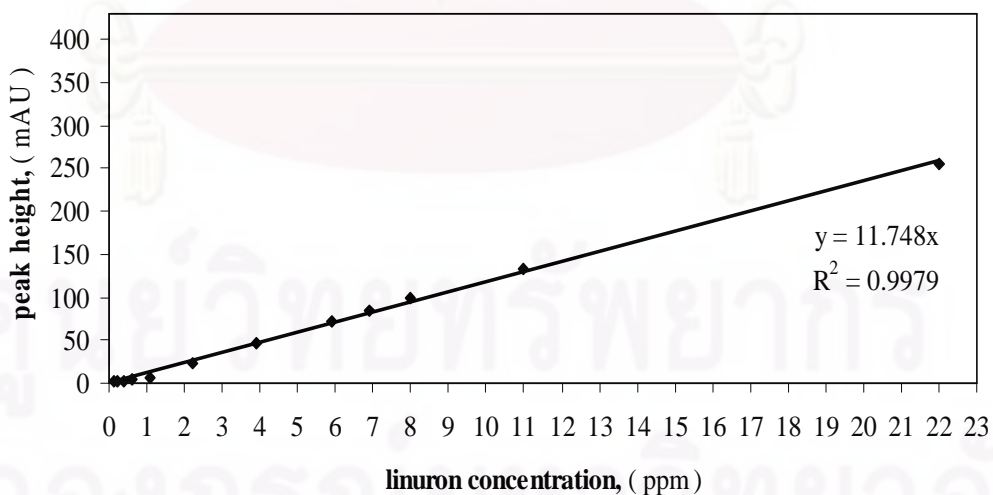
Figure B.2.   The calibration curve of linuron.

$y = 11.748x$
$R^2 = 0.9979$
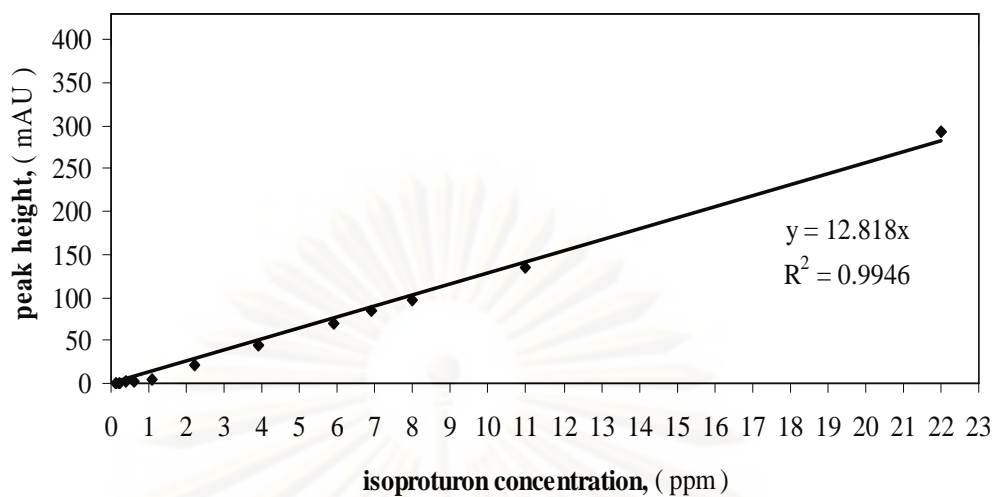
Figure B.3.   The calibration curve of isoproturon.
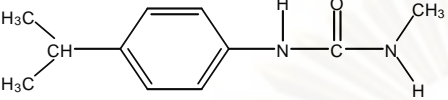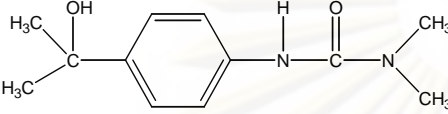
APPENDIX C

MASS SPECTRA OBTAINED FROM LC/MS

Some of the identified intermediate reported here were also identified and reported earlier by M.V.P. Sharma et al. (2008). The intermediate compounds during isoproturon degradation are identified based on LC–MS data. The data show the formation of several intermediates and some are identifiable by m/z ratios of main MS fragments as shown in Table C.1. Based on the results, a plausible mechanism is proposed for photocatalytic degradation of isoproturon. Isoproturon adsorbed over zinc oxide surface. When a photon of ultra-band gap energy ($hv > E_g$) is absorbed by ZnO, it results in promotion of electrons (e^-) from valence band (VB) to conduction band (CB), with the concomitant generation of a hole (h^+) in the valence band. In the aqueous medium the holes react with water molecules and forms hydroxyl radicals. On the other side, electrons react with oxygen molecules to form superoxide radicals and these inturn react with protons (H^+) to generate another OH radical. All OH radicals attack at different functional groups of isoproturon giving rise to several consecutive reactions. The intermediates formed by the attack of OH radicals on the aromatic ring are identified and the abstraction of hydrogen atoms of the methyl group is followed by addition of oxygen and decarboxylation, which leads to the formation of dealkylated intermediates. The photoreactivity is also related to the donor or withdrawing effect induced by different substituents of the aromatic ring (S. Parra et al., 2002). The first hydroxylation that can occur either on the aromatic ring or on the alkyl groups leading to different monohydroxylated intermediates. Furthermore, it forms di- and poly-hydroxylated compounds and later successive oxidations lead to ketones, organic acids and ultimately lead to complete mineralization.
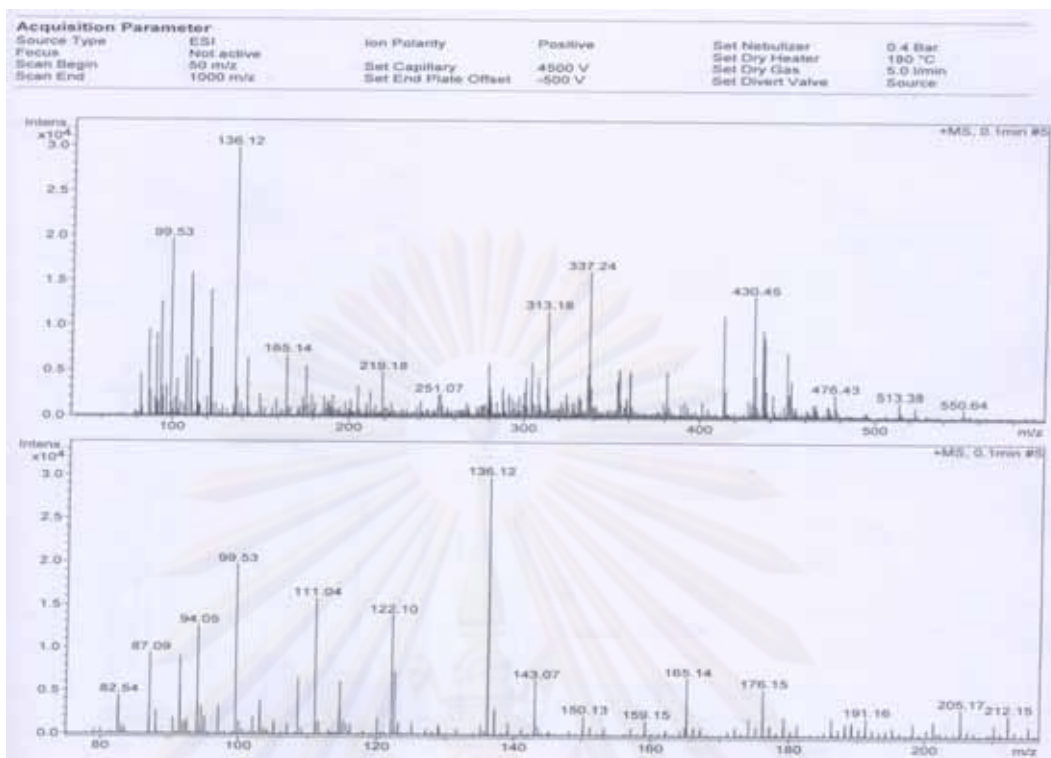
Table C.1. Mass spectral data for photocatalytic degradation of isoproturon as
analyzed by HPLC-MS

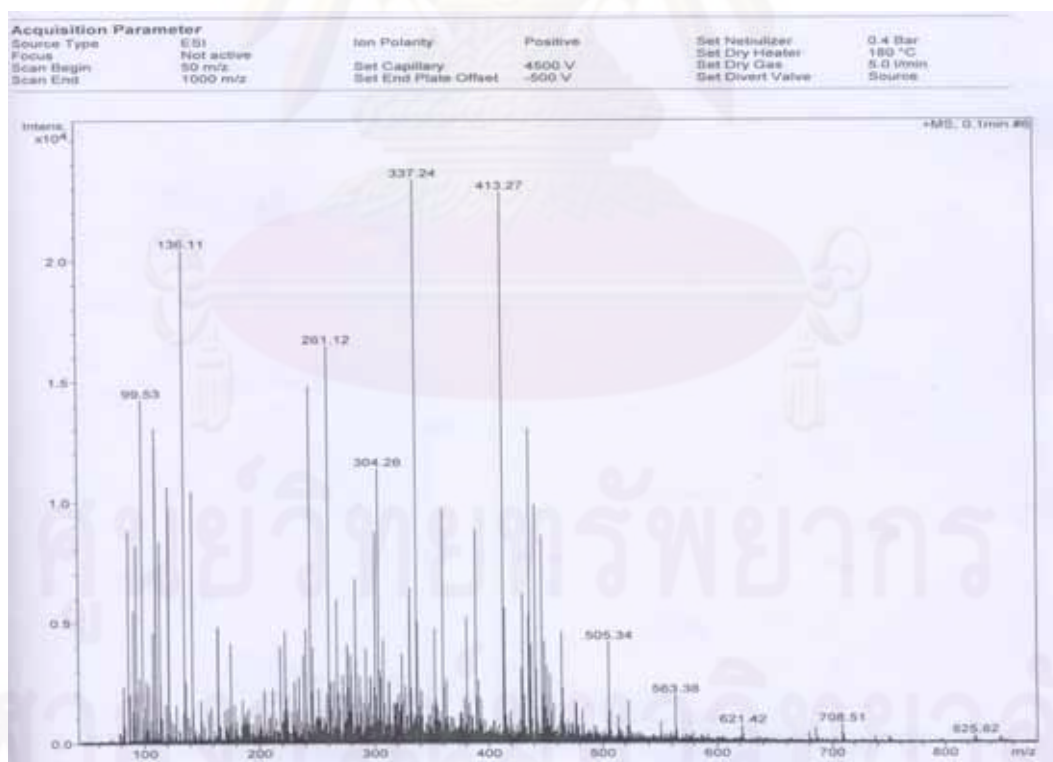| Compound structure	Intermediates (M+1/mol. wt.)	m/z ratios of main mass (MS) fragments
	193/192	193, 151, 136, 94
	223/222	223, 205, 165, 134
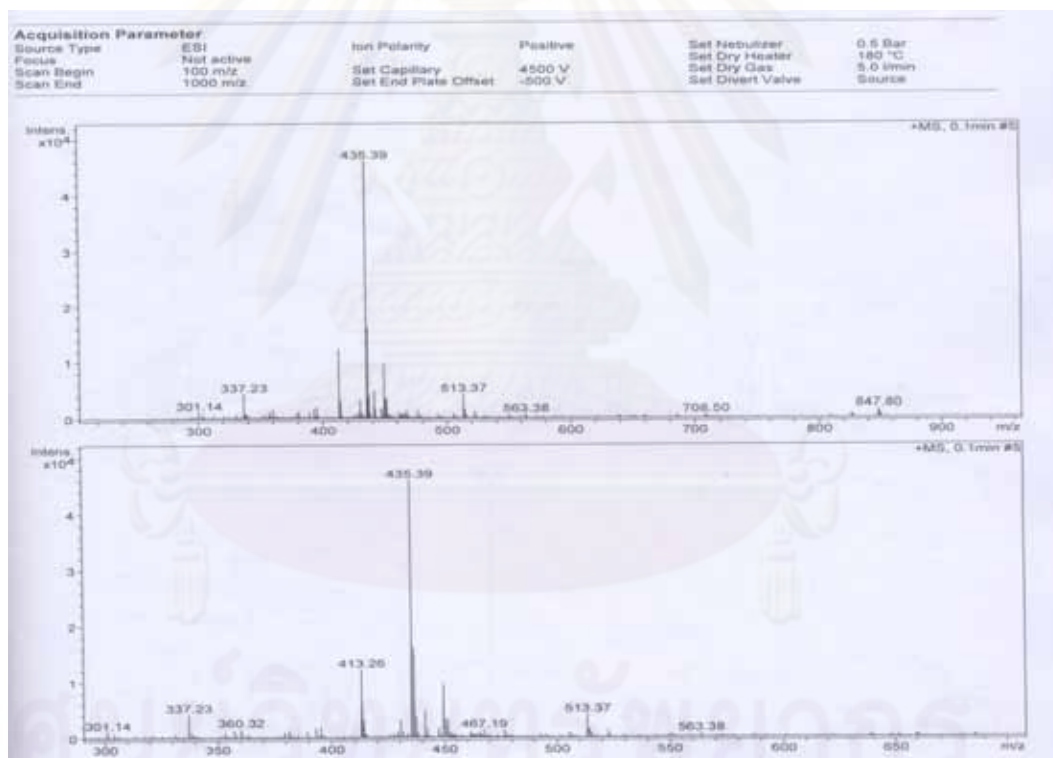
(a)

Figure C.1. Mass spectra at retention time of: (a) 6.6 min, (b) 8.2 min, (c) 10.3 min,
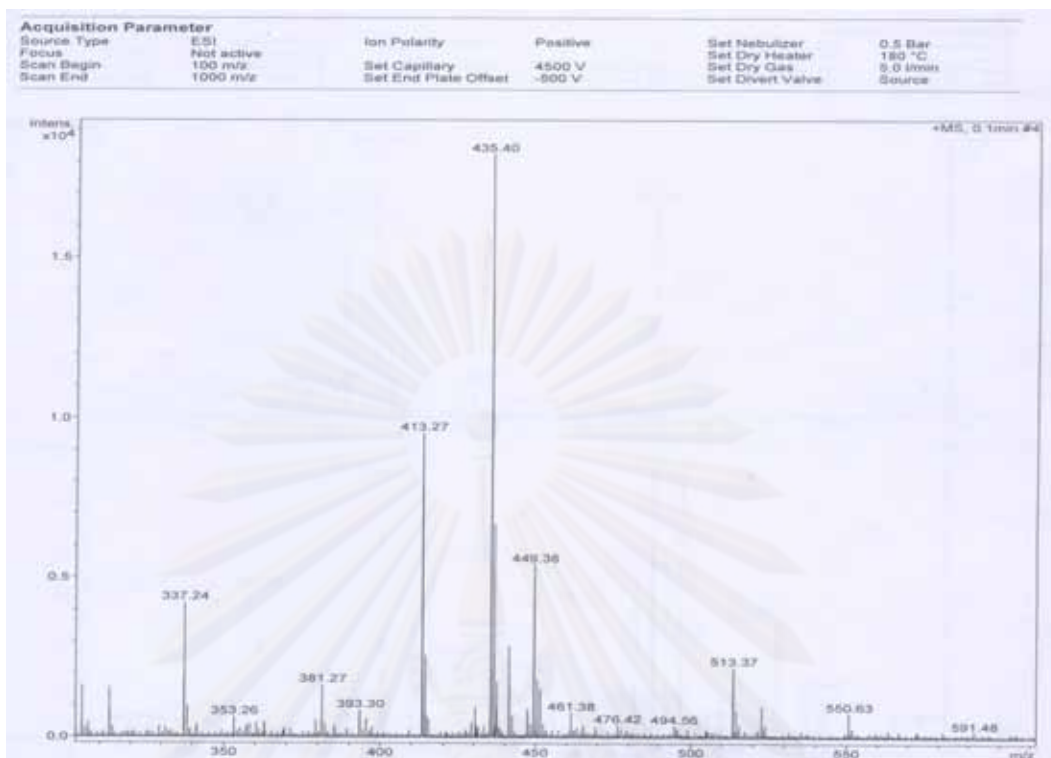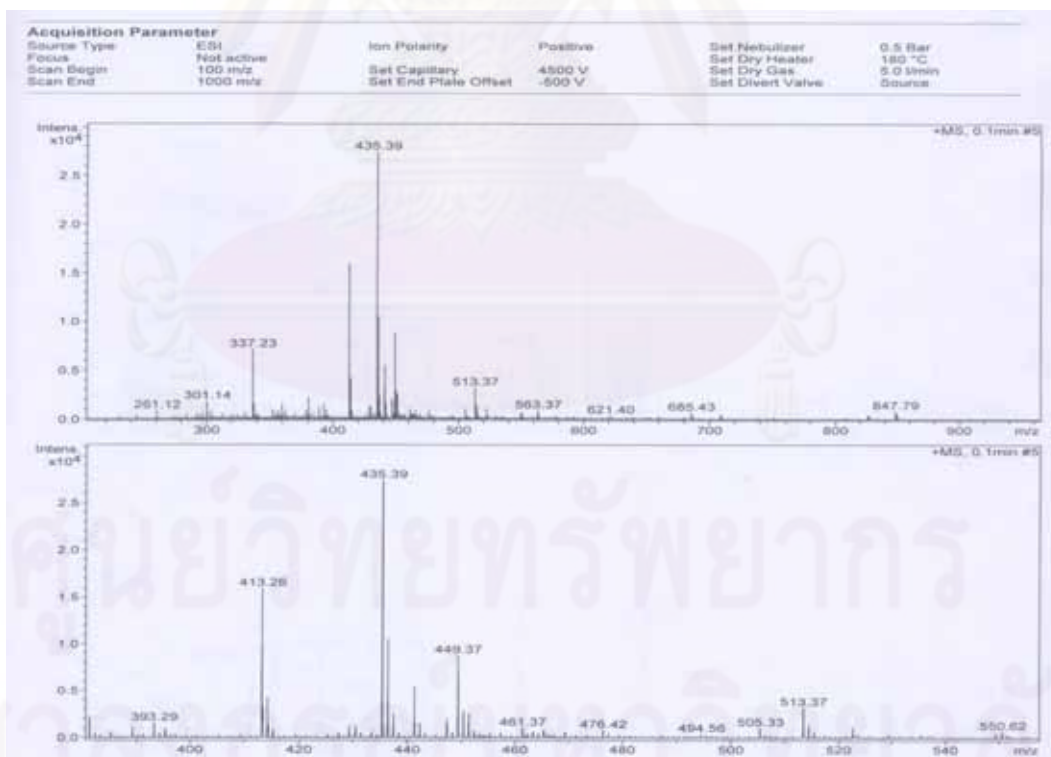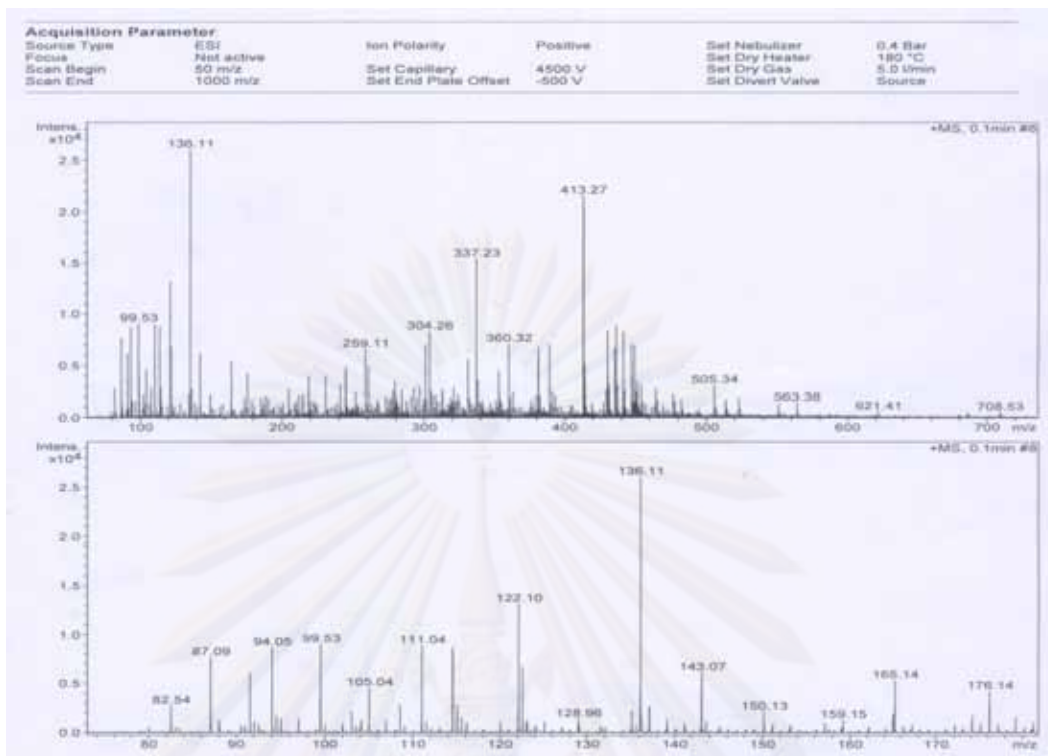(d) 11.2 min, (e) 11.7 min, (f) 12.2 min, (g) 12.9 min, (h) 13.3 min and (i)
15.3 min.

(b)

(c)

Figure C.1. (continued)

(d)

(e)

Figure C.1. (continued)

(f)
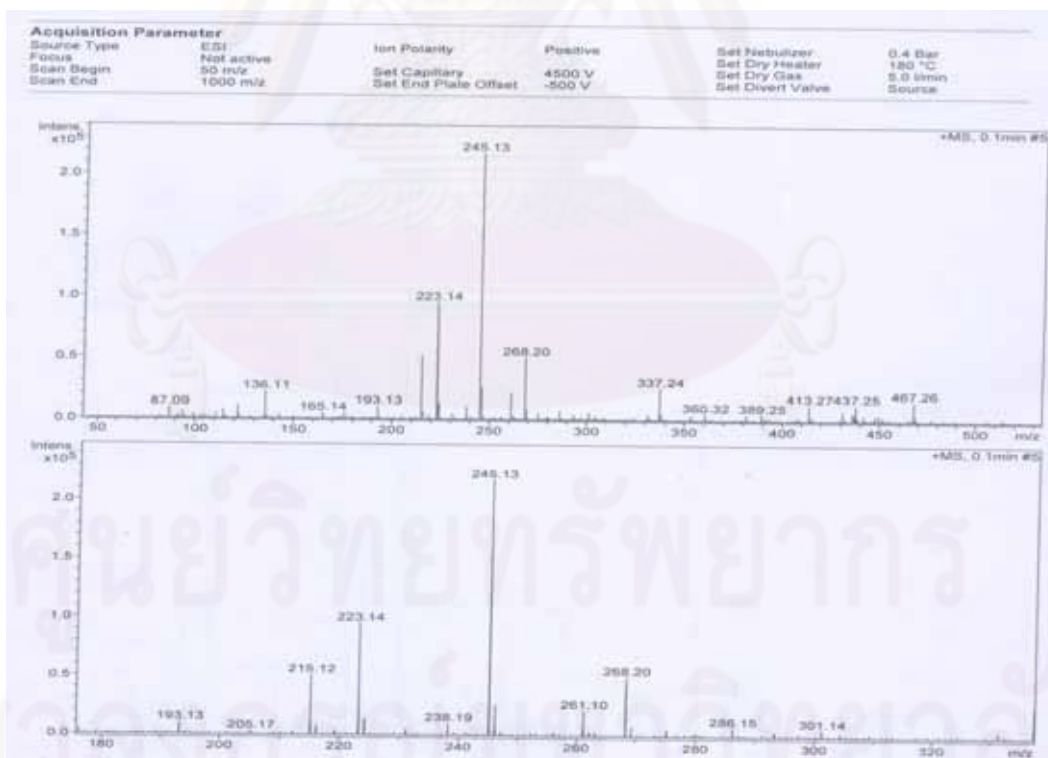
(g)

Figure C.1. (continued)
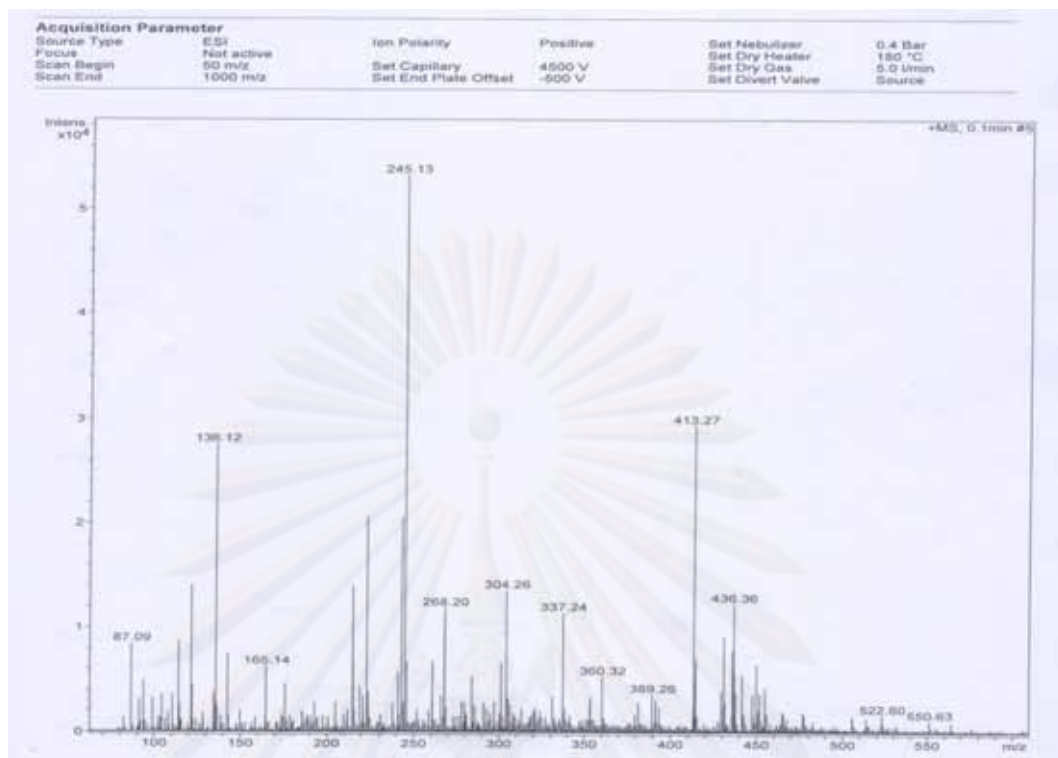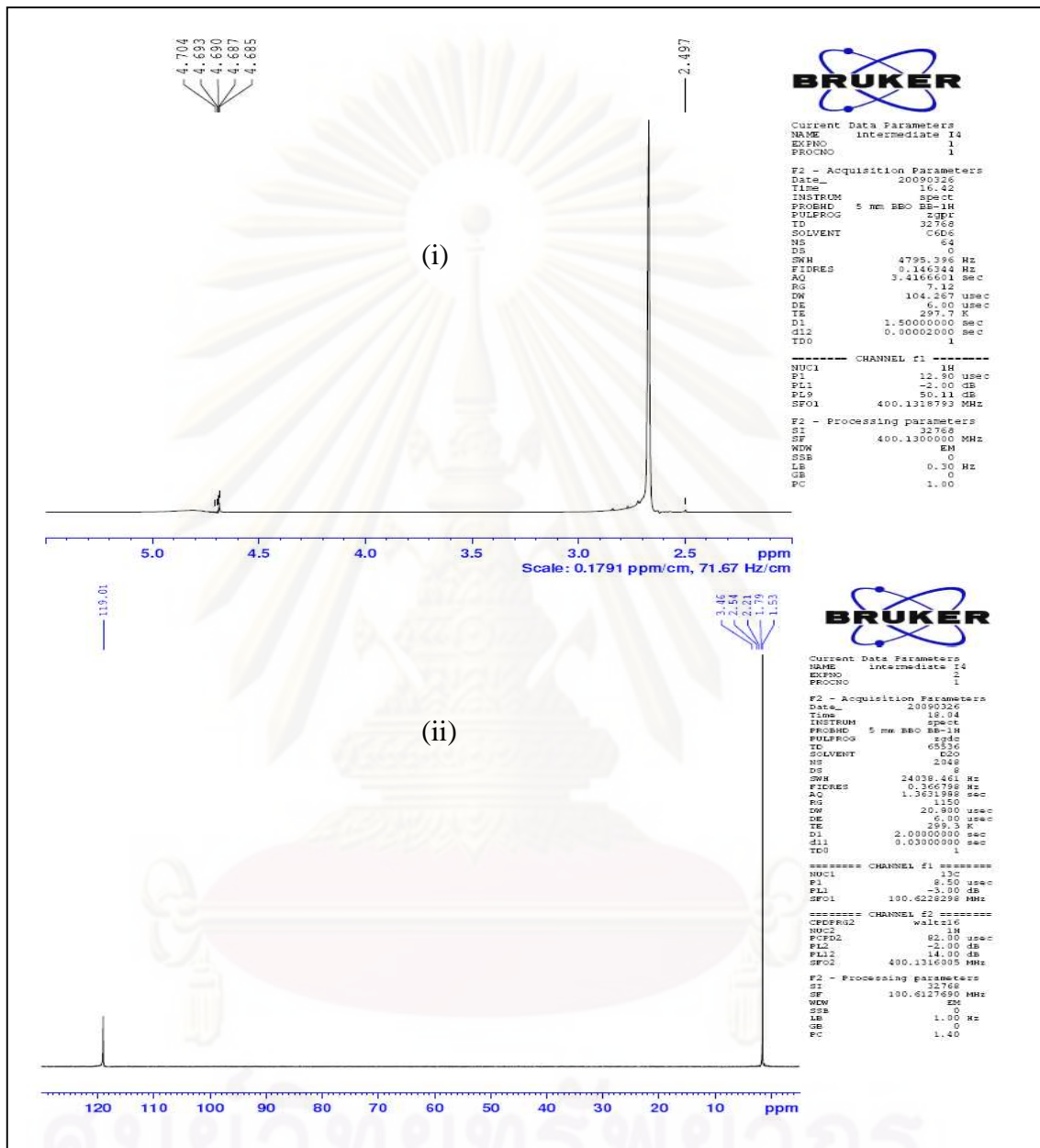
(h)
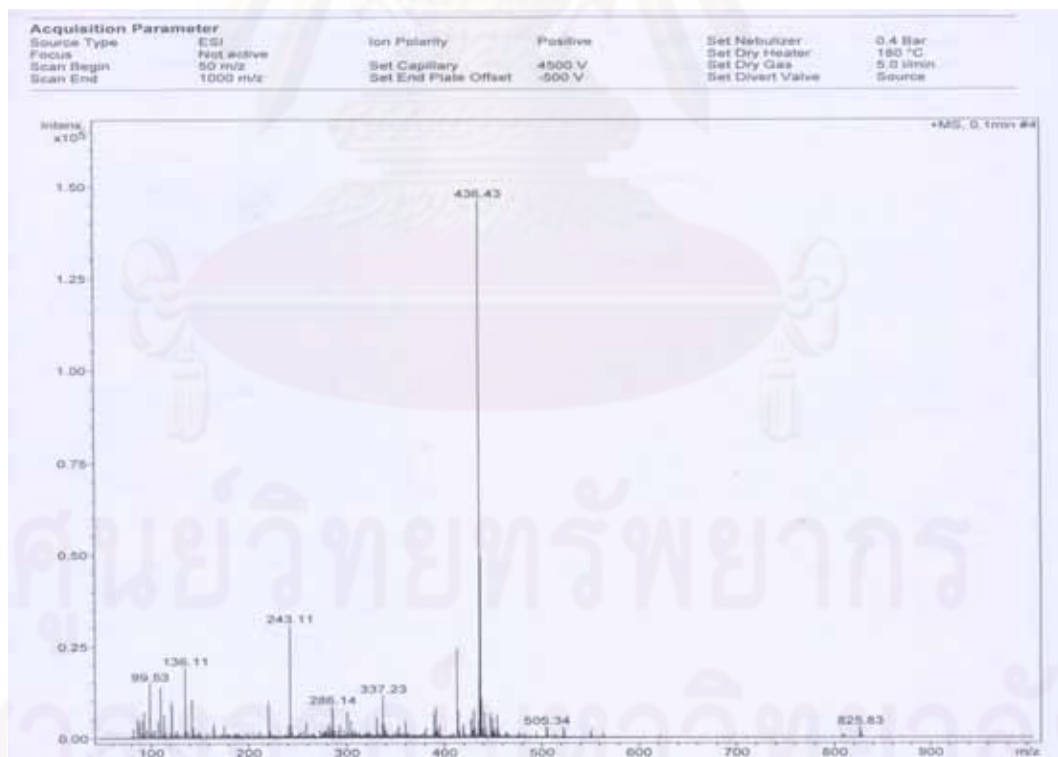
(i)

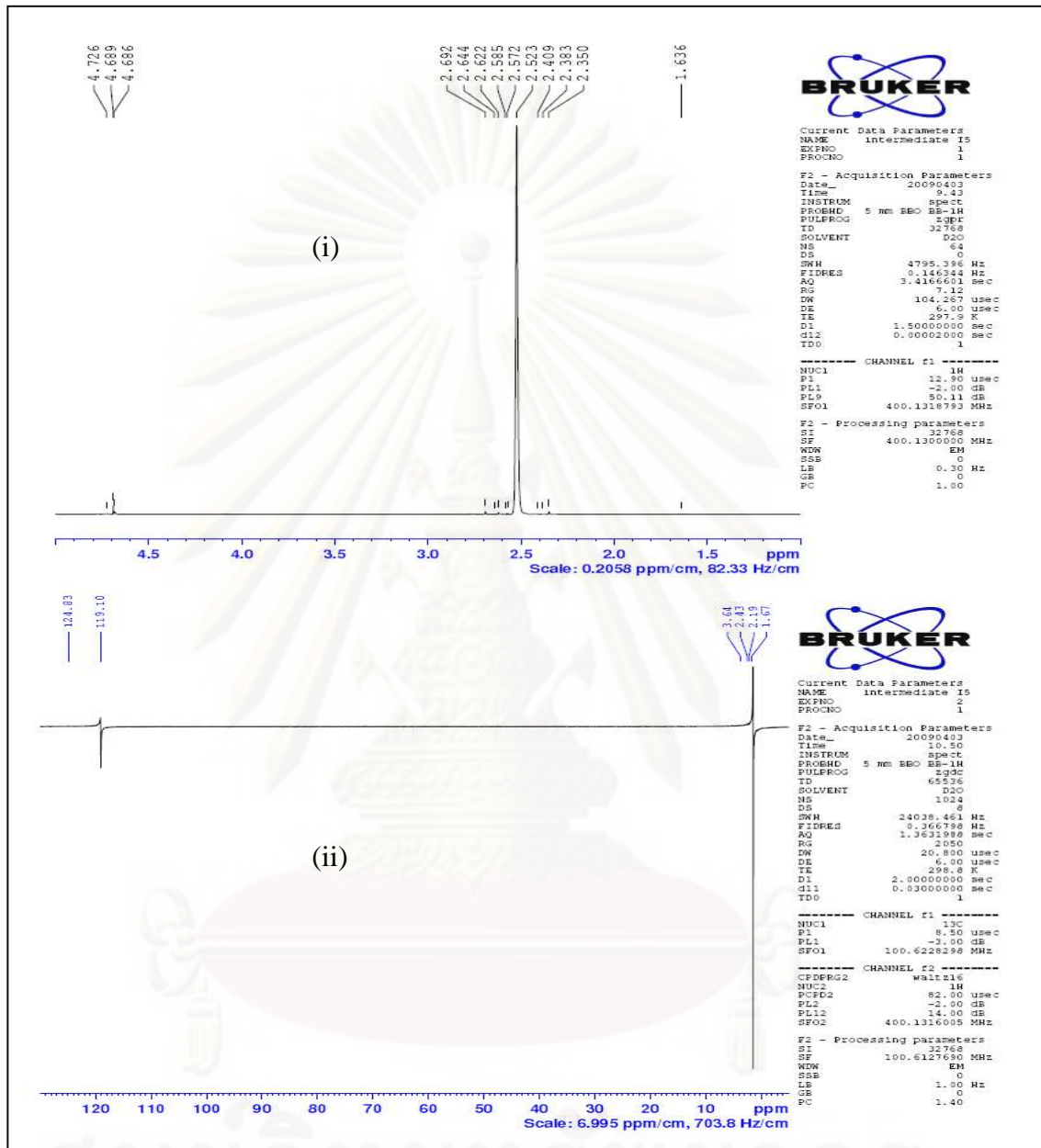**Figure C.1.** (continued)

APPENDIX D

SIGNAL OF NMR
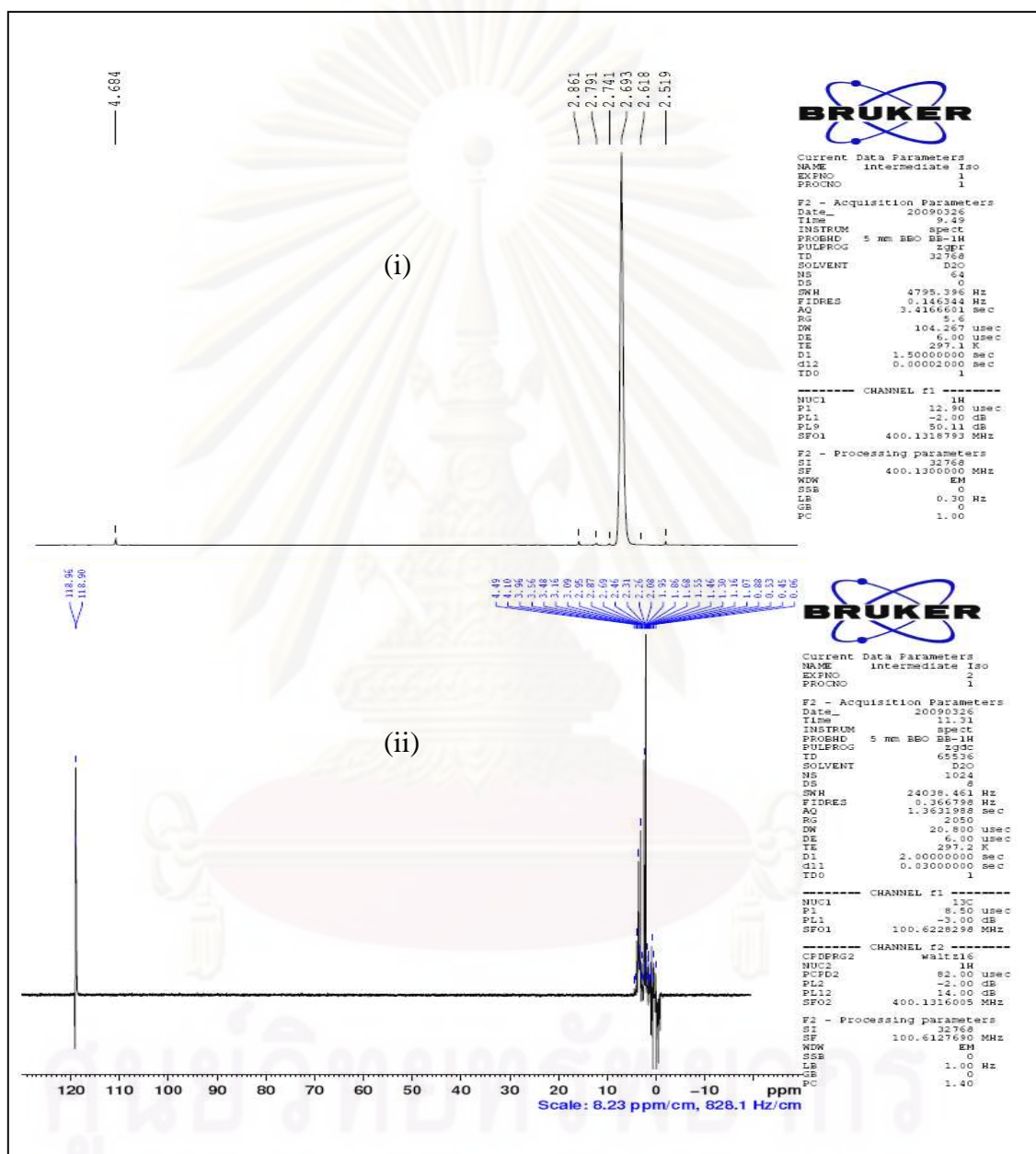
(a)

Figure D.1. NMR signal for proton mode (i) and carbon mode (ii) at retention time

of: (a) 6.6 min, (b) 8.2 min, (c) 10.3 min, (d) 11.2 min, (e) 11.7 min, (f)

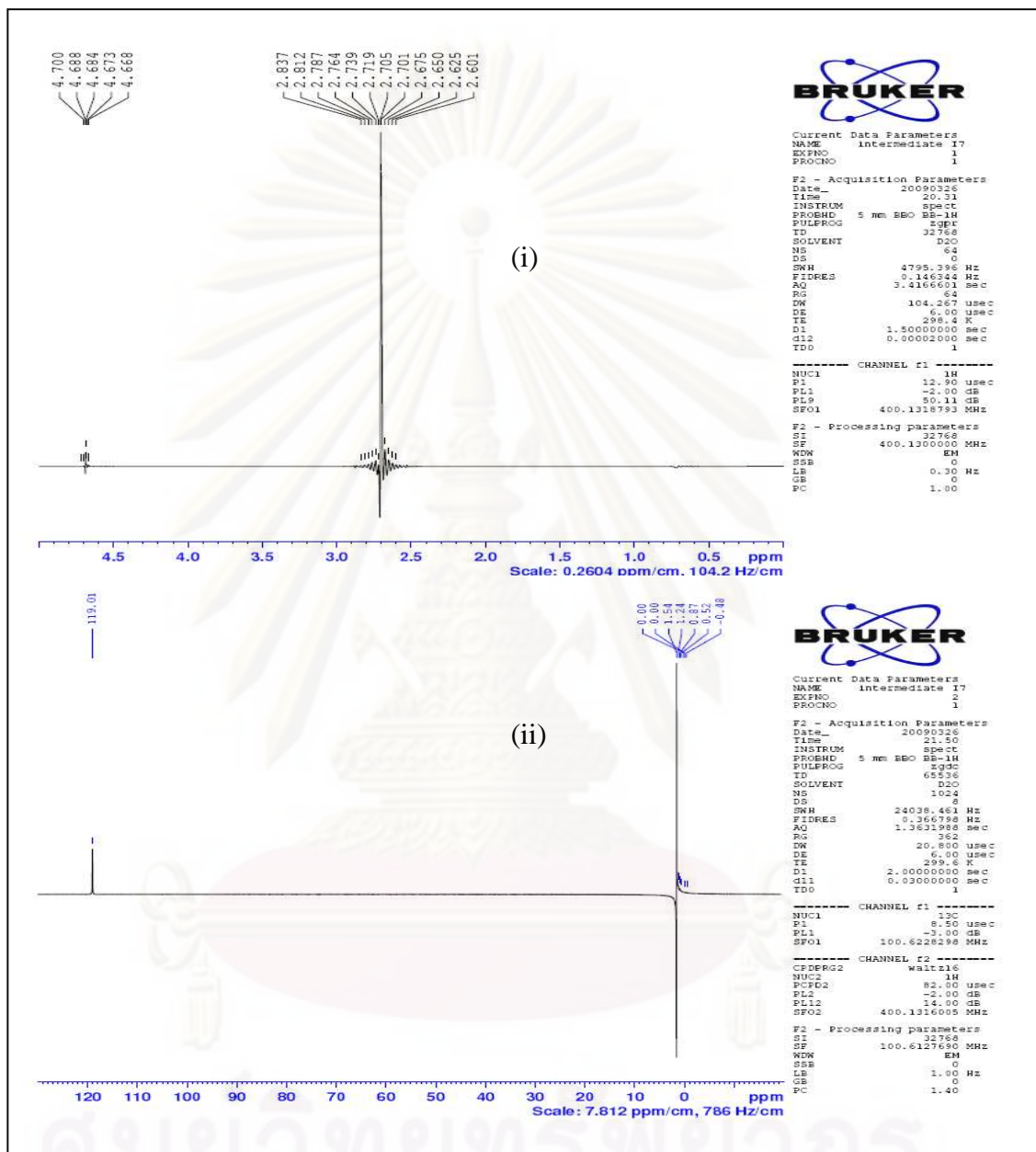12.2 min, (g) 12.9 min, (h) 13.3 min and (i) 15.3 min.
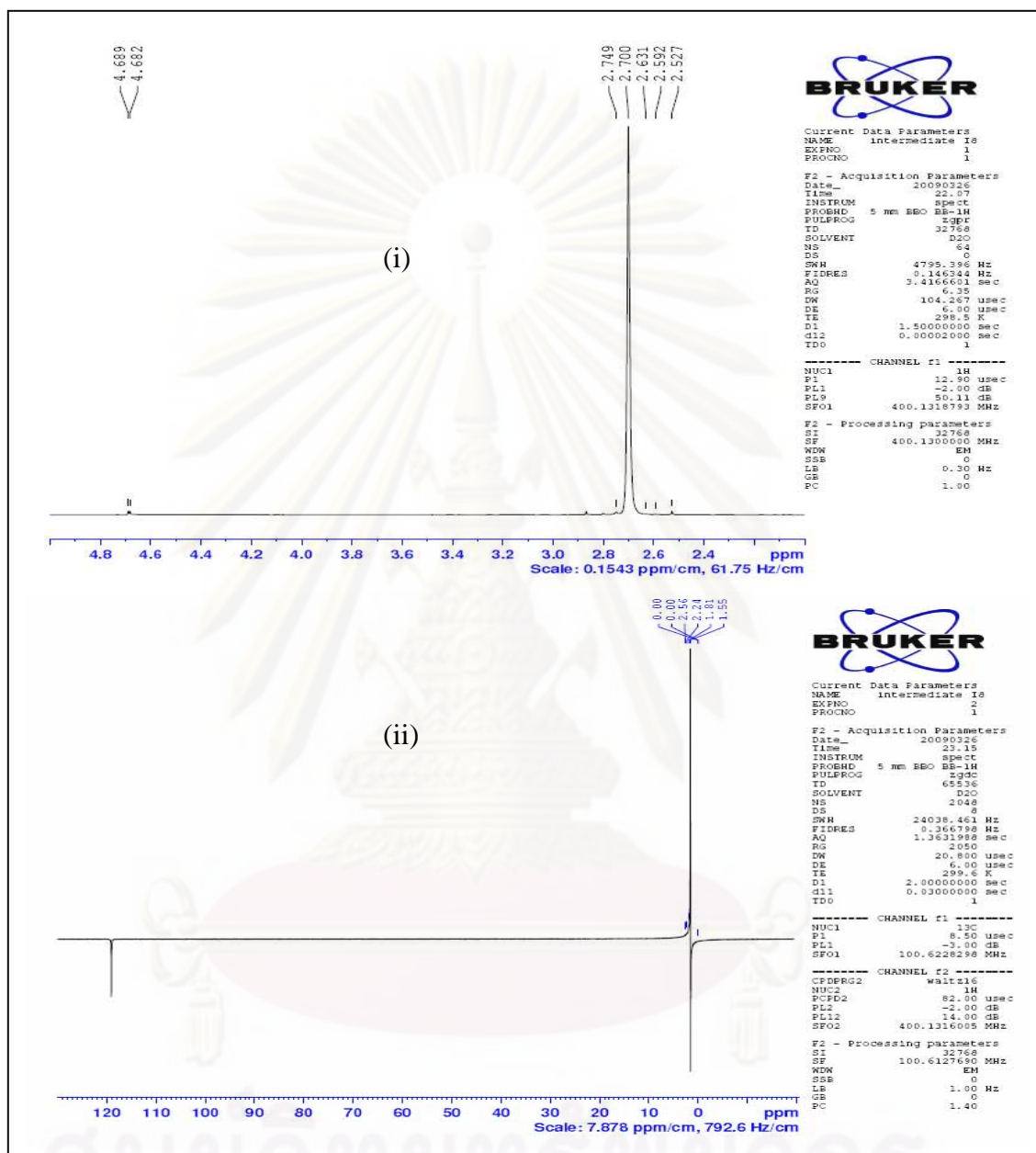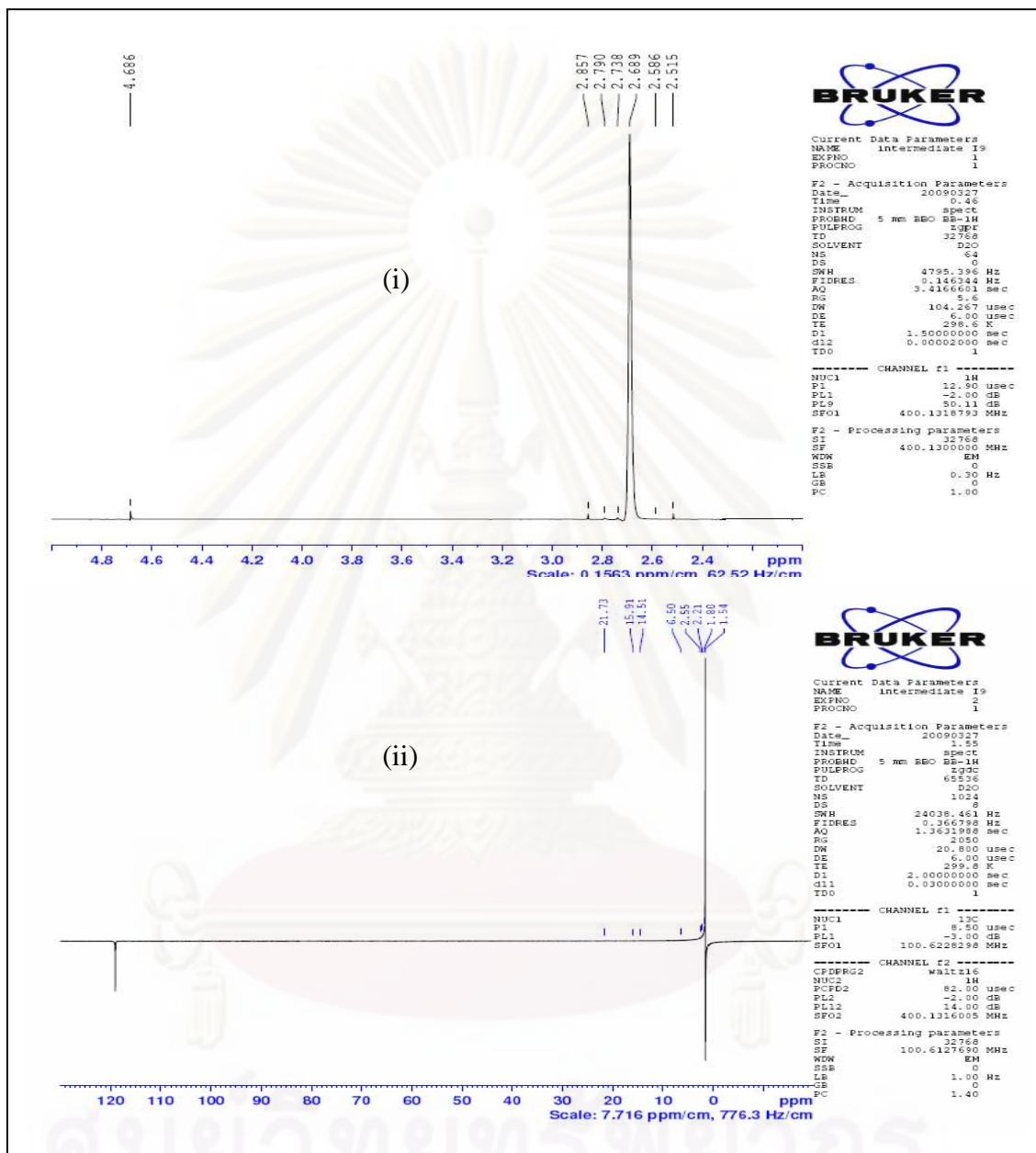
(b)

Figure D.1. (continued)

(c)

Figure D.1. (continued)

(d)

Figure D.1. (continuoed)

(e)

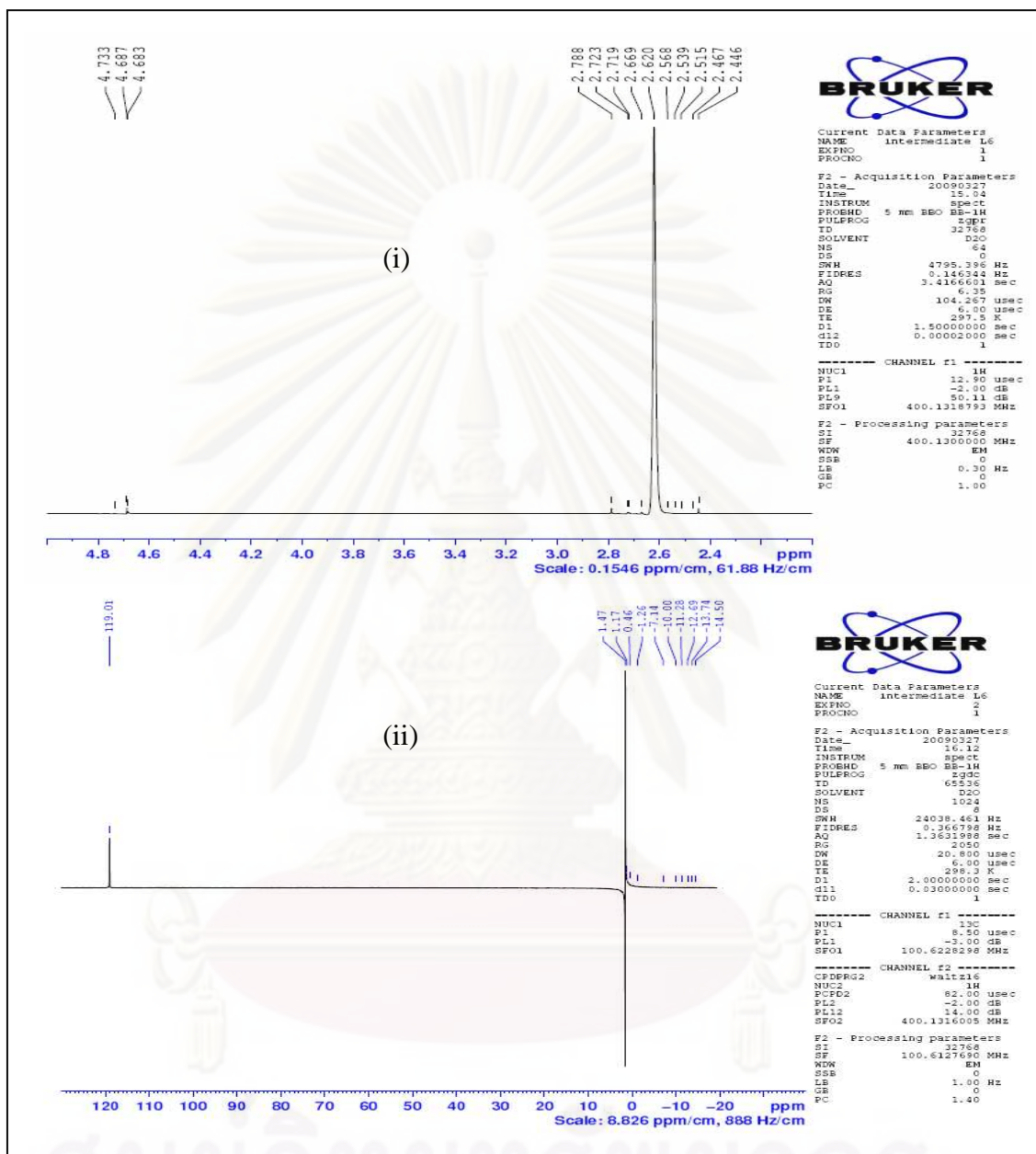**Figure D.1.** (continued)
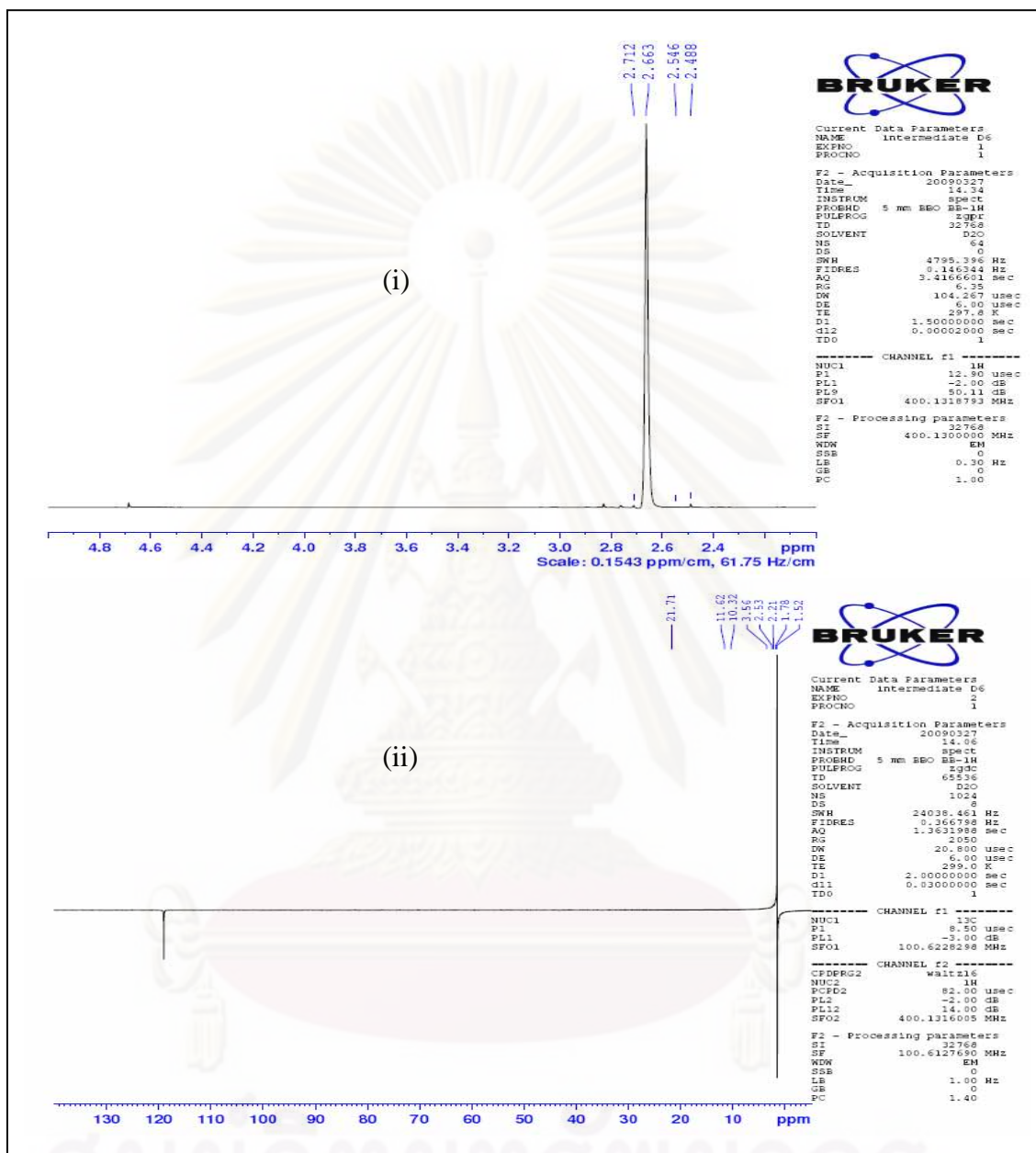
(f)

Figure D.1. (continued)

(g)

Figure D.1. (continued)

(h)

Figure D.1. (continued)

(i)

Figure D.1. (continued)

APPENDIX E

LIST OF PUBLICATIONS

1. Kamonrat Apichatsanee, Alisa S. Vangnai and Varong Pavarajarn. "Photocatalytic Degradation of Diuron on Nanosized ZnO powder: An investigation of Kinetics and Generated Intermediates", 5th Thailand Materials Science and Technology Conference (MSAT-5), September 16-19, 2008.

EO 02

Photocatalytic Degradation of Diuron on Nanosized ZnO powder: An investigation of Kinetics and Generated Intermediates

Kamolrat Apichatsanee[1], Alisa S. Vangnai[2] and Varong Pavarajarn[1,*]

[1]Department of Chemical Engineering, Faculty of Engineering, Chulalongkorn University, Bangkok 10330

[2]Department of Biochemistry, Faculty of Science, Chulalongkorn University, Bangkok 10330

*Corresponding author: Phone 0-2218-6890, Fax 0-2218-6877, E-mail: fchvpv@eng.chula.ac.th

Abstract

In the present paper, the degradation of diuron [3-(3,4-dichlorophenyl)-1, 1-dimethylurea], which is one of the most commonly used herbicides in Thailand, by photocatalysis using nanosized ZnO powders was investigated. It was found that although diuron is chemically stable, over 99% removal of diuron was achieved within 1 h of the photocatalytic degradation process. The reaction kinetics as well as intermediates formed during the reaction are also reported.

1. Introduction

The use of agrochemicals such as herbicides and insecticides is one of the main environmental problems at presence because agrochemicals are commonly toxic and can contaminate both soil and aquatic systems for very long time. Among such agrochemicals, diuron [3-(3,4-dichlorophenyl)-1, 1-dimethylurea], is one of the most commonly used herbicides, belonging to the family of halogenophenylureas. It is considered as highly toxic, bio-recalcitrant and chemically stable with a half-life over 300 days [1].

One of the waste treatment technologies for the elimination of toxic chemicals is semiconductor-assisted photocatalytic process. Many kinds of semiconductor have been studied as photocatalysts. The most widely used semiconductor is TiO_2 due to its high efficiency, photochemical stability, non-toxic nature and low cost. On the other hand, ZnO is also a semiconductor having similar band gap as TiO_2. The advantage of ZnO, comparing with TiO_2, is that it absorbs over a larger fraction of UV spectrum and the corresponding threshold of ZnO is 425 nm [2].

In this work, the photodegradation of diuron, using nanosized ZnO powder as catalyst is investigated. Both the degradation kinetics and the formation of intermediates during the photocatalytic degradation of diuron are reported.

2. Materials and Method

Diuron (98%, Sigma-Aldrich) was first dissolved in deionization water. The concentrations of the aqueous diuron solution investigated were 1 and 10 ppm, respectively. Then, ZnO nanoparticles (obtained from Univenture PLC, Thailand) were added into the solution in the ratio of 1 mg of ZnO to 10 ml of solution. The mixture was kept in the dark for 30 min to allow the complete adsorption of diuron on the surface of ZnO. The photocatalytic reaction was initiated by irradiating the mixture to light from 6 UV-A lamps (Phillips TLD 15W/05). During the experiment, the mixture was constantly agitated by a magnetic stirrer.

Diuron degradation was periodically monitored by using a reverse-phase liquid chromatography system, with UV detector (HPLC-UV, Agilent Technologies, series 1200) and C-18 column (ZORBAX SB-C18, 5 μm particle size, 4.6x150mm). The solution of 70% acetronitrile-30% water was used as mobile phase (flow rate of 1.5 ml/min).

3. Results and Discussion

Figure 1 shows the disappearance of diuron by the photocatalytic degradation, using ZnO as catalyst. It should be noted that C is the diuron concentration at time t, while C_0 is the initial diuron concentration. It was found that, regardless of the initial concentration of diuron, the degradation reached about 99% of initial

EO 02

concentration within about 60 min. Comparing with the resulted in literature, this results confirmed that ZnO was more active toward the photodegradation of diuron than TiO$_2$ [3]. The reaction reached the stage of very slow progress after 60 and 90 min for 1 ppm and 10 ppm initial diuron concentration, respectively.
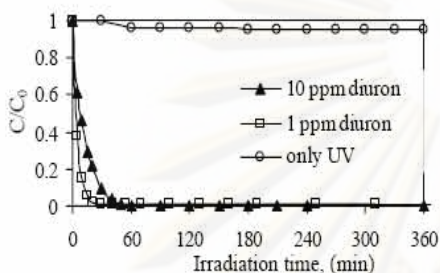

Figure 1. Results for the photocatalytic degradation of diuron.

The degradation can well represented by the pseudo-first order kinetics model, according to the Langmuir-Hinshelwood kinetics model. As shown in Figure 2, the pseudo-first order linear transforms of the results shown in Fig.1, i.e. the plot of ln (C_0/C) versus time, fitted well with the model. The apparent rate constants of the degradation (k_{app}) are reported in Table 1.
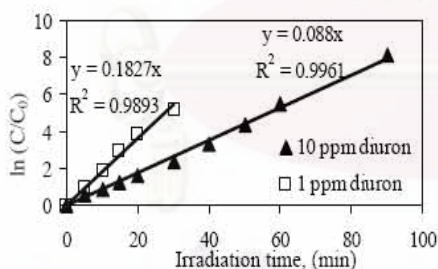

Figure 2. First-order linear transform of the degradation of diuron.

Table 1. Pseudo-first order kinetic rate constants of the photocatalytic degradation of diuron.

Initial diuron concentration (mg/l)	k_{app} (min^{-1})
1	0.1827
10	0.0880

As indicated in Table 1, the rate of degradation depends upon the initial concentration. At high concentration of diuron, greater amount of diuron adsorb on the surface of ZnO, which results in fewer active sites for the generation of hydroxyl radicals. Moreover, the fraction of photon intercepted by the species in the solution before they can reach the catalyst surface is increased if the concentration of diuron in the solution is high [3].

The intermediates generated during the photocatalytic degradation of diuron were also monitored by HPLC. It was found that intermediates from the degradation of diuron with the initial concentrations of 1 ppm and 10 ppm were the same. The results are illustrated in Figure 3.
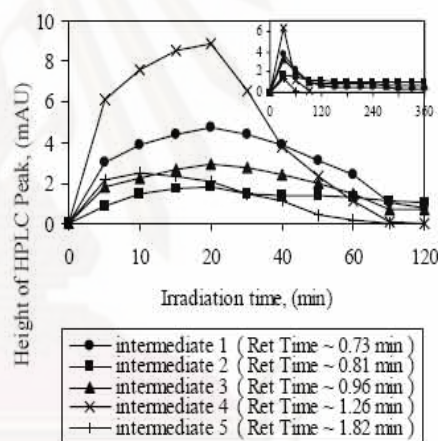

Figure 3. Results for the intermediates generated during the photocatalytic degradation of diuron.

Although the chemical structures of the intermediates were not identified in this present work, the result confirms that the degradation of diuron generates lots of intermediates. All intermediates were formed in the highest concentration within the first 20 min of the reaction. Then, subsequent degradation of the intermediates occurred. The intermediate 4 and 5 could not be detected after 90 min of irradiation time. However, some intermediates, e.g. intermediate 1-3, remain stable even after 6 h of the reaction (see inset in Figure 3). Further, identification of the degradation intermediates by

EO 02

using GC/MS and NMR will be discussed in our next paper.

4. Conclusion

Zinc oxide has high activity toward the photo-catalytic degradation of diuron in aqueous solution. About 99% degradation was achieved within relatively short period of time. The degradation follows the Langmuir-Hinshelwood kinetics model, but the reaction rate depends upon the initial concentration of diuron in the solution. Moreover, many intermediates are formed during the degradation of diuron.

References

[1] El Madani, M., et al., "Photocatalytic degradation of diuron in aqueous solution in presence of two industrial titania catalysts,either as suspended powders or deposited on flexible industrial photoresistant papers," Applied Catalysis B-Environmental, 2006. 65(1-2): p. 70-76.

[2] Daneshvar, N., et al., "Photocatalytic degradation of the insecticide diazinon in the presence of prepared nanocrystalline ZnO powder sunder irradiation of UV-C light," Separation and Purification Technology, 2007. 58(1): p. 91-98.

[3] Klongdee, J., et al., Activity of nanosized titania synthesized from thermal decomposition of titanium (IV) n-butoxide for the photocatalytic degradation of diuron. Science and Technology of Advanced Materials, 2005. 6(3-4): p. 290-295.

VITA

Miss Kamonrat Apichatsanee was born on February 3, 1980 in Nakornratchasima, Thailand. She received the Bachelor's Degree in Chemical Engineering from Suranaree University of Technology in December 2006, She entered the Master of Engineering in Chemical Engineering at Chulalongkorn University in June, 2007.